UNIVERSITY FEDERICO II OF NAPLES

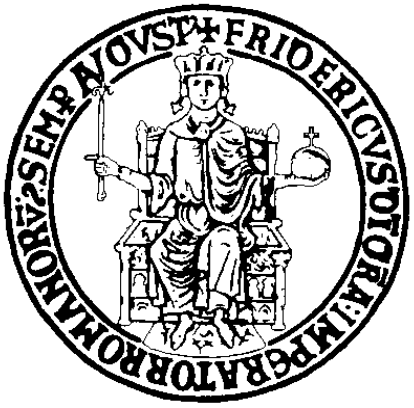

Department of Chemical, Materials and Industrial Production Engineering

PHD THESIS IN
CHEMICAL ENGINEERING

DIELECTRIC HEATING OF FOOD AND POLYMERIC MATERIALS

Scientific Committee
Prof. Roberto Nigro
Prof. Francesco Marra
Eng. Fernando Bressan

Candidate
Ing. Marica Di Domenico
MATR. DR993089

XXXIII CYCLE

A Matteo

SUMMARY

INTRODUCTION 6
1. STATE OF ART 7
1.1 TRADITIONAL TREATMENT TECHNOLOGIES 7
1.1.1 HEAT TREATMENTS 8
1.1.1.1 PASTEURIZATION AND STERILIZATION 8
1.1.1.2 DRYING 10
1.1.2 HEAT TREATMENT PLANTS 12
1.1.2.1 PASTEURIZATION 13
1.1.2.2 STERILIZATION 19
1.1.2.3 DRYING 20
1.1.3 REACTIONS INDUCED BY HEAT DURING THERMAL TREATMENTS 22
1.2 INNOVATIVE TECHNOLOGIES: RADIO FREQUENCY AND MICROWAVE 25
1.2.1 DIELECTRIC HEATING PROCESSES 27
1.2.1.1 PASTEURIZATION AND STERILIZATION 27
1.2.1.2 DRYING 28
1.2.2 DIELECTRIC TREATMENT PLANTS 29
2. AIM OF THE THESIS 39
3. MATERIALS 40
3.1 REFERENCE MATERIAL: WATER 40
3.2 FOOD PRODUCTS 41
3.2.1 LIQUID MATERIALS 41
3.2.1.1 RAW MILK 41
3.2.1.2 ALMOND MILK 43
3.2.1.3 FRUIT JUICES 45
3.2.2 FLUID MATERIALS 46
3.2.2.1 PUREES 46
3.2.2.2 ICE CREAM PREPARATIONS 47
3.2.3 SOLID MATERIALS 47
3.2.3.1 SUNFLOWER SEEDS 47
3.2.3.2 FLAX SEEDS 48
3.3 POLYMERS 49
4. METHODS 49

4.1 SYSTEMS FOR MEASURING DIELECTRIC PROPERTIES....50
4.2 LABORATORY SCALE TREATMENT SYSTEMS....54
4.2.1 CONTINUOUS SYSTEM....55
4.2.2 STATIC SYSTEM....57
4.3 NUMERICAL MODELING SYSTEMS: FEM 3D....62
4.3.1 COMSOL MULTIPHYSICS®....63
4.3.2 RF APPLICATOR MODEL FOR LIQUIDS....65
4.3.2.1 RF APPLICATOR MODEL....66
4.3.2.2 MESH CONSTRUCTION AND MODELING PARAMETERS....69
4.4 EXPERIMENTAL SYSTEM....80
4.4.1 PASTEURIZER....81
4.4.2 RF SYSTEM....83
4.4.3 PACKAGING MACHINE....84
4.4.4 EXPERIMENTAL TESTS....85
4.4.4.1 ENERGY BALANCE....85
4.4.4.2 PRELIMINARY TEST WITH WATER....86
4.4.4.3 RAW MILK TEST....87
5. RESULTS....88
5.1 DEVELOPMENT OF TEST PROTOCOLS AND IMPEDANCE MEASUREMENTS....88
5.1.1 LIQUID MATERIALS....88
5.1.1.1 RAW MILK....88
5.1.1.2 ALMOND MILK....90
5.1.1.3 FRUIT JUICES....93
5.1.2 FLUID MATERIALS....96
5.1.2.1 PUREES....96
5.1.2.2 ICE CREAM PREPARATIONS....99
5.1.3 SOLID FOOD MATERIALS....102
5.1.3.1 SUNFLOWER SEEDS....103
5.1.3.2 FLAX SEEDS....107
5.1.4 SOLID POLYMER MATERIALS....110
5.2 SIMULATIONS AND EXPERIMENTAL TESTS....116
5.2.1 SIMULATION WITH WATER....116
5.2.2 SIMULATION WITH MILK....122
5.2.3 RESULTS OF EXPERIMENTAL TESTS....125

5.2.3.1 PRELIMINARY TEST 124
5.2.3.2 TESTS WITH MILK 126
5.2.3.3 COMPARISON BETWEEN SIMULATIONS AND EXPERIMENTAL TESTS 128
6. CONCLUSIONS 132
APPENDIX I 133
APPENDIX II 148
BIBLIOGRAPHY 153

INTRODUCTION

In modern society, an essential trait of industrial processes is to carrying out treatments to modify chemical-physical characteristics of material in a way that is functional to the industrial needs and aims. Among the industrial applications in the food sector, for example, it is common to heat food in order to eliminate microorganisms harmful to human health or to increase the products' shelf-life. The primary purpose of thermal processes in the food industry is to reduce or destroy microbial and enzymatic activity and to produce physical or chemical changes in order to achieve the required quality standards. There are multiple types of thermal processes applied to the food industry such as hot air drying. This is a traditional drying method used in many stages of food processing processes. With regard to plastic pellets or wood, on the other hand, hot air heat treatments are usually used with the aim of eliminating excess moisture and increasing the mechanical properties of materials.

One of the most important applications of hot air drying is precisely the sterilization and dehumidification of materials or the pasteurization of food. However, this process has several disadvantages: long treatment times, high energy consumption, low heating efficiency especially in the case of materials with a low moisture content and the possible browning or blackening of dried products that affect the overall quality, price and appeal on the market.

For these reasons, new technologies have been studied to replace or help traditional technologies. Currently, the interest of the industrial panorama for dielectric heating applications is growing and strengthening, pushed by the prospect of ensuring a faster, more homogeneous and more efficient heating process than those traditionally used, limiting the inconveniences related to a not uniform heating within the material matrix, or to the achievement of excessively high temperatures.

To provide proper heating, it is necessary to quantify the dielectric properties of the materials in terms of dielectric constant (ε') and loss factor (ε''). Dielectric properties are fundamental to understanding the electrical behaviour of a material: ε' is related to the ability to store electricity in the presence of an external field and ε' refers to energy dissipation in the form of leaks. Data on dielectric properties are critical to the development of heat treatments using radio frequency (RF) or microwave (MW) energy and are essential for estimating the uniformity of heating in electromagnetic fields: the properties of a product are a general guide to select the optimal frequency range and the system power.

There are many different ways and tools to measure and estimate the dielectric properties of materials, and if, in the case of liquids, determining such quantities is quite simple, as regards solids and especially granular solids, there are many problems in carrying out tests.

The purpose of this work is to define a measurement protocol and provide data on the dielectric properties of various types of materials, both liquid and solid, of food origin and more. Furthermore, have been provided the theoretical equations that describe the dielectric properties of the materials analysed as a function of temperature.

This thesis work was carried out in collaboration with Officine di Cartigliano, one of the first companies in Italy to design and use radio-frequency heating systems, today a leader in the sector.

1. STATE OF ART

Reduction of production costs has always been one of the driving forces of the industrial world towards the improvement and research of innovative production methods that at the same time lead to an increase in product quality. The heat treatment processes are and remain the main methodology through which the industry achieves the sterilization, drying and increase of the shelf-life of a wide range of products, not only food, without compromising their quality and safety. Recently, however, traditional heat treatment methodologies are being accompanied by innovative methods that respond not only to the need to make these processes faster and cheaper, but also to preserve the peculiar and interesting properties of the products subjected to the treatments, such as for example nutritional characteristics or attributes related to quality.

1.1 TRADITIONAL TREATMENT TECHNOLOGIES

The heat treatments allow the achievement of a wide range of results, such as, for example, the inactivation of pathogenic microorganisms. Fresh foods, undergo a series of physical and chemical transformations more or less quickly and often those transformations make them inedible. The deterioration of food in general is a problem that mankind has always tried to solve. The cause of this deterioration is due to microorganisms such as bacteria and fungi (molds and yeasts). The life of microorganisms depends on various environmental factors of a physical, chemical and biological nature. Among the physical factors, temperature plays a

role of primary importance, and is the parameter on which we mainly act as a method of sanitation by means of heat treatments.

1.1.1 HEAT TREATMENTS

The heat treatments mainly have a dual purpose: to destroy human pathogenic microorganisms and reduce the endogenous microflora to the lowest possible level, in order to increase the products shelf-life. Depending on the time required to carry out the treatment and its temperature, the population of vegetative cells of pathogens, such as Escherichia Coli, Salmonella or Listeria Monocytogenes, as well as of sporogens, such as Clostridium Botulinum, Clostridium Perfringens or Bacillus Cereus, can be reduced considerably. Other heat treatments can be designed to destroy altering microorganisms, such as Alicyclobacillus Acidoterrestris, a fearful non-pathogenic sporogenic, but altering the quality of fruit and vegetables [1].

The sanitation methods used are mainly two, based on a different time-temperature combination: pasteurization and sterilization. Drying, on the other hand, has the purpose of reducing the moisture content of the product to such a low level as to prevent the proliferation of microorganisms.

1.1.1.1 *PASTEURIZATION AND STERILIZATION*

Pasteurization (by the name of Pasteur) is defined as the heat treatment designed to destroy the pathogenic forms, and most of the vegetative ones, of the microorganisms present in the food and deactivate the enzymes with a minimal alteration of the chemical, physical and organoleptic characteristics of the food. Pasteurization, in fact, is for foods that are more sensitive to heat and which can therefore be subjected to mild heating, in order to preserve the organoleptic and nutritional qualities, such as milk, fruit, vegetables, pork, wine or beer. Pasteurization is also defined as "mild heat treatment" to avoid microbial and enzymatic deterioration, in fact it is not able to destroy all microorganisms. It is typically used to extend the shelf-life of food at low temperatures, usually 4°C for several days, such as in the case of milk, or for several months, such as for fruit stored in jars [2]. The severity of the heat treatment and the consequent extension of the shelf-life are mainly determined by the pH of the food. Pasteurization is performed through three methodologies: high, low and rapid, as shown in table 1, and is usually followed by rapid cooling of the product. During the pasteurization, temperatures are not so high to devitalize the thermophilic microorganisms

or the spores.

Sterilization is a more drastic treatment than pasteurization and aims to destroy all microbial forms, including spores, yeasts, moulds and vegetative bacteria. It can be defined as that heat treatment designed to destroy all microorganisms that can reproduce in the food during storage and distribution, in fact it allows products to be stored even at room temperature with a prolonged shelf-life. Sterilization procedures involve the use of heat, radiation or chemicals or the physical removal of cells [2]. The thermal conditions necessary for sterilization depend on various factors, among which the pH of the food plays a fundamental role. Sterilization temperatures for acidic foods are around 100°C; for foods at low acidity or neutral, temperatures of 115-120°C are needed, with times not less than 20 min. The heat treatment can be carried out on solid or liquid food already closed in a metal or glass container, or on unpackaged liquid food, which will then be collected in a sterile container (table 1). In the first case, it will be a classic sterilization, to be carried out in an autoclave if temperatures above 100°C are required. In this case, the sterilization process consists of four distinct phases. In the first step, the product must be heated to a temperature of 110-125°C to ensure sterilization. In the second step, the product takes a few minutes to equilibrate, because the surface is hotter than the central part of the container and this cause a temperature gradient. The equilibration stage allows to reduce the temperature gradient. In the third phase, the product must be kept at this temperature for a certain period to ensure a predetermined sterilization value. Finally, the product must be cooled mainly to stop further heat treatment and avoid the product cooking.

In the second case, the food will be brought to the sterilization temperature, for the necessary time, in a heat exchanger or, more rarely, by direct injection of superheated steam; then it will follow the traditional hot filling in glass containers, also sterilized (for example, in the packaging of fruit and tomato juices) or the cold aseptic filling in flexible multilayer containers. These sterilization systems, carried out mainly, but not only, on milk, are indicated with the initials UHT (Ultra High Temperature), since the temperature reaches and goes over 140°C, while the times are reduced to a few seconds [3].

Table 1 – Heat Treatments types and characteristics

Type of heat treatment	Temperature	Time	Remarks
Low pasteurization	60-65°C	30 min	Used for wine, beer, milk for cheese making
High pasteurization	75-85°C	2-3 min	Method once used for milk, now replaced by HTST
Fast pasteurization o HTST (High Temperature Short Time)	75-85°C	15-20 sec	Conducted on liquid foods that flow in a thin layer between two heated metal walls (also called stassanization)
Classic sterilization or appertization	100-120°C	≥ 20 min	Carried out on canned foods in an open bath (acidic foods) or in an autoclave
Indirect UHT	140-150°C	Few seconds	Carried out on bulk food in heat exchangers
Direct UHT or uperization	140-150°C	Few seconds	Carried out by injection of superheated steam into the bulk product

The heat treatments of pasteurization and sterilization are both based on the combination of time and temperature parameters: the killing of microorganisms takes place, in fact, thanks to the heat supplied to the food, which must reach the microorganism and invest it for a certain amount of time. A living organism subjected to the effect of high heating will first undergo an increase in the speed of metabolic reactions and subsequently a denaturation of vital proteins, until its death. In order for the heat treatment to be effective, not only the reached temperature level is important, but also the relationship between this factor and the time of application of the temperature itself [4]. Time and temperature of the treatment are established on the basis of the heat resistance of the microorganism to be inactivated or destroyed, its microbial load prior to the treatment, the final one to be obtained and the chemical-physical characteristics of the product.

1.1.1.2 *DRYING*

Drying is an operation that has the purpose to obtain the solid-liquid separation. In the vast majority of cases, the liquid to be separated is a solvent, and almost always water. In the case of food, drying involves the elimination of almost all of the water, passing from values of 65-

95% to a water content at which the deterioration due to microbial action is greatly reduced, that is about of 10-15% water [5]. Drying does not kill microorganisms, but it stops their development. Dehydration or drying consists of heating the product under controlled conditions to evaporate most of the water it contains [6]. While some materials have moisture only on the outer surface, and are, therefore, easy to dry through the use of hot air flows, others materials absorb water even in their innermost areas. In these cases, the drying of the material becomes a problem that is far from trivial.

The industrial drying methods originated with the first dryers, that is artificially heated environments where the products to be treated circulate or stand. The manufacturing process involves three stages:

- Preparation of the product to be dried;
- Drying;
- Packaging.

If the preparation (washing, concentration of liquid products, cutting of the material, etc.) and packaging (in containers impermeable to light, air but above all humidity) are very important for the final result, the heart of the procedure remains the heat treatment aimed at removing the water from the product. In this phase two aspects are of fundamental importance:

- The transfer of heat from the source to the product;
- The transfer of water from the product to the outside.

Heat transfer generally takes place using conduction, convection or radiation mechanisms in order to transport energy from a heat source (hot gas or heated metal surface) to the material to be dried. On the other hand, the mass transfer during drying can be controlled by the diffusion rate of moisture (liquid or vapor) within the matrix of the material or by the rate of evaporation of moisture from the surface of the product to the medium of drying [7]. The water transport mechanisms include capillary flow, surface diffusion and liquid diffusion while the vapor transport mechanisms consist of Knudsen diffusion, reciprocal diffusion, Stefan diffusion, Poiseuille flow and condensation-evaporation [8].

The mechanisms of heat and mass transfer are usually influenced both by the differences in temperature and concentration of the water, and by the velocity field of the air, together with the properties of the materials themselves. In general, heat, mass and momentum transfer

occur in at least two distinct subdomains (air and product) and occur simultaneously both externally and internally to the product matrix itself. The drying process can be outlined as follows [9]:

- Convective and conductive heat transfer in the air;
- Convective and diffusive transfer of water into the air;
- Heat transfer mainly by conduction inside the solid;
- Mass transfer within solid by diffusion (liquid or vapor);
- Evaporation of humidity at the air-product interface;
- Air flows (laminar or turbulent) around the material.

In particular, the process of releasing water from the product consists of three phases: at the beginning, the water migrates abundantly from the innermost to the outermost layers through the porosity of the material, and when it reaches the surface it evaporates. Later, once the larger channels have dried, the residual water slowly diffuses outwards through the micropores. Finally, the product tends to thermohygrometric equilibrium with the surrounding environment.

Conventional thermal dryers have several limitations, including non-uniformity of product quality due to too much and/or reduced drying caused by long, inadequate or non-uniform product exposures to the processing conditions. Long drying times result from the low thermal efficiency between the drying medium and the dried materials. In case the treatment concerns food products, there is also the possibility of thermal degradation of nutrients and generation of unpleasant aromas due to exposure to higher temperatures. Furthermore, in some cases, conventional dryers require large volumes with low production capacity. These limitations result in poor drying performance and very high operating costs [7].

1.1.2 HEAT TREATMENT PLANTS

Drying, pasteurization, sterilization and other thermal processes are treatments, by giving heat, which are applied in food processes to destroy microorganisms and viruses that can harm public health or cause significant economic damages. The plants used for the different types of process have some parts that are common and others that are specialized for the specific type of treatment. However, for each of these, the heat exchange operations are

fundamental. These operations require a suitable service fluid (hot and cold), separated by a wall or in direct contact with the product, depending on the technologies. In heat recovery plants, the hot service fluid is the same product leaving the pasteurization, which heats the incoming product through an exchanger.

The heart of each thermal process follows the following steps:

1. Heating - Product temperature rises to a lethal level for target microorganisms;
2. Holding - The product is kept in temperature for a time sufficient to reach the required extent of destruction of microorganisms;
3. Cooling - The temperature is lowered as quickly as possible to minimize thermal damage to the product and block the proliferation of any thermophiles present.

The holding phase is crucial. Although part of the destruction of microorganisms occurs in the final stages of heating and in the initial stages of cooling, the holding is usually designed, in terms of temperature and time, to reach the full extent of the destruction of pathogens by itself. The relatively modest extent of destruction that occurs during heating and first cooling should be considered as a safety margin.

For these reasons, several new treatment technologies, including microwaves and radiofrequency heating, have been studied to improve, replace or complement conventional heat treatment technologies.

1.1.2.1 *PASTEURIZATION*

A typical plant for HTST pasteurization consists of the following equipment:

- A tank of the raw product;
- A raw product pump;
- One exchanger;
- A pasteurization temperature control system;
- An in-line filter or a centrifuge;
- A dosing pump and a flow control;
- A holding tube;

- A temperature-activated deviation system;
- A differential pressure control system;
- A process registration and control system.

Figure 1 shows a simplified diagram of a pasteurization plant. The raw product is pumped from the tank to the recovery section of the exchanger, where it is preheated by the hot pasteurized product coming from the holding tube. The preheated product can pass through a filter or a centrifuge. After recovery heating, the product is pumped by the metering pump to the heating section of the exchanger. Here its temperature is raised by hot water or vacuum steam. The holding at this temperature is achieved by passing the product through a tube of such dimensions that, at the flow rate of the pump, the minimum residence time in the tube is greater than or at least equal to the minimum dwell time required. The product temperature is monitored downstream of the holding tube. If this is greater than the one required, the deviation system at this point allows the product to flow forward towards the recovery section. In the recovery section, the pasteurized product is pre-cooled by releasing heat to the incoming raw product. Final cooling take place in the properly section in which cold water and icy water (sometimes also glycol solution from the refrigeration system) are commonly used.

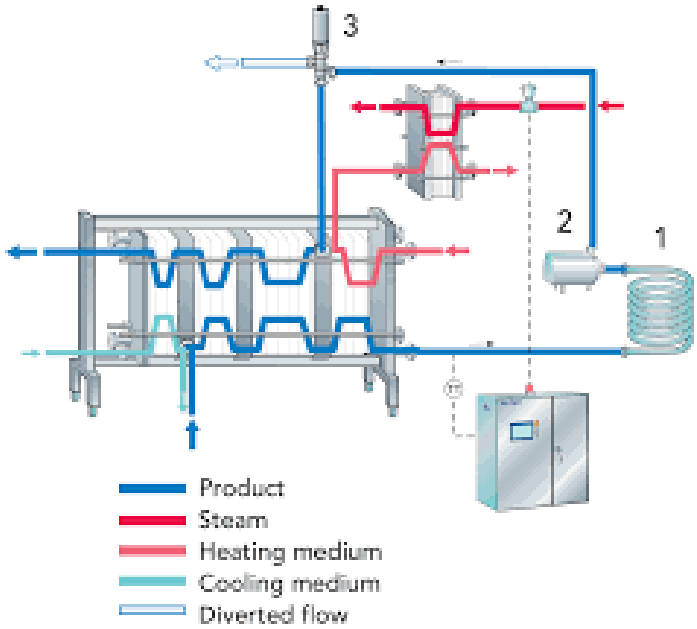

Figure 1 Pasteurization plant scheme

If the product temperature at the end of the holding tube is lower than required, the under-pasteurized product is diverted back to the feed tank. The plant must be designed to operate

without contamination of the final product with the raw product in the recovery section or contamination by a non-potable exchange medium in any of the other sections. If the product is not immediately packaged, it must be stored at refrigerator temperature in clean and disinfected tanks and protected from post-pasteurization microbial contamination.

Among the most important elements of a pasteurization plant, there is undoubtedly the heat exchanger. Its function is to heat the raw material to the pasteurization temperature and, after the holding stage, to cool it to the required temperature. There are different types of heat exchanger, but the most used types for pasteurization are:

- Tube-in-tube exchangers

The tube-in-tube exchanger consists of two concentric tubes, in the central section of which the food fluid flows and in the outermost section the service fluid flows. These exchangers can withstand high pressures and achieve good heat transmission efficiency. Some types of heat exchanger have the internal surface of the tube corrugated, in order to generate the turbulence of the fluids and further improve the heat exchange. They are simple to make and easy to inspect, they also allow perfect counter-current and are modular. Due to the large surface area of the outer tube, they have high heat losses, which often require insulation. To obtain greater efficiency from the tubular exchanger, it is possible to increase the heat exchange surface by approximately double, by assembling a third tube, inside the tube in which the liquid to be heated flows (figure 2). In the section of the pipe it can therefore be observed that the cold fluid, in perfect counter-current, flows between the two service fluids [10].

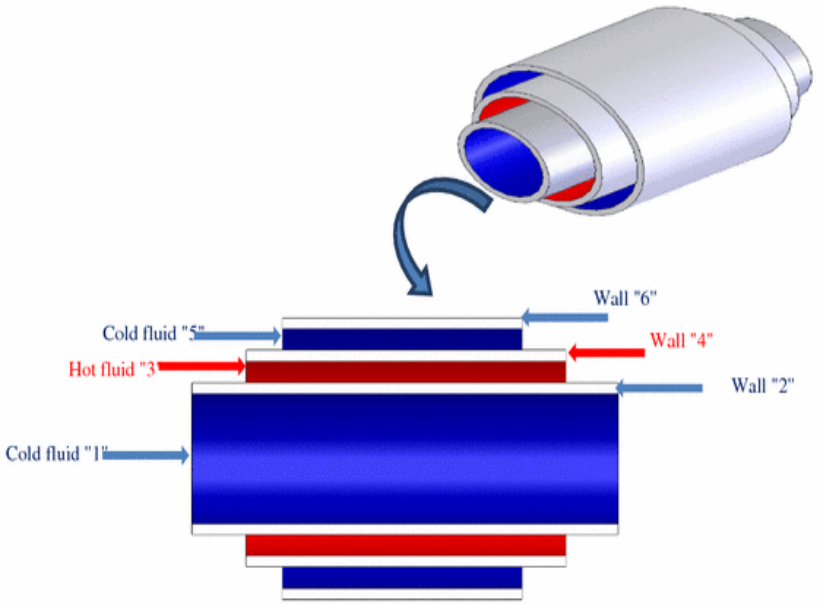

Figure 2 Three concentric pipes heat exchanger: in blue the fluid to be heated and in red the service fluid, in perfect counter-current

Furthermore, the flow of the product to be heated can be multitubular or monotubular (figure 3):

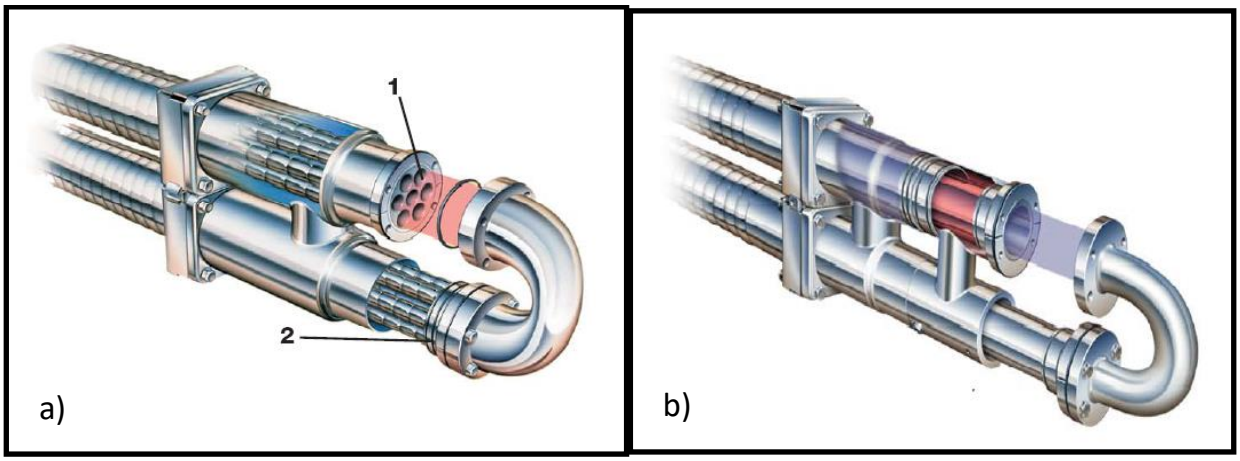

Figure 3 Multitubular exchanger a) and monotubular b)

- Plate exchangers

Plate heat exchangers are made by assembling a certain number of rectangular stainless-steel plates, crossed by holes through which the service fluid and the fluid to be treated flow. The passage of the two fluids is regulated by the seals on each plate, which allow the sliding in the section first of one, then of the other liquid, interspersing a passage of product to be treated with a service one. Their working is illustrated in figure 4:

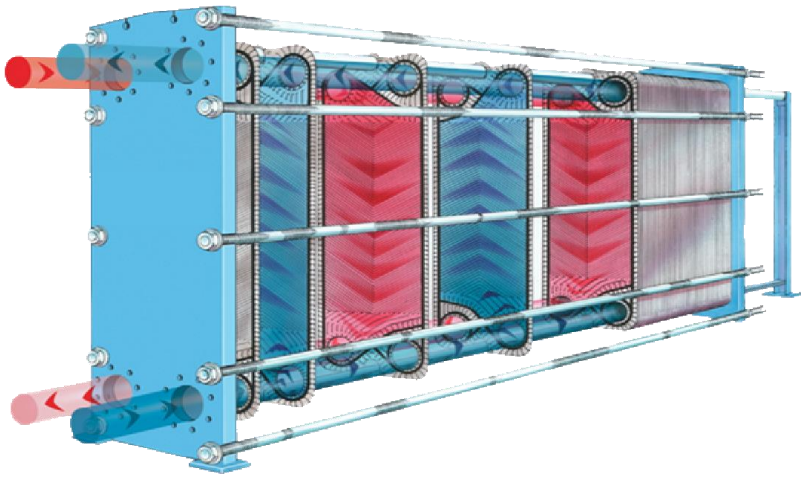

Figure 4 Plate heat exchanger with parallel assembly: the service fluid in red and the product to be heated in blue

The plates are hung and tightened with threaded bars and nuts on the side members, they are modular and can be inspected; furthermore, they are deep drawn to allow greater resistance to high pressures and to increase the turbulent motion of the fluids, which growths the efficiency of heat transmission. The system is advantageous both from the point of view

of the overall dimensions, as it is very compact, and as regards the heat losses, which are very low. On the other hand, it requires careful maintenance of the gaskets, as the risks of leakage are high, and of the plates, which are easily encrusted due to the limited thickness that separates them. The high modularity allows the plates to be assembled in different ways (parallel, mixed and in series). The assembly of the plates in parallel allows the creation of the perfect counter-current, against a limited exchange surface, since the fluids undergo only one passage along the plate (inlet and outlet from the same side, as image above). On the other hand, with series and mixed assemblies, the perfect counter-current is not achieved but more fluid passages can be obtained along the plates.

In the heat recovery section of the exchanger, heat is transferred from the pasteurized product to the incoming raw product. The recovery efficiency (η_{RE}) is defined as the percentage ratio between the heat supplied by the recovery section and the total heat theoretically required to bring that unit of mass to the pasteurization temperature (the one required at the beginning of the holding tube).

Assuming the mass flow rate equal to the two extremes of the recovery section and realistically assuming that the specific heat of the product is independent of the temperature in the range considered, we can write an efficiency as a function of temperatures, rather than heat flows:

$$\eta_{\mathrm{RE}} = \frac{t_r - t_{in}}{t_p - t_{in}} \qquad (1)$$

where:

t_{in} = temperature at the inlet of the pasteurizer (°C)
t_r = temperature after recovery, before heating (°C)
t_p = pasteurization temperature (°C).

Recovery yields of 94% or higher are normal in modern plate pasteurizers. A 94% efficiency means that operating energy costs only 6% of what it would have cost without recovery. Obviously, a high yield lowers the operating cost, but high yields require large exchange surfaces (for example greater number of plates) in the regenerator. The increase in the surface increases a lot with the increase in efficiency for η_{RE} above 90%. In fact, if the temperature of the raw product entering the recuperator is very close to that of the

pasteurized product leaving the recovery unit (small ΔT), the quantity of heat exchanged over time is lowered. For example, to pass from a η_{RE} of 0.90 to one of 0.93, a 50% increase in the exchange surface is required. Therefore, if a high yield decreases operating costs, it increases investment costs. The recovery section is therefore very delicate and must be sized to obtain a balance of the two costs. The optimum is calculated on the basis of factors such as the inlet temperature of the product (t_{in}), the temperature of the cold water available, the relative costs of cold water, steam and refrigeration, maintenance costs and expected life of the exchanger. A further disadvantage in the high-performance system is that it has a low start-up speed to reach the operating temperature and the sterilization temperature during the washing phase. The problem is avoided by bypassing the regeneration section until the temperature has been reached, making sure to wash the recovery section first to avoid the cooking of the residual product. Some systems have an additional heating section, used only for cleaning, while in others preheated water is introduced.

The holding pipe is placed immediately downstream of the exchanger and keeps the product, in a continuous flow, at a fixed temperature and for a time not lower than the established ones. It consists of a number of straight sections mounted one above the other in a vertical plane. The sections are connected by 180° bends, which can be easily disassembled for inspection and cleaning. The straight sections are inclined upwards by about 1° to prevent the formation of air bubbles. The length of the pipe is defined as the distance between the beginning of the first straight section and the diversion valve, located at the highest point. The tube is neither heated nor cooled in any point, but at most isolated. In this case the temperature drop is negligible, but it can be greater than 2°C for an uninsulated pipe of 20 mm in diameter. The thermometer on the holding tube is mounted long before the diverter valves to compensate for the delay in opening which would otherwise allow a small amount of unpasteurized milk to pass before the valve has time to open. Such a problem would cause contamination of all the already pasteurized milk. The average residence time is given by:

$$t_m = \frac{L}{u_m} = \frac{L}{\frac{Q}{\pi r^2}} = \frac{L \pi r^2}{Q} = \frac{tube\ volume}{volumetric\ flow\ rate} \qquad (2)$$

where:

t_m = average holding time (s)
L = tube length (m)
u_m = average flow velocity (m/s)

r = inner radius of the tube (m)

However, it must be considered that viscosity creates a velocity profile in the pipe section, the shape of which depends on the type of flow, laminar or turbulent. The holding time must therefore be programmed so that the fastest element has a residence time greater than or equal to the desired one. This ensures that no point of the product remains under-pasteurized. The holding time is measured by injecting NaCl at the beginning of the tube and measuring the electrical conductivity at its end.

1.1.2.2 *STERILIZATION*

The purpose of sterilization is to allow the product to be stored for long periods at room temperature without danger of microbiological damage. The process must therefore be able to reduce the spores of thermophilic bacteria to acceptable levels. Sterilization can be done in two ways:

- Continuously - the product is processed in a continuous flow, then cooled and aseptically packaged. In the treatment of milk this process is called UHT and is equivalent to HTST pasteurization, but with higher temperatures and shorter times;
- In container - the product is treated after being hermetically packaged.

After or before the heat treatments, a homogenization treatment is very often necessary, which mainly serves to break any fat globules into much smaller particles (figure 5) in order to decrease the tendency of the globules to group or coalesce.

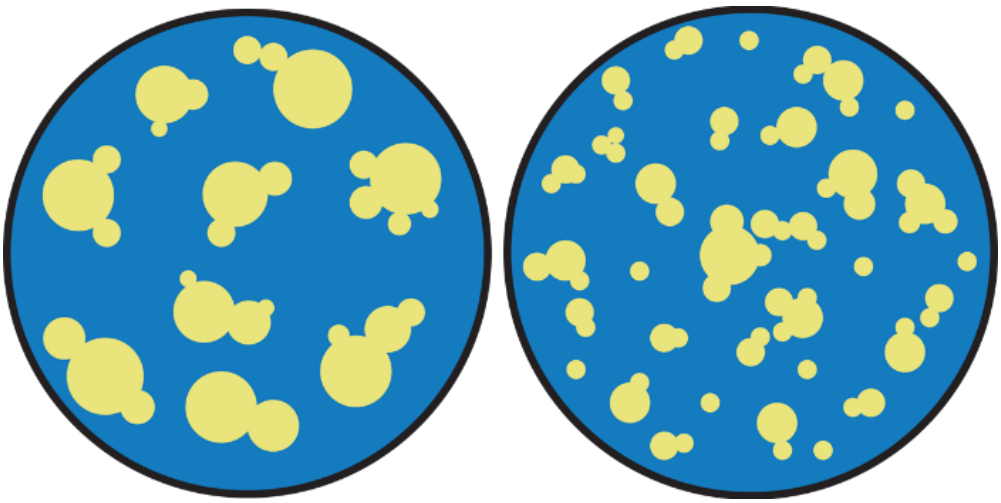

Figure 5 Fat globules reduced to smaller particles

The product is homogenized with a special mechanical equipment in which the liquid is forced through a small passage at high speed (figure 6). The disintegration of the original fat globules is achieved by the contribution of a combination of factors, in particular turbulence and cavitation. Homogenization reduces the size of the fat globule from an average of 3.5 µm in diameter to less than 1µm. This is accompanied by a four- to six-fold increase in the fat/plasma interfacial surface.

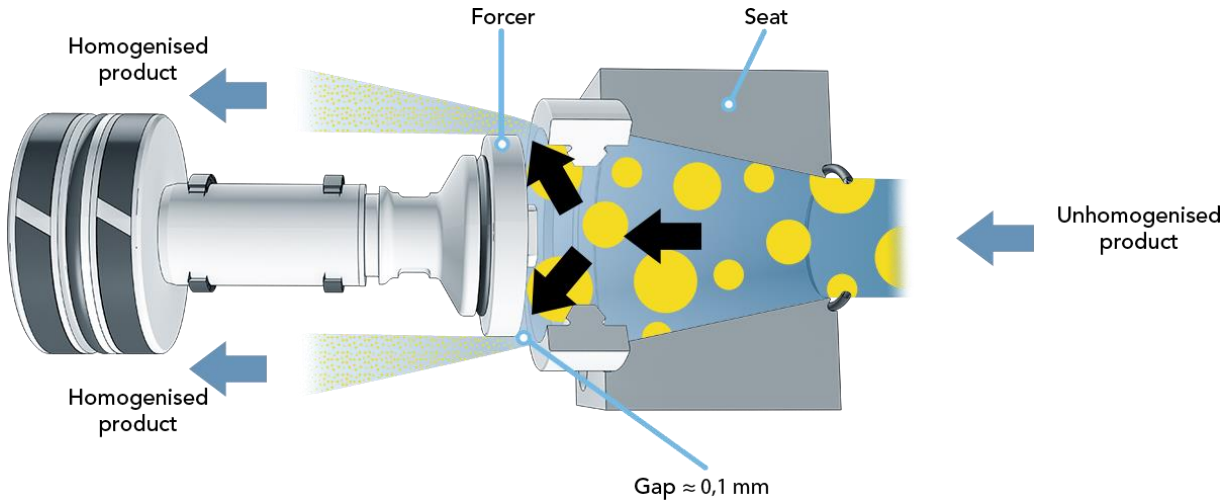

Figure 6 The liquid is forced through narrow openings where the fat globules are reduced into smaller particles

1.1.2.3 *DRYING*

Drying is an economically much more expensive process than other techniques for the preservation of food and non-food products, as it requires large amounts of energy. For this reason it is important to work in optimal conditions in order to limit energy consumption [11].

There are hundreds of different types of dryers, based on different principles, the most important are listed below:

- Production capacity (kg/h)
- Initial moisture concentration
- Particle size distribution
- Drying curve
- Maximum temperature to which the product can be exposed
- Toxicological properties of the product
- Isotherms of humidity

- Solubility of the solid in the liquid

- Contamination by drying gases

- Corrosion

- Physical properties of the materials involved

Table 2 shows the types of dryers most used depending on the nature of the product to be treated [12]:

Table 2 Dryer Selection versus feedstock form

Feed Nature	**Liquids**			**Free-Flowing Solids**					**Formed Solids**
	Solution	**Slurry**	**Pastes**	**Powder**	**Granule**	**Fragile Crystal**	**Pellet**	**Fiber**	
Convection Dryers									
Belt conveyer dryer					x	x	x	x	x
Flash dryer				x	x			x	
Fluid bed dryer	x	x		x	x		x		
Rotary dryer				X	x		x	x	
Spray dryer	x	x	x						
Tray dryer (batch)				x	x	x	x	x	x
Tray dryer (continuous)				x	x	x	x	x	
Conduction Dryers									
Drum dryer	x	x	x						
Steam jacket rotary dryer				x	x		x	x	
Steam tube rotary dryer				x	x		x	x	
Tray dryer (batch)				x	x	x	x	x	x
Tray dryer (continuous)				x	x	x	x	x	

1.1.3 REACTIONS INDUCED BY HEAT DURING THERMAL TREATMENTS

The action of high temperatures, sufficient to destroy microorganisms and inactivate enzymes, causes significant variations in the chemical, physical and organoleptic characteristics of the food. Some of these transformations are exploited to improve the characteristics of the product, but are generally undesirable. For example, one of the effects obtained through heat treatments is the coagulation of proteins: denaturation makes possible the metabolism of proteins by enzymes. As a result of denaturation, sulfhydryl groups are released, which give to the food the taste of cooked. If the heat treatment is prolonged, increase in viscosity, coagulation and precipitation occur. The nutritional value of proteins is also reduced by the Maillard reaction in which lysine is mainly involved, which is also the most sensitive to high temperatures. The functionality of proteins depends on the interactions between protein molecules and solvent (water), salts (ions) and other food components. The development of the structure of protein gels and the formation of stable emulsions and foams involve the protein-protein interaction. The speed and extent of the protein-protein interaction could affect water immobilization and fat stabilization and ultimately the texture of the final products [13].

However, as already mentioned, the thermal treatment processes have some undesirable effects. Among all, the destruction of the characteristics that attribute quality to food products is certainly one of the most relevant aspects. In particular, the loss of heat labile nutrients, such as vitamins B_1, B_{12} and C, is strongly dependent on the temperatures and the type of environment in which the heat treatments take place [14] and it is a very important aspect especially for foods with a high vitamin content such as fruit and vegetables. Furthermore, the appearance of undesirable colours or pigments is also of great importance for the sensory quality of food. Chemical changes in pigments such as carotene and chlorophyll are produced by the heat and oxidation that occurs during drying. In general, the longer the process and the higher the temperature, the greater the pigment losses [15]. Furthermore, the appearance of a browning following a heat treatment can not only alter the colour, but also the flavour, aroma and nutritional value of food products. Three mechanisms may be involved in the development of browning, namely the caramelization of sugar, the Maillard reaction and the oxidation of ascorbic acid. Heat-induced caramelization of sugars can occur in acidic or alkaline conditions and is associated with the production of flavours

with unique characteristics [16]. Some of these flavours have bitter or burnt notes. On the other hand, the Maillard reaction involving the condensation of amino groups with sugars can also contribute to serious problems during the processing and storage of food products, as well as lead to the formation of melanoidins, brown and high molecular weight compounds, resulting in a loss of nutritional value. The Maillard reaction has been extensively characterized and is strongly influenced by temperature, water activity and pH. Finally, the degradation of ascorbic acid is the main cause of the darkening of a number of products, including fruit juices and concentrates [11].

As for the changes in the texture of foods due to heat treatments, the most important are certainly originating from the gelatinization of starch, the crystallization of cellulose and internal tensions due to localized variations in humidity. For example, with heating the starch granules are gelatinized causing the destruction of the intermolecular hydrogen bonds, this destruction depends on the temperature, the water content and the duration and speed of heating [17]. Of course, the gelatinization process is also closely related to the initial structure of the starch: the greater the breakdown of the hydrogen bridges, the greater the moisture absorbed by the starch, until the network of starch micelles separates and spreads in the aqueous medium. This involves a decrease in viscosity and consequently a change in the initial texture of the food [18].

The internal tensions due to the viscosity variations generated by the aforementioned reactions generate cracks and compressions which manifest themselves as permanent alterations in the cells, giving them a rough appearance. The temperature and speed of dehydration have a great influence on the texture of the food and, in general, faster processes and higher temperatures cause more damages. The high temperature, in fact, causes profound physical and chemical alterations on the surface of the food, thus leading to the formation of a hard-impenetrable surface layer, which keeps the food dry on the surface but moist inside. Drying also causes some changes in the mechanical properties, structure, volume, porosity and density of foods [19].

All of these effects affect the overall quality of foods, their price and marketability.

Furthermore, heat treatments are usually food preservation processes that require the use of a lot of energy and long treatment times [20], [21].

In heat exchange equipment, when a food liquid comes into contact with a hot surface, some

of its components can deposit on the surface, causing an increase in resistance to heat transport. This phenomenon of increasing the thickness of the product on the exchange surface is called fouling. This effect is observed when a liquid is placed in contact with subcooled surfaces. Fouling on the heat exchange surfaces not only increases the thermal resistance but can also restrict the passage area to the liquid flow. Furthermore, noble components of the food liquid are lost in the deposited layer. Figure 7 shows what are the effects of fouling on the surfaces of the exchangers.

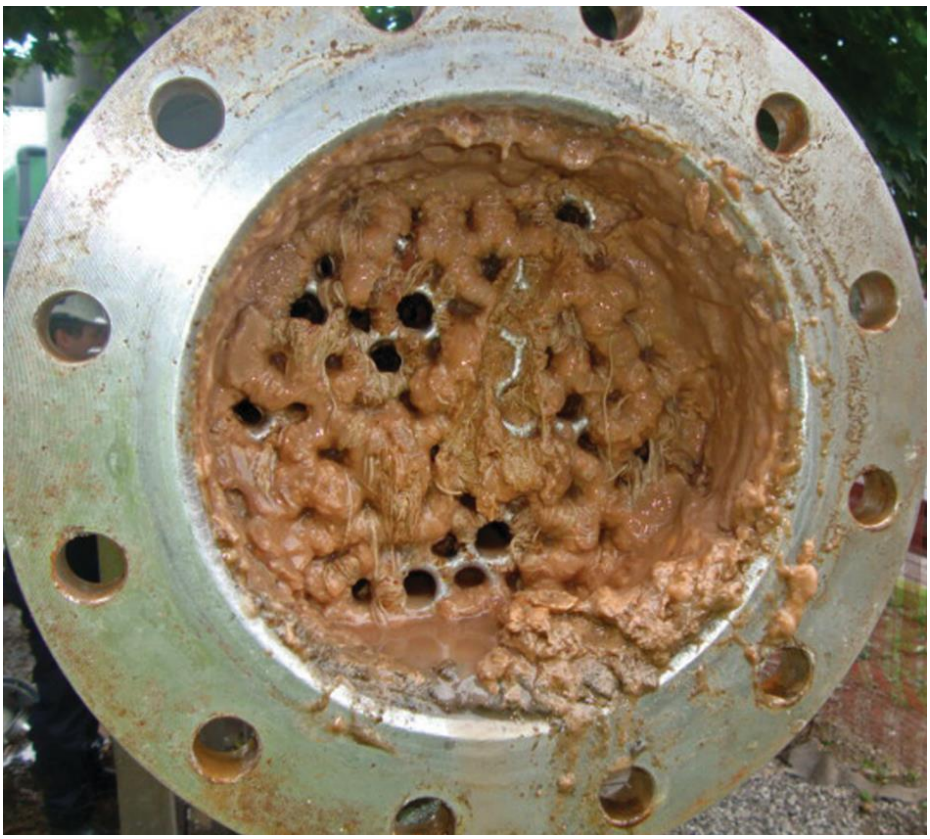

Figure 7 Effect of fouling on the exchange surfaces

The best remedy for the fouling phenomenon is to wash the exchange surfaces with very strong chemical agents, which are however also pollutants for the environment.

Fouling is a major problem in process chemistry. Its role is even stronger in the food industry, where many heat-sensitive components are treated that can deposit on the heat exchange surfaces. It is for this reason that process operations involving heating or cooling require frequent daily cleaning. Some of the most common types of fouling and their basic mechanism are highlighted in the table 3:

Table 3 Common fouling mechanisms on the surfaces of heat exchangers

Type of fouling	Dirt mechanism
Precipitation	Precipitation of dissolved substances. Salts such as $CaSO_4$ $CaCO_3$ cause fouling
Chemical reaction	The surface of the material behaves like a reactant; chemical reactions of proteins, sugars and fats
Particulate matter	Accumulation of fine particles suspended in the processed liquid on the exchange surface
Biological	Attachment of micro and macro organisms to the exchange surface
Freezing	Solidification of liquid components on subcooled surfaces
Corrosion	The exchange surfaces react with the environment and corrode

The deposit layer has a different composition than the liquid which causes fouling. Fouling deposits come from a series of complex reactions, and in the heating process these reactions are accelerated by temperature. To compensate the reduced heat transfer rate due to increased thermal resistance, a larger heat transfer surface is required, which increases the cost of heat exchange equipment. For a heat exchanger with a dirty surface, the reduced rate of heat transfer is compensated by using higher temperature gradients across the heat transfer medium. As a result, the energy requirement to operate the heat exchange equipment increases significantly.

1.2 INNOVATIVE TECHNOLOGIES: RADIO FREQUENCY AND MICROWAVE

The possibility of heating, sterilizing and drying materials using electricity has proved to be an exceptional discovery for our life, and has allowed to resolve delicate issues relating to the food sector and that of the production of material goods. Electric current can be used, for example, as a source for heating materials. This can be done both directly, when it is applied directly to the product (ohmic heating), and indirectly, when the electrical energy is converted into electromagnetic radiation that generates heat inside the product (microwave heating, MW, and radio frequencies, RF). These methods allow the material to be heated quickly and volumetrically, guaranteeing, into materials with suitable dielectric properties, the achievement of the predetermined temperature increase objectives, without altering its

fundamental characteristics (nutritional, mechanical, chemical, etc.). Electricity can also be used to sterilize materials without excessively increasing their temperature (Pulsed Electric Field Technology), minimizing the risk, in the case of foods, of compromising their nutritional and organoleptic characteristics.

New technologies have been developed in the field of the treatment of materials with electricity, which are strongly affecting the industrial and commercial world. The most used and effective are:

- Ohmic heating
- Pulsed Electric Field (PEF) technology
- Microwave heating
- Radio frequency

Among these, radiofrequency (RF) and microwave (MW) turn out to be ones of the most advantageous and effective. Radio frequency technology is one of the most promising technologies for the food processing industry. Previously used mainly in the telecommunications field, RF technology has expanded into other fields, including sterilization, pasteurization and drying of food, disinfestation of agro-food products, drying of wood, leather, paper; it is used in medical instruments and, more recently, it has been used for the extraction of nutraceuticals. Speed, efficiency, safety and convenience are some of the advantages offered by this system. Microwave heating applications are limited to a few frequency values for ISM applications in order to avoid interference with frequencies used for telecommunication purposes. Typical frequency ranges are 925∓25 MHz and 2450∓50 MHz, with penetration thickness varying between 3-8 cm at 2450 MHz and 8-22 cm at 915 MHz, depending on moisture content. In particular, in microwave ovens for domestic use frequencies of 2450 MHz are used. Microwave heating in food is due to the coupling of electrical energy of an electromagnetic field in a microwave cavity containing the food, the subsequent dissipation of thermal energy to the inside the product.

The fundamental relationships of dielectric heating are well known in the literature and to make this work smoother, they have been reported in Appendix I. These relationships are of a general and apply to both radio frequency and microwave fields.

Many studies have been conducted on dielectric properties of dry and wet food products in liquid, grain or flour form, such as raw cow milk [22], fruit juices [23], bean [24], flaxseeds [25], cereal grains [26], sunflower seeds [27], almond [28], legumes [29] and others. However, almost all of these studies aimed at measuring dielectric properties at specific or at narrow ranges of frequencies. Instead, in literature there are not many data regarding the dielectric properties of polymers and if there are, they are always limited to very narrow ranges or specific frequencies. This is because there is not much industrial interest in the use of radiofrequency or microwave technologies for heating or drying polymers, but rather in the use of specific polymers for the construction of components and equipment that induce electromagnetic fields and heating.

1.2.1 DIELECTRIC HEATING PROCESSES

The main sectors in which radio frequency or microwave technologies are starting to play a leading role are the heat treatment of food and the drying of materials. In the first case, it allows to extend the shelf-life of the product without particularly damaging its nutritional and organoleptic properties. In the second, dielectric heating technology solved the problem of drying materials that have water even in their innermost areas, a result that a simple flow of hot air that laps the material has enormous difficulty in reaching.

1.2.1.1 PASTEURIZATION AND STERILIZATION

As already mentioned, dielectric heating technology has found wide application in food pasteurization and sterilization processes. Compared with traditional techniques, it offers numerous advantages. In particular, this kind of technologies allow for rapid and volumetric heating, ensuring greater uniformity of heating between the outer surface and the central core of the material. Consequently, the risk of reaching excessive temperatures along the external surface of the material is also avoided, which can always cause loss of the nutritional value of the processed food. The advantages of a dielectric heating treatment, compared to a traditional treatment method, with all the problems related to it, are:

- Volumetric heating;
- Reduction of process times (figure 8);
- Uniformity of the temperature;
- The food can be processed directly inside the packaging;

• The nutritional and organoleptic properties are preserved;

• High level of control over the process;

• Fewer problems of fouling of the heat exchangers.

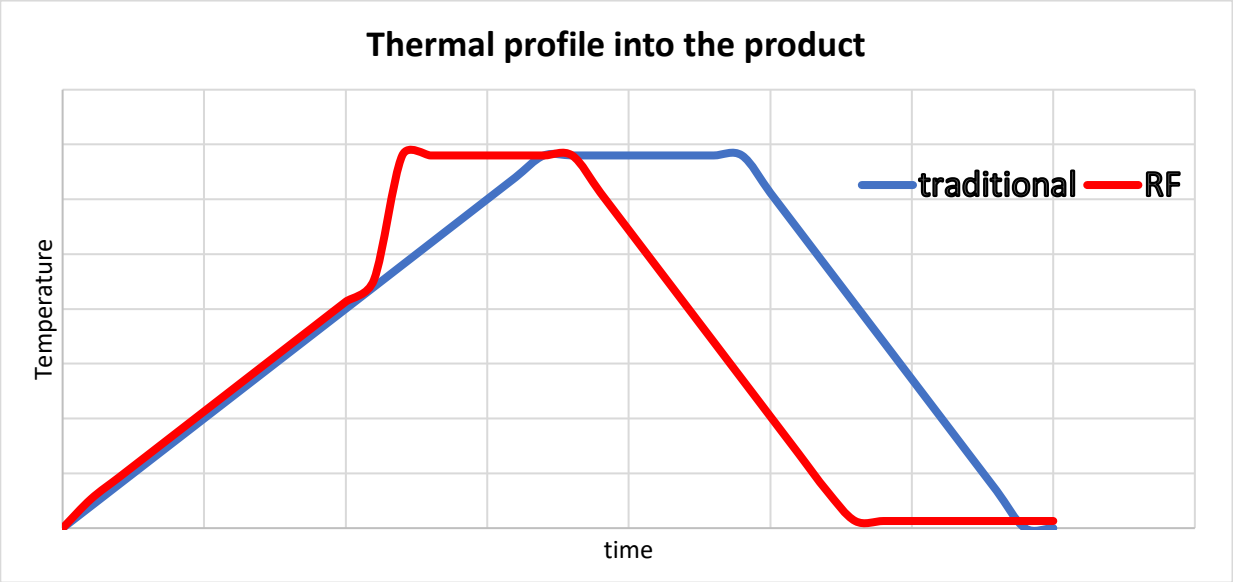

Figure 8 Comparison between the thermal profile of a traditional vs a radiofrequency pasteurization

For example, in figure 8, the thermal profiles inside the same product are shown in the case of a traditional heating and an innovative one with the use of the radiofrequency system. As is evident, the use of radio frequencies allows to reach the desired temperature much earlier than the traditional system. Both types of systems will be illustrated below in detail.

1.2.1.2 DRYING

The drying industry has also found important advantages in the use of dielectric heating technology. In fact, while some materials have moisture only on the external surface, and are therefore easily dried through the use of hot air flows, others absorb water even in their innermost areas. In these cases, the drying of the material becomes a really difficult problem to solve, and dielectric heating can play a fundamental role in its resolution. The use of dielectric drying can offer many benefits compared with conventional drying, including faster line speeds, more consistent moisture levels, lower drying temperatures, and smaller equipment. Conventional heating (for example, conduction, convection, conduction–convection, and radiant) has a heat source on the outside and relies on transferring the heat to the surface of the material and then conducting the heat to the middle of the material. Heating using RF or MW is different, as it heats at the molecular level and therefore heats

from within the material, raising the temperature in both the middle as well as the surface. A conventionally dried product is hot and dry on the outside and cold and wet on the inside due to external heat and internal mass transfer resistance across the material in and outward, respectively. This is not efficient, because the dry outer layer acts as an insulating barrier and reduces conductive heat transfer to the middle of the product. With dielectric drying, where the heating is from within, there is no hot, dry outer layer. Dielectric heating has great potential to get the center hot enough, because the energy penetrates evenly. Also, because the product is heated throughout, the water at the center is heated and moves to the surface. In general, because of the heat losses at the surface, RF-dried products are hot and dry on the inside and cooler and wetter on the outside [30]. The combination of two technologies, RF heating to heat the inside and move the water to the surface and conventional methods to remove the outside moisture, offers a great opportunity to overcome problems associated with heat and mass transfer [31].

1.2.2 DIELECTRIC TREATMENT PLANTS

Dielectric heating, whether it occurs with the use of radio frequencies or with microwaves, is governed by the same physical laws, which arise from the application of Maxwell's laws. What differentiates the two systems are the technical solutions that characterize each specific application. Dielectric heating takes place in a section of the materials treatment plant which can be schematized as shown in the figure 9:

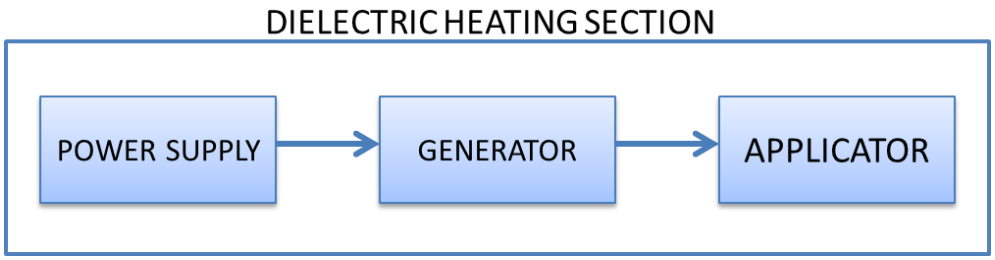

Figure 9 Block diagram of the dielectric heating section

Each block performs its specific task through dedicated components. The power supply section consists of an inverter, a power transformer, a rectifier circuit and an electrical panel (figure 10). The inverter is an electronic device directly connected to the 400 V industrial power grid, which, through PLC control, allows to adjust the value of the input voltage to the machine. The power transformer operates in alternating current and has the function of increasing the voltage value of the output current from the inverter. The rectifier circuit (Graetz bridge) transforms the input current from alternating to direct and sends it to the

generator, in particular to the anode. All these components are controlled by an electrical panel.

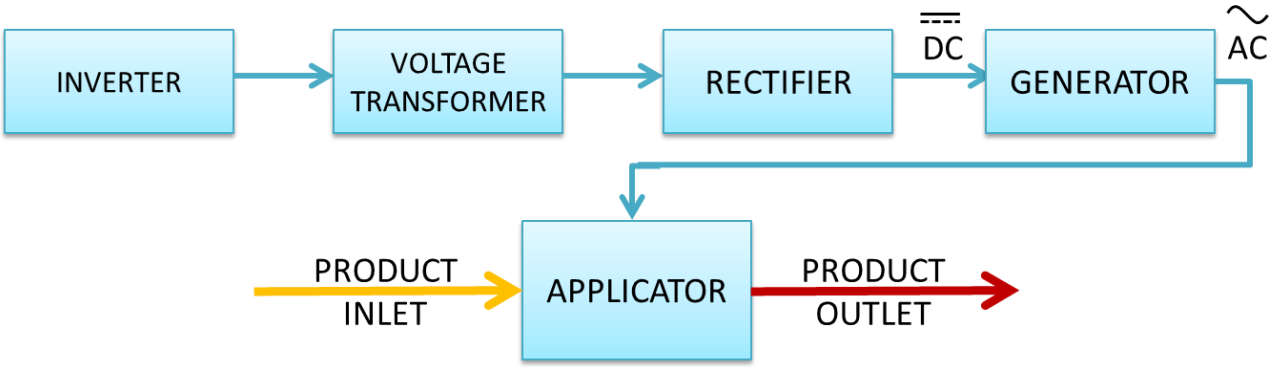

Figure 10 Block diagram of the main components of the dielectric heating section

The second block of the dielectric heating section is the generator that consists of three main components: triode (for RF technology) or the magnetron (for the MW system), LC oscillating circuit and the variable capacitor. The triode or the magnetron, as appropriate, is the key component of the generator.

The constructive simplicity of the RF generator, whose heart is the triode, is clearly superior to the MW one, generated by the magnetron. The RF, however, is effective only with regular geometries, while the MW are equally effective also on irregular geometries. Comparing the reliability costs and operating costs of microwave heating with respect to RF heating we must refer to the most expensive part: triode for radio frequencies, magnetron for microwaves. For the same kilowatts, the cost of an industrial triode is significantly lower than that of an industrial magnetron. In addition, the average life of the properly sized triode on a well-maintained RF heating system is approximately 20,000 hours (3 years or more), compared to a typical magnetron life of 3000-6000 hours [30]. The triode is the key component of the RF generator. It is powered by the rectifier circuit of the power supply section, and outputs a power signal that is alternated at high frequency. It is formed by a filament which acts as an anode (positive pole), a plate which acts as a cathode (negative pole) and a grid interposed between them (figure 11). These three components are kept under vacuum inside a tube or ampoule.

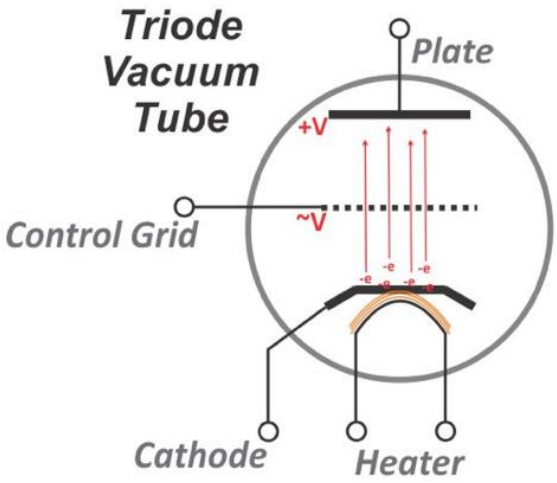

Figure 11 Triode scheme

Electrons are released by the thermionic effect from the cathode, which is heated by current flowing through a thin metal filament. In some triodes, the filament itself is the cathode, while in most cases the filament heats a separate cathode electrode. All the air is removed from the tube, in order to allow the electrons to move freely. Electrons are attracted to the positively charged plate (anode) and flow through the spaces between the grid wires, creating a current that can be through the tube from the cathode to the plate. The magnitude of this current can be controlled by a voltage applied between the cathode and the grid. A negative voltage on the grid will repel some of the electrons, so there will be fewer passes through the plate, resulting in reduced current. A positive voltage on the grid will instead attract more electrons from the cathode, so more electrons will reach the plate, increasing its current. Therefore, a low power signal applied to the grid can control a much more powerful plate current, resulting in amplification.

The magnetron, shown in figure 12, consists of a chamber with a circular section surrounded by lobes, in which the vacuum has been carried out, the structure of which constitutes the anode, with zero electric potential. In the center there is a wire kept incandescent, the cathode, and at a negative electric potential, constant or impulsive, very high compared to the anode. In the direction normal to the electric field, constituted between cathode and anode, a magnetic field produced by a permanent magnet is maintained. The filament and the cathode consist of a single electrode made of helical-shaped tungsten wire, with a number of turns varying between 8 and 12, with a radius approximately equal to the length. The cathode is coated with a material suitable for emitting electrons. The electrons emitted by the thermionic effect from the filament tend to move towards the walls of the chamber, kept at zero potential, which correspond to the anode. The presence of the magnetic field,

however, causes a curvature in their trajectory due to the Lorentz force, leading them to follow a cycloid path. On the perimeter of the room there are openings suitably spaced and communicating with cavities. The electrons, reaching the edge of the cavities, unite in beams that oscillate at radio frequency, depending on the size of the magnetron, due to the effect of the crossed fields (magnetic field and electric field). A part of this field is picked up by a loop, called pick-up, connected to a wave guide (a metal tube capable of conveying microwaves), and sent from this to the user load, whether it is a transmitting antenna, or the microwave chamber.

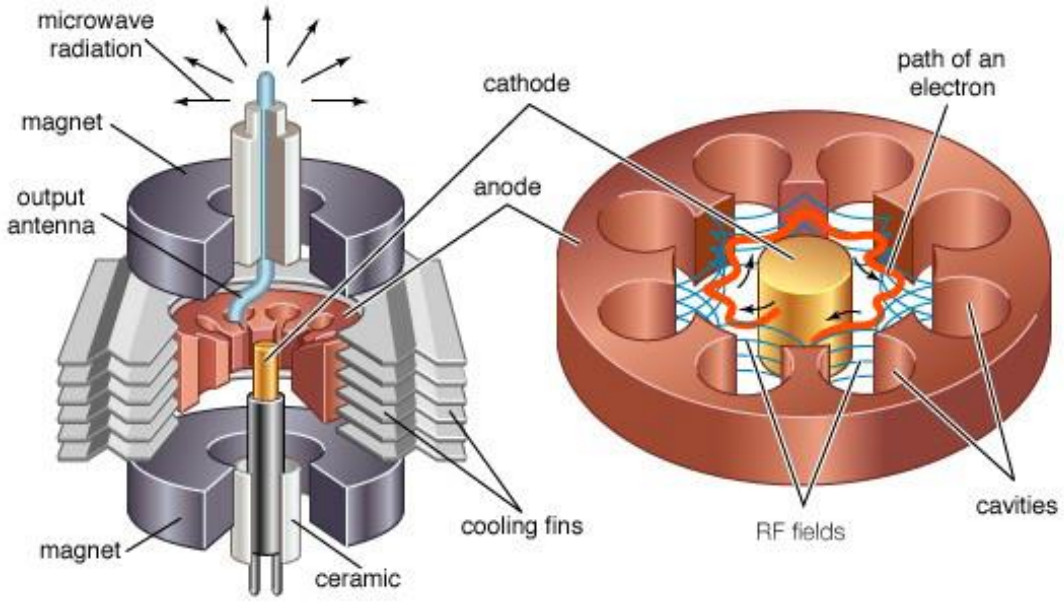

Figure 12 Magnetron scheme

The LC oscillating circuit is composed of an inductance and a capacitance in parallel. It provides an output signal at the operating frequency. This result is achieved by modulating the resonant frequency through the geometric characteristics of the capacitor and inductance, whose sizing is of fundamental importance in the design phase. Finally, the variable capacitor is arranged in series downstream of the oscillating circuit LC. Changing the distance between the plates or, what is the same, the thickness of the dielectric changes the frequency of oscillation. These adjustments can be made remotely via PLC; however, only slight changes, about 0.5-1 cm, can be made in order to improve the coupling, increasing the power and modifying only minimally the resonant frequency of the oscillating circuit (which must be as close as possible to the operating frequency).

All the components presented are cooled by a fan, which feeds air to a duct that reaches all parts of the power supply section and the generator.

It is very important to understand what is the best way to transfer energy by the generator of electromagnetic filed to the product. In order to ensure maximum transfer of electrical power from the generator to the applicator, it is necessary that the two impedances, the generator and the applicator, are equal to each other. For this reason, when designing a dielectric heating system, an automatic impedance matching system must always be provided, which controls the impedance of the applicator, making sure that this is always the same as that of the electromotive force generator.

The efficiency of the power transfer is determined, depending on the particular product, by the particular configuration of the electrode system. Modeling systems are currently available to allow designers to optimize the electrode system for a particular product. The configuration of the electrodes that make up the applicator is very different between systems that treat liquid material and systems that treat solids:

- Liquids

The applicators of the liquid treatment plants consist of an optimized configuration of electrodes that surround a U-shaped Teflon tube, into which the product flows continuously. The electrodes are perforated in the center and coaxial to the Teflon tube. Each of them is connected by a horizontal metal bar to the corresponding electrode placed on the contiguous Teflon branch, so that they are isopotential. Of the pairs of electrodes, some are connected to the generator and energized at the working frequency, others are grounded. The electrodes are in aluminium, the connections between them in copper. Parallel to each of the two vertical branches of the Teflon tube in which the product flows are installed two tubes filled with Teflon which act as an electrically insulated mechanical support. Other metallic mechanical seals are mounted at the upper and lower ends. The electrodes have the function of generating an electric field that flows in the Teflon tube, transparent to radio frequencies. The alternating electric field generates heat inside the material through the mechanisms presented in Appendix I. The applicator is located inside a steel compartment that acts as a mechanical support, as a screen for electromagnetic fields towards the external environment and as a closure of the electrical circuit to earth (figure 13).

Figure 13 Example of applicator of a liquid RF system

- Solids

The configurations mostly used in RF systems for solids or granular materials are basically of three types: the through-field or flat plate electrode configuration, the staggered configuration and the strayfield configuration.

a. Through-field or flat plate electrode

   The through-field electrode is the simplest type of electrode, as well as the first to have been used. It consists of two parallel plates, usually of aluminium, between which the material to be heated is placed (figure 14).

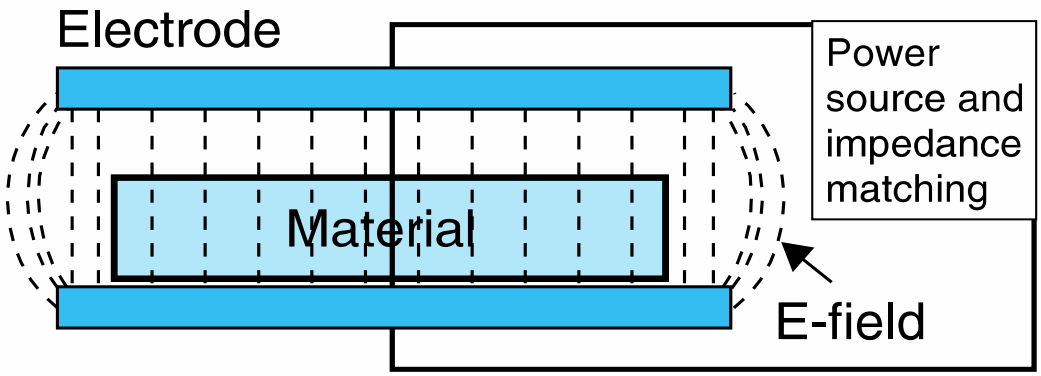

Figure 14 Through-field or flat plate electrode

This system is typically used for batch or continuous heat treatments, to process products of 10 mm or more in height, or product beds made from irregularly shaped pieces typically 5 mm or more in height [32].

b. Staggered electrode

The staggered electrode consists of a series of parallel bars arranged on two planes in a staggered way, a configuration that has proved convenient from the point of view of the uniformity of the distribution of the electric field along the material (figure 15).

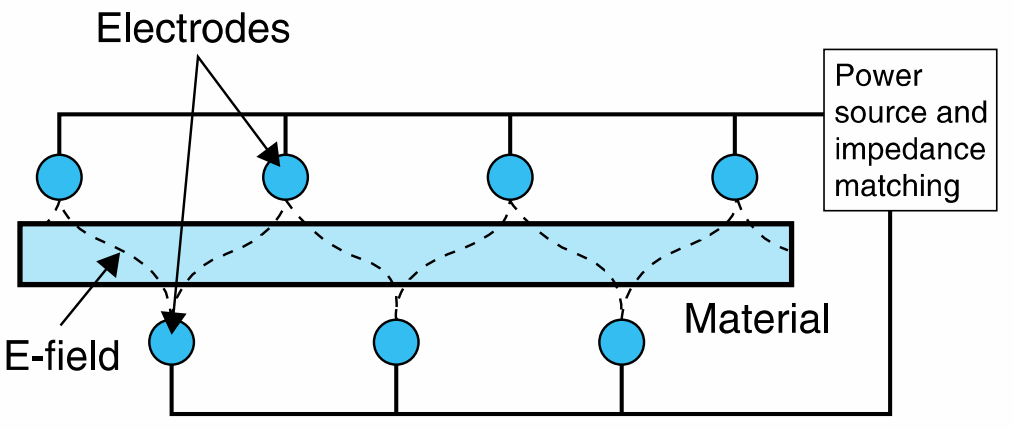

Figure 15 Staggered or rod electrode

This electrode system is generally used for the treatment of products having a thickness between 1mm and 6mm in monolayer. In this way, electromagnetic energy is transferred much more effectively, for the same product, compared to the through-field configuration [32].

c. Strayfield electrode

In case you want to heat very thin products (for example <1 mm thick), a third type of electrode system is available, known as strayfield or fringe-field (figure 16).

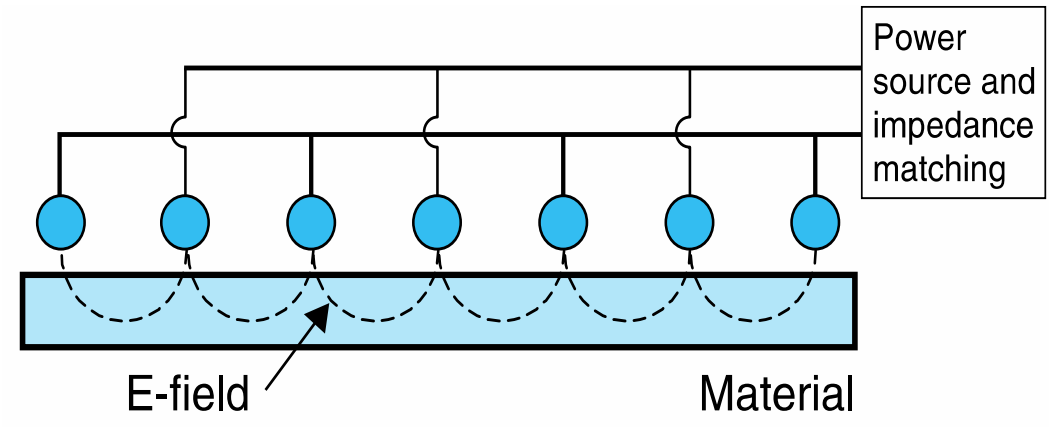

Figure 16 Strayfield or fringe-field electrode

Compared to those presented previously, which had different polarities on two opposite sides with respect to a plane passing through the product to be treated, this system provides for the presence of both polarities of the electrode above (or below) the sample. Figures 17a) and 17b) show how the electric field between the rods is transferred to the product:

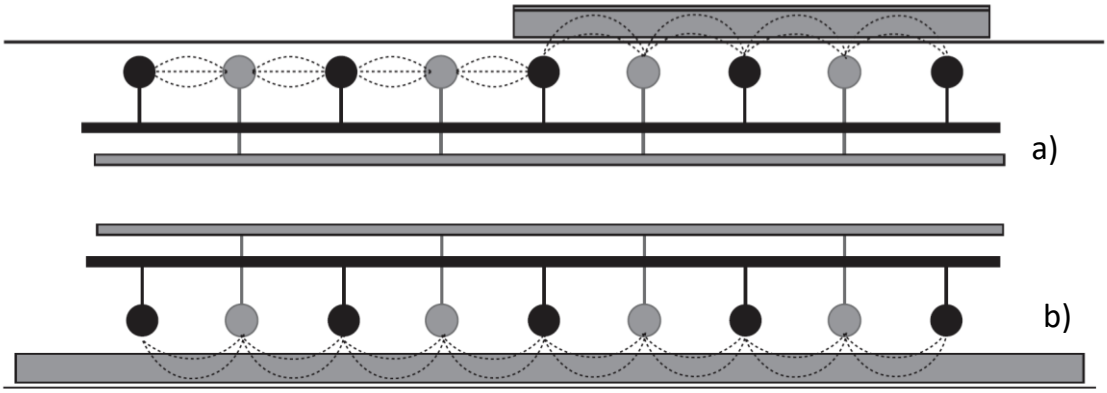

Figure 17 a) Strayfield and b) inverted strayfield electrode

This system is normally found in dryers used for water-based coatings on paper, but it can be safely used for applications on food, for example those in which only drying or heating of the surface is desired [32].

Microwave heating applicators fall into three broad categories: multimode resonant, single-mode resonant, and traveling wave applicators. By far the most widely used is the multimode resonant cavities applicator. A mode corresponds to a fixed field pattern within a metal cavity at a specific resonant frequency. A multimode cavity is typically rectangular in shape, with large-enough dimensions to sustain many different modes over the frequency spectrum of the magnetron. The familiar domestic microwave oven is an example of a multimode applicator. Most industrial microwave systems are simply a scaled-up version of the domestic microwave oven; however, besides being larger and more powerful than its domestic counterparts, industrial microwave systems have open ends to allow products to move from one end to the other on a conveyor belt. Because the frequency range of a magnetron can excite multiple modes in large cavities, those multimode cavities are generally considered to provide relatively good uniform heating. Since each mode has its own specific heating pattern, in particular hot and cold regions, and there are many modes with their own distinct patterns, the overall combined pattern tends to be better than an applicator with a single mode [33]. A domestic microwave oven either uses a rotary metal mode stirrer at the top of the cavity to change field patterns or a rotary turntable to move foods through field patterns to improve

heating uniformity. Similarly, mode stirrers and/or conveyor belts are used in multimode microwave tunnels in industrial systems (figure 18).

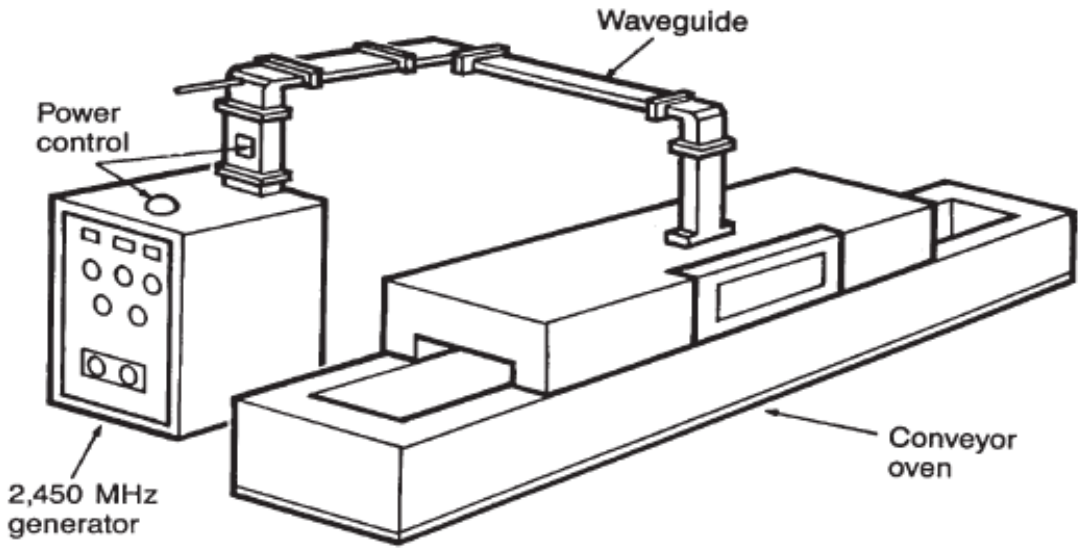

Figure 18 A multimode 2450 MHz industrial microwave system

Unlike multimode cavities, a single-mode cavity, as its name implies, can sustain only one mode. The advantage of a single-mode cavity is that the heating pattern is well defined within the frequency range of the magnetron. The most common mode used for a cylindrical cavity is the TM_{010}, which has a uniform electric field along its cylindrical axis [33]. An example of a single-mode cavity is shown in figure 19. A piece of rectangular waveguide is excited at one end and shorted at the other. A plunger is used to tune the system so that optimum power is coupled to the load.

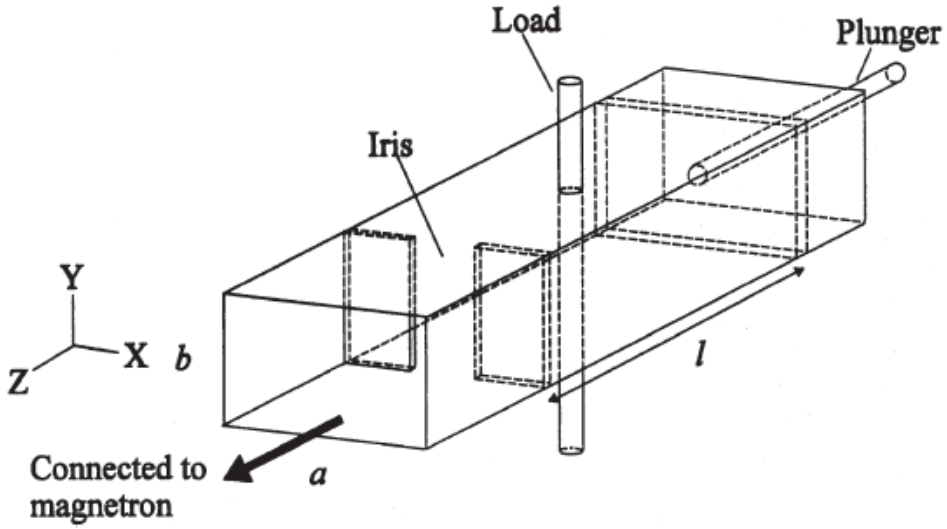

Figure 19 A single-mode cavity system

By matching a source to a load, a traveling wave is produced. Figure 20 shows an example of travel wave applicator for drying sheet materials such as paper:

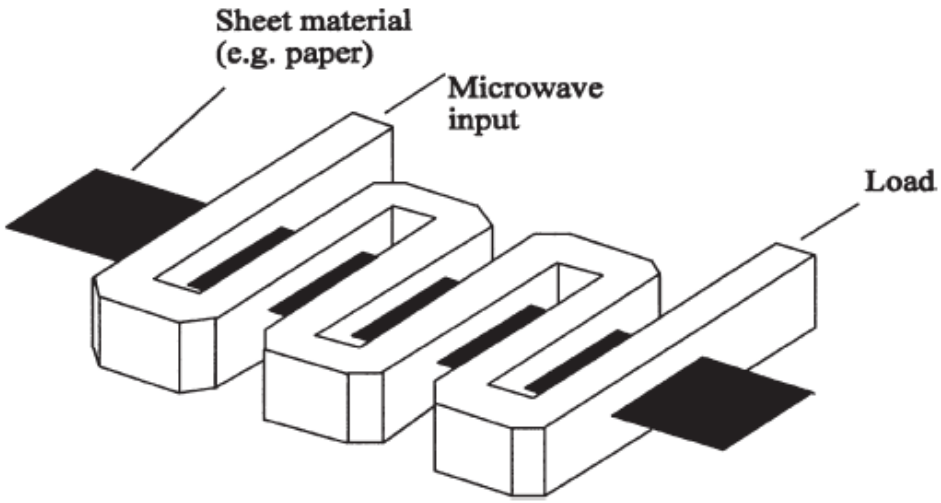

Figure 20 Travel wave applicator for heating sheet material

Generally, the design of the product transport system depends on the type of product and process. However, some rules are common to all transport systems [30]:

• The conveyor belt must be inert with respect to the absorption of electromagnetic energy

• Any joint present must be inert to electromagnetic absorption, otherwise it can fail. Joints in metal and materials with high loss factors should be avoided.

• The conveyor belt must always be equipped with an automatic system that blocks the delivery of electromagnetic energy whenever the conveyor belt breaks or becomes blocked. This avoids the risk of fires due to the continuous heating of a by now dry product.

Design approaches and methodologies may vary depending on the particular electrode system used for heating the material of interest.

Major generator cooling systems use air, water, or a combination of the two. The simpler low-power systems are often air-cooled. The efficiency of the air flow through a dielectric heating generator that works continuously is of vital importance for the reliability of the system. Unfortunately, it is a fact that in the industry, especially due to dust and other contaminants, air cooling systems are inefficient, due to the rapid clogging of the filters. Generally, machines with capacities greater than 25 KW must be water-cooled to be efficient. A well-designed machine must include demineralized water, to prevent clogging of pipes and other parts of the system. In addition, demineralized water has a very low conductivity, a fundamental feature to prevent this from negatively affecting the efficiency of the product's absorption of electromagnetic energy. A good flow and temperature control system of the cooling water is

also essential, in order to avoid temperatures that are too high but also too low, which can cause condensation of the water itself, with the risk of corroding the equipment.

2. AIM OF THE THESIS

The purpose of this PhD thesis is to collect different data regarding the dielectric properties of a wide range of materials, liquids and solids, of food and non-food origin in a wide spectrum of frequencies and in particular focusing on the frequencies used for industrial treatments, that are 27.12 MHz for radio frequencies and 2.45 GHz for microwaves. Furthermore, while testing liquid products is relatively simple, this is not the case for solid materials. Therefore, another fundamental objective of my studies was to formulate a unique measurement protocol for solid and granular materials, which would guarantee the reproducibility of the measurements and which would allow to easily determine the dielectric properties of the aforementioned materials both in the radio frequency range than in the microwave one.

Finally, simulations were conducted with the use of the COMSOL Multiphysics® software using the data produced by the measurements of the dielectric properties of the water and milk to obtain a prediction model of the heating reached using an RF treatment system for liquids.

3. MATERIALS

The activities carried out in this thesis work can be divided according to the type of materials analysed. In particular, the following products were considered:

1. Reference material: water
2. Food products
3. Polymers

The materials and methods used for each activity will be presented in the next paragraphs.

3.1 REFERENCE MATERIAL: WATER

Water was used as a reference material both for the setup of the different systems used for the measurements that will be illustrated in detail below, and as a control material for the goodness of the data, as all the properties of water, including the dielectric properties, are well documented in the literature. In particular, since the characteristics of tap water may vary depending on the geographical location, we chosen to use bottled water with the following chemical-physical characteristics:

Table 4 Chemical-physical properties of bottled water

Chemical - Physical Properties	
Specific electrical conductivity at 20°C [µS/cm]	668
pH at the temperature of the water at the source	7.06
Free carbon dioxide at source [mg/L]	50
Fixed residue at 180°C [mg/L]	440

Table 5 also shows the concentrations of the dissolved elements:

Table 5 Chemical-physical properties of bottled water

Dissolved Elements [mg/L]	
Calcium	124
Magnesium	29.8
Sodium	4
Potassium	1.2
Bicarbonates	498
Sulphates	17.6
Chlorides	6.6
Nitrates	2
Nitrites	< 0.002

3.2 FOOD PRODUCTS

The food products analysed are of different nature and chemical composition, so they have been divided as follows:

- Liquid materials
- Fluid materials
- Solid materials

3.2.1 LIQUID MATERIALS

The first group of materials includes liquid food and in particular:

- Raw milk
- Almond milk
- Fruit juices

3.2.1.1 *RAW MILK*

Milk is the complete and indispensable food of the offspring of mammals in the first period of life. Biologically, milk is the product of the secretion of the mammary glands of female mammals, intended for feeding the young. It appears as an opalescent white liquid, with a characteristic smell and sweetish taste. Being a food with high nutritional value and high biological value, milk is an essential component of a healthy diet for all age groups. To date, it represents one of the main protein food sources for humanity. In particular, cow's milk has been one of the cornerstones of human nutrition since historical times; consequently, it is the subject of intense scientific and industrial research.

Cow's milk that has not undergone any type of treatment is defined as "raw", such as, for example, freshly milked milk shown in figure 21:

Figure 21 Raw milk

Milk is a complex multi-component system. It is mainly made up of water, carbohydrates (mostly lactose), lipids, proteins (mainly casein) and a small part of mineral substances and organic acids, non-protein nitrogenous substances (NPN), vitamins, gases and microelements, as shown in the table 6:

Table 6 Raw milk composition

	Composition (%)				
	Water	**Carbohydrates**	**Lipids**	**Proteins**	**Minerals & others**
Raw Milk	87.5	4.9	3.5	3.1	1

Milk is formed by an aqueous phase in which are dispersed:

- Carbohydrates in solution;
- Proteins, mainly casein micelles, in a colloidal state;
- Lipids, in the form of droplets, in emulsion;
- Minerals, vitamins and enzymes.

As regards food safety, the CE Regulation 853/2004 authorizes the marketing of raw milk for direct human consumption and establishes that each state can decide to prohibit or regulate the sale. In Italy, the State Regions Conference of 25 January 2007 regulates the trade of raw milk and defines the microbiological/hygienic criteria for production. 'Raw milk' must be

clearly stated on the label. The direct sale of raw milk is a rapidly expanding phenomenon. The milk from the stable is filtered and refrigerated, that is brought to a temperature between 0 and 4°C and then distributed through self-service vending machines. The bottles can be found on site or brought from home. It does not undergo any heat treatment (pasteurization or sterilization), nor homogenization; it is therefore consumed naturally. From the point of view of taste, it is rich in non-homogenized fat, therefore tastier than packaged milk, furthermore the nutritional qualities of this milk are undoubted, as it does not undergo any decay of the thermosensitive substances present.

3.2.1.2 *ALMOND MILK*

Two types of almond milk were tested:

- Almond milk

Almond milk is made by blending almonds with water and then straining the mixture to remove the solids. It has a pleasant, nutty flavour and a creamy texture similar to that of regular milk. For this reason, it is a popular choice for people following a vegan diet and those who are dairy allergic or intolerant to lactose.

During processing, almonds and water are blended and then strained to remove pulp. This leaves a smooth liquid. In most commercial almond milks, thickeners, preservatives, and flavourings are usually added to improve flavour, texture, and shelf life. The concentration of nutrients in almond milk depends on how many almonds went into making it, the amount of added water it contains, and whether or not it contains any added vitamins and minerals. Almond milk is an excellent and natural source of vitamin E, which is a fat-soluble antioxidant that helps protect the body from free radical damage. Some varieties are fortified with calcium and vitamin D, which are important nutrients for bones health.

Figure 22 Hawaiki almond milk

The tested almond milk (figure 22) was bought in a local supermarket and kept at a temperature of 4°C, it is mainly made up of water, carbohydrates, lipids and proteins as shown in table 7:

Table 7 Almond milk composition

	Composition (%)				
	Water	**Carbohydrates**	**Lipids**	**Proteins**	**Minerals & others**
Almond Milk	85.6	10.5	2.6	0.8	0.5

- Organic almond milk

Organic almond milk differs from the previous one because there are no added substances to improve its flavours or nutritional properties.

Figure 23 Milbona organic almond milk

The tested sample (figure 23) was bought in a local supermarket and kept at a temperature of 4°C and is composed as follows (table 8):

Table 8 Organic almond milk composition

	Composition (%)				
	Water	**Carbohydrates**	**Lipids**	**Proteins**	**Minerals & others**
Organic Almond Milk	92.3	6.0	1.0	0.3	0.4

3.2.1.3 FRUIT JUICES

Fruit juices are popular beverages worldwide. Fruits are widely recognized sources of a significant number of beneficial nutrients including vitamins, minerals, phytochemicals, and dietary fiber that have been associated with lower risks of cardiovascular disease and obesity. For children and adolescents aged 2–18 years, it is recommending a daily fruit intake of 1–2 cups depending on age, sex, and physical activity level. However, most children (particularly after the preschool years) still fail to consume the recommended amount of total fruit per day. The role of 100% fruit juices in total fruit intake amongst children, especially younger children, continues to be controversial. After 1 year of age, fruit juices may comprise up to half of the recommended total daily fruit intake but intakes among 1 to 3-year old children should be limited to 110 g per day and among those 4 to 6 years of age to 110–170 g per day [34].

Figure 24 Zuegg a) Cranberry b) Pomegranate c) Pear juices

In particular, three types of fruit juices (figure 24) were considered for the evaluation of the dielectric properties. They were bought in a local supermarket and their compositions are summarized in table 9:

Table 9 Composition of the tested fruit juices

	Composition (%)				
	Water	**Carbohydrates**	**Lipids**	**Proteins**	**Minerals & others**
Cranberry juice	84.69	14.56	0	0.14	0.61
Pomegranate juice	84.74	15.0	0	0.16	0.1
Pear juice	91.84	7.5	0	0.12	0.54

3.2.2 FLUID MATERIALS

This category includes fluid food materials (neither liquid nor solid):

- Purees
- Ice cream preparations

3.2.2.1 PUREES

For this group of materials, fruit purees with and without pieces were taken into account and in particular strawberry and peach purees (figure 25) are tested with and without pieces.

Figure 25 Peach puree a) without pieces and b) with pieces

The purees were provided by Officine di Cartigliano and their compositions are reported in table 10:

Table 10 Strawberry and peach puree compositions

	Composition (%)				
	Water	**Carbohydrates**	**Lipids**	**Proteins**	**Minerals & others**
Strawberry puree	82.03	14.43	0.36	1.08	2.1
Peach puree	87.24	10.2	0.21	0.87	1.48

3.2.2.2 ICE CREAM PREPARATIONS

For this category, different ice cream preparations are provided by Officine di Cartigliano and their compositions are reported in the following table:

Table 11 Composition of different ice cream preparations

	Composition (%)				
	Water	**Carbohydrates**	**Lipids**	**Proteins**	**Minerals & others**
Black Cherry	59.8	21.9	10.8	2.9	4.6
Fig	55.8	25.7	14.1	2.4	2.0
Strawberry	58.6	22.1	12.3	3.4	3.6
Wild Strawberries	57.9	22.2	11.8	3.3	4.8
Wild Berry	59.5	21.0	10.5	4.1	4.9
Pineapple Jelly	25.7	61.3	5.9	3.8	3.3
Toffee Milk topping	36.0	53.6	8.9	0.3	1.2
Bourbon Vanilla	61.1	23.3	8.4	2.7	4.5
VQS Strawberry	58.3	22.8	11.7	3.1	4.1
Eggnog	61.4	20.3	12.6	4.2	1.5

3.2.3 SOLID MATERIALS

This category includes granular solid food materials and the considered products are the following:

- Sunflower seeds
- Flax seeds

3.2.3.1 SUNFLOWER SEEDS

Sunflower seeds (figure 26) were bought in a local market and their composition is shown in table 12:

Figure 26 Sunflower seeds

Table 12 Sunflower seeds composition

	Composition (%)				
	Water	**Carbohydrates**	**Lipids**	**Proteins**	**Minerals & others**
Sunflower seeds	1.18	23.32	55.2	17.28	3.02
Almonds	5.61	21.35	48.93	21.15	2.96

3.2.3.2 FLAX SEEDS

Also flax seeds (figure 27) were bought in a local market and their composition is reported in the table 13:

Figure 27 Flax seeds

Table 13 Almonds composition

	Composition (%)				
	Water	**Carbohydrates**	**Lipids**	**Proteins**	**Minerals & others**
Flax seeds	6.55	31.88	42.16	17.29	2.32

3.3 POLYMERS

For the polymers' category, many types of polymers are considered. The first tested was Nylon 6,6. It was bought from Rgpballs S.r.l. in the form of spheroids of different sizes and in particular samples with a diameter of 2 mm, 4 mm (figure 28), 1 cm and 2.5 cm are selected.

Figure 28 4mm Nylon 6,6 spheres

4. METHODS

The activities carried out in this thesis work can be divided into three parts:

1. Measurement of dielectric properties. As said previously, these properties are of fundamental importance both for the understanding of the phenomenon and for the computer modeling of the dielectric heating process;
2. Laboratory scale heating systems. These systems allowed us to simulate dielectric heating in the laboratory;
3. FEM simulation of the RF heating process, in order to obtain a prediction of radio-frequency heating based on laboratory results.

The methods used for each activity will be presented in the next paragraphs.

4.1 SYSTEMS FOR MEASURING DIELECTRIC PROPERTIES

The dielectric properties of the products of interest were measured using a system consisting of an apparatus for measuring the dielectric properties. These measurements are of fundamental importance for the understanding and modeling of the physical phenomenon.

The dielectric properties measuring system (figure 29) consists of three main components:

- the E4991B impedance analyser with the Option 010 probe connection kit (Keysight Technologies, Microlease s.r.l, Milan, Italy);
- the N1501A coaxial probe (Keysight Technologies, Microlease s.r.l, Milan, Italy);
- software for processing permittivity measurements, installed on an external PC, directly connected to the analyser.

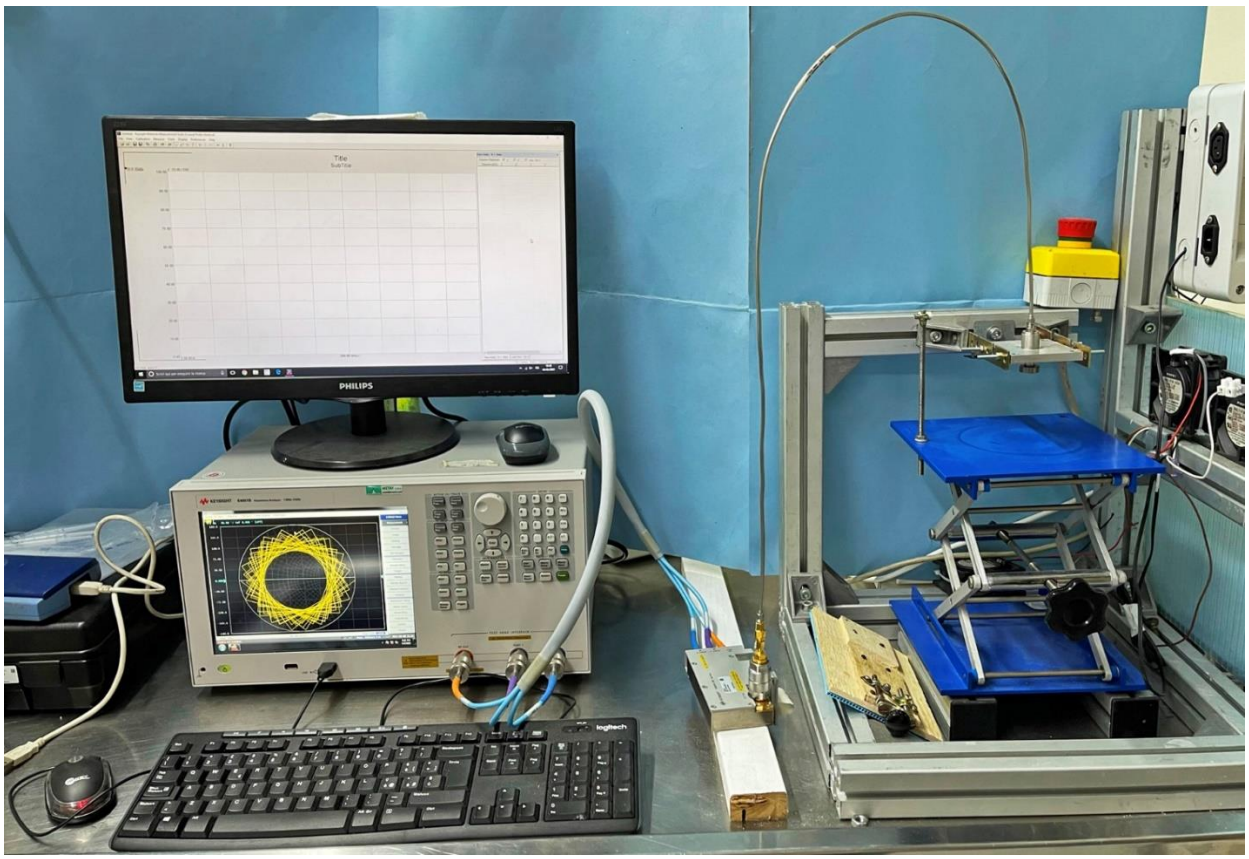

Figure 29 Dielectric heating measuring system

The impedance analyser E4991B with the Option 010 probe connection kit (figure 30) has a frequency range spreading from 1 MHz to 3 GHz. It allows to evaluate the permittivity and the loss tangent of various materials using a semi-rigid cable connected to the probe.

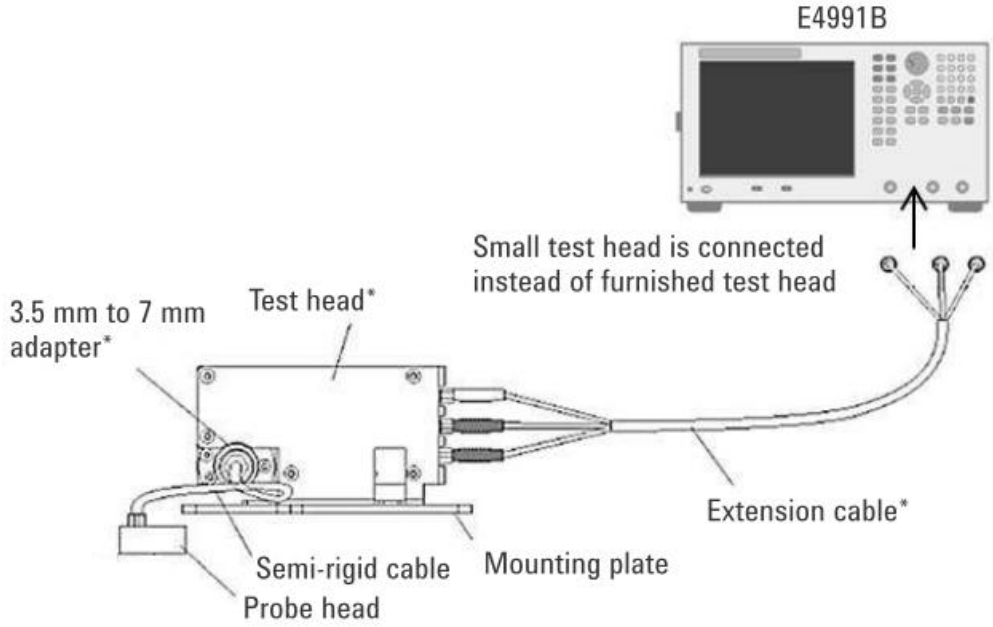

Figure 30 Connection diagram of the impedance analyser with the coaxial probe connection kit

Specific probes are commonly used for dielectric parameters characterization: the three most popular methods are: open-ended coaxial probe, transmission line and resonant cavity method. The probe method is based on a coaxial line ending abruptly at the tip that is in contact with the material being tested. The probe method is the easiest to use because it does not require a particular sample shape or special containers and allows measurements in a wide range of frequencies that spreads from 1 MHz to 3 GHz. The only flaw of the use of this method is that it requires perfect contact between the probe surface and the sample surface. Therefore, there is difficulty pairing the probe with a granular matrix. High temperature probe characteristics are reported in table 14:

Table 14 High temperature probe characteristics

Frequency Range (nominal)	10 MHz to 3 GHz
Temperature range	–40 to +200 °C
Temperature slew rate	< 10 degrees/minute
Immersible length (approximate)	35 mm
Connector	3.5 mm male
Repeatability and resolution	Two to four times better than accuracy
Material Under Test (assumptions)	Material is “infinite” in size, non-magnetic, isotropic, and homogeneous. Solids have a single, smooth, flat surface with gap-free contact at the probe face.
Sample size (requirements)	Diameter: > 20 mm Thickness: $\frac{20}{\sqrt{\lvert\varepsilon_r^*\rvert}}$ mm Granule size: < 0.3 mm

Expected Value (requirements)	Maximum recommended $\varepsilon_r' < 100$ Minimum recommended loss tangent > 0.05
Accuracy	Dielectric constant, $\varepsilon_r' = \varepsilon_r'$ ± 0.05 $\lvert\varepsilon_r^*\rvert \cdot \varepsilon_r'' = \varepsilon_r''$ ± 0.05 $\lvert\varepsilon_r^*\rvert$

One of the most important properties of the high temperature probe is the range of frequencies which allows to investigate which, although very wide, involves measurement problems in the radio frequency range, as it is very close to the lower limit of the measurement scale. These difficulties are clearly visible especially with materials that have poor dielectric properties and manifest themselves with a wave pattern of the curves representing the dielectric constant and the loss factor.

The probe head (connector) of the Option 010 connection kit of the impedance analyser must always be calibrated before and sometimes even during a prolonged measurement session. The known standards used in calibration are:

- Open (figure 31a);
- Short (figure 31b);
- 50 Ω Load (figure 31c);
- Low loss capacitor (figure 31d).

a) b)

c) d)

Figure 31 Standards used for probe head calibration

On the screen of the impedance analyser (figure 29), it is possible to evaluate the goodness of the calibration on a Smith chart.

The coaxial probe (figure 32) is connected to the impedance analyser test head using a semi-rigid connection cable. The coaxial probe is comparable to a cutting section of a transmission line.

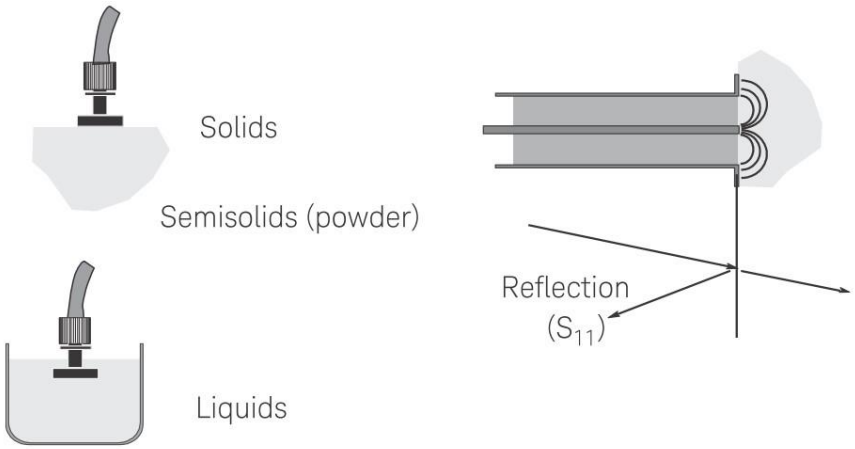

Figure 32 Coaxial probe measurement method

Material properties are measured by immersing the probe in liquid or by contacting the flat face of a solid or granular material. The fields at the end of the probe enter the material and change as they pass through it. The reflected signal s_{11} can be measured and correlated to equation $\varepsilon_r = \varepsilon_r' - j\varepsilon_r''$ ((A-8)). For this reason, it is absolutely necessary that the probe is in perfect contact with the surface of the material to be measured.

The probe (figure 33a) is equipped with a glass-to-metal hermetic seal, which makes it resistant to corrosive or abrasive chemicals and is called “high temperature” because it is able to withstand a range between -40°C to +200°C, which allows measurements as a function of frequency and temperature. Before the measurement, the probe tip must be calibrated. It is necessary to correct for directivity, tracking and source errors that can manifest themselves in a measure of reflection. To resolve these three types of errors, three well-known standards are measured. The difference between the expected and measured values is used to remove the systematic error (therefore repeatable). The three known standards are:

- Air (open type calibration);
- Short circuit (short type calibration, figure 33b);
- Distilled and de-ionized water (load type calibration).

Figure 33 High temperature probe a) and shorting block b) for calibration

The water temperature affects the dielectric properties and must be entered in the software before starting the calibration. There are additional sources of errors that can undermine the accuracy of the measurement, even after calibration. The three main ones are:

- Cable stability;
- Air gaps;
- Thickness of the sample.

The frequency range investigated in the measurements is between 1 MHz to 3 GHz, and the dielectric properties were measured on 500 linearly spaced points. This range includes the frequency of interest used in radio frequency (27.12 ± 0.16272 MHz) and the microwave-based ISM applications (2450∓50 MHz). The computer and proprietary software are used to control the system and save the data.

4.2 LABORATORY SCALE TREATMENT SYSTEMS

Since it was not possible to use a laboratory-scale radiofrequency heating system, a conductive heating system was built that simulated as much as possible the heating rate of

an industrial electromagnetic system. The measurement of the dielectric properties of the chosen materials were carried out in two different treatment systems:

- Continuous system
- Static system

In the following paragraphs, the two systems will be described in detail.

4.2.1 CONTINUOUS SYSTEM

The measurements of the dielectric properties of the liquid products were carried out under flow conditions, with the use of a closed system in which, once loaded, the liquid recirculates continuously at a settable speed and temperature (figure 34):

Figure 34 Liquid flow system with adjustable temperature

The system is insulated with insulating materials in order to reduce as much as possible the dispersion of heat along the pipes and surfaces of the tank.

As can be seen in the scheme of figure 35, the probe is placed on the bottom of a cylindrical tank and is completely in contact with the liquid. The product is loaded through an opening from above (figure 35, the green arrow). Once filled with liquid, the system is set in motion by a MARCO UP 12/OIL 24 V pump, controlled by a voltage generator that allows to modulate the flow rate. The liquid is then pumped into the measuring system, crossing it from bottom

to top (blue arrows in figure 35). At the same time, it is possible to start the heating system, consisting of a series of flexible silicone heaters placed on the lateral surface of the tank and regulated by an electrical cabinet that allows to choose the temperature.

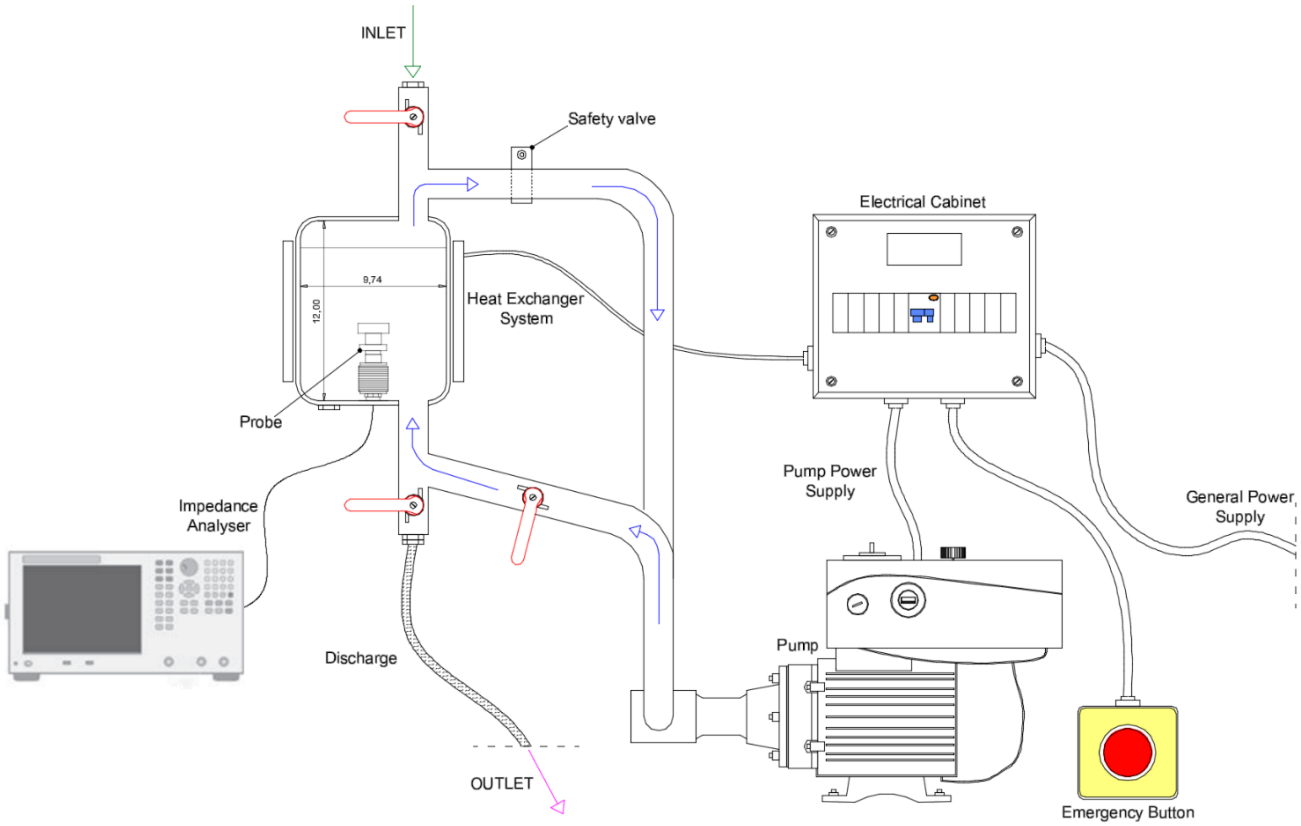

Figure 35 Continuous system scheme

The system is also equipped with a safety valve for vapours venting in case the pressure becomes excessive, an emergency button to shut down all systems at the same time and taps for liquid loading and unloading (magenta arrow in figure 35) and washing.

This system allowed to simulate a very rapid continuous heating, even if not as fast as a dielectric heating can be, but at the same time it made possible to measure the dielectric properties along the entire heating phase, without having to interrupt it to carry out the measurements. Furthermore, this system, being under pressure, allows the achievement of very high temperatures and therefore the measurement of the dielectric parameters up to about 150°C. Table 15 shows the temperature and flow rate ranges that have been reached with the use of the continuous system:

Table 15 Properties of the laboratory scale continuous system

Temperature	T_{amb} – 135°C
Flow rate	300 – 500 L/h

The data obtained from these tests made it possible to derive an equation describing the behaviour of the dielectric properties as the temperature varies.

4.2.2 STATIC SYSTEM

It was not possible to use the continuous heating system for fluid and solid products, due to the presence of the pump because in the first case it would have irremediably changed the structure of the samples and in the second case it is simply impossible to use it. For these reasons, it was necessary to devise another heating system fast enough to simulate the electromagnetic one. This led to use a microwave oven for heating the samples, so they could then be manually and quickly measured with the probe. This naturally involves a type of heating in time steps, during which the sample is exposed to the electromagnetic field and heated, interspersed with the dead times necessary to carry out the measurements of the dielectric properties.

The products were heated with the Whirlpool Extra Space microwave oven (figure 36a) and at each step temperatures and dielectric properties were measured respectively with a Pico Technology thermocouple (figure 36b) and dielectric properties measurement system in its original configuration, like previously shown in figure 29.

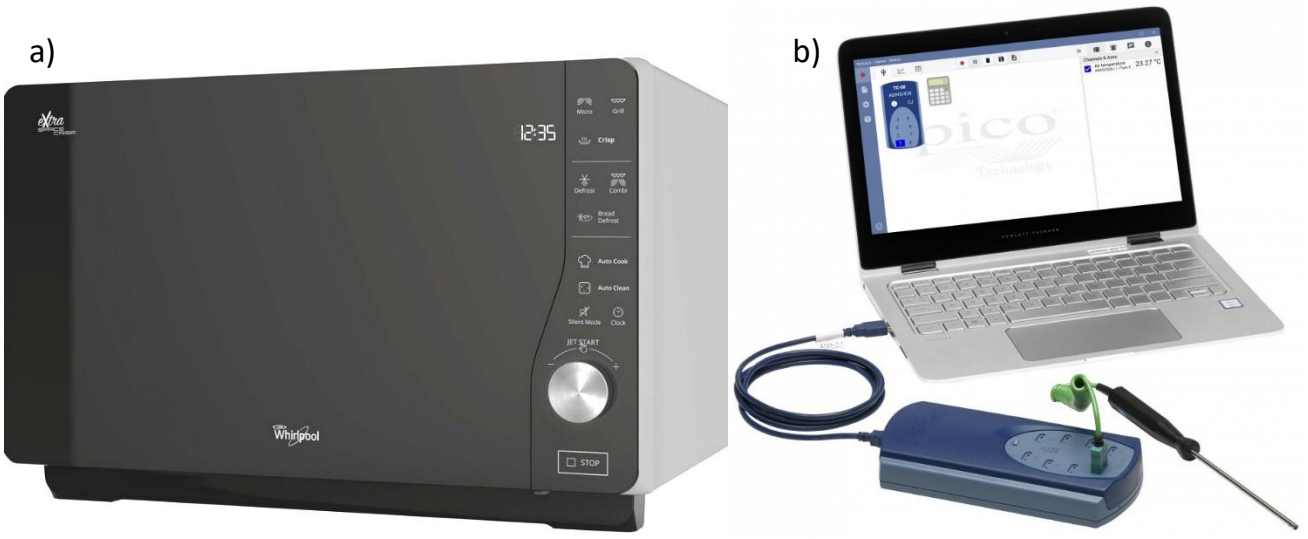

Figure 36 a) Whirlpool Extra Space microwave oven and b) Pico Technology thermocouple

Heating and the consequent evaluations at the radiofrequency could not be performed because a laboratory scale radiofrequency generator could not be recovered. To perform the heating inside the microwave, the fluid samples were collected in glass backers, closed with a heat-resistant polymer film in order to avoid evaporation of the sample. Only a small hole

was made in the film to avoid overpressure in the containers and thus allow the escape of a small part of the steam. Naturally with this system it was not possible to go beyond about 90°C both for the start of the boiling phase and for the handling of the samples.

In order to evaluate the effective energy deposited by the microwave inside a sample, preliminary tests were carried out with the use of water, which, as previously mentioned, was used as a reference material both for the setup of the different systems used for the dielectric properties measurements, and as a control material for the goodness of the data. For this purpose, tests were carried out to evaluate the real power supplied by the microwave oven in water samples of different volumes during a microwave heating. The samples were heating in steps of 10 seconds and at each step the temperature was measured; 50°C was not exceeded to avoid evaporation of the samples. The Whirlpool Extra Space oven works at 800 W, but only a portion of the power will be transferred to the product in the form of heat and it is evaluated using equation (A-20), reported in Appendix I. In the following table the results of these tests are shown:

Table 16 Evaluation of the average power transferred to various volumes of water

Mass (g)	T (°C)	P (W)	$\overline{P}$ (W)
1000	26.0	-	567.12
	30.0	556.00	
	34.2	583.80	
	38.2	556.00	
	42.3	569.90	
	46.4	569.90	
800	25.6	-	553.22
	30.95	594.92	
	35.8	539.32	
	40.8	556.0	
	45.5	522.64	
600	25.5	-	508.74
	31.8	525.42	
	37.5	475.38	
	43.8	525.42	
400	25.0	-	528.2
	34.6	533.76	
	44.0	522.64	
100	26.4	-	419.78
	41.5	419.78	
50	25.3	-	238.14
	36.5	238,14	

As is evident from table 18, as the volume decreases, the power transferred to it is less. Another way to show this trend is through the graph in figure 37 where it is evident that as the volume of the sample subjected to microwaves increases, the greater the power deposited and tending almost to a plateau. When, on the other hand, the volumes are very small, the deposited power is much smaller and in particular the power deposited inside a becher containing 50 mL of water is just about 238.14 W.

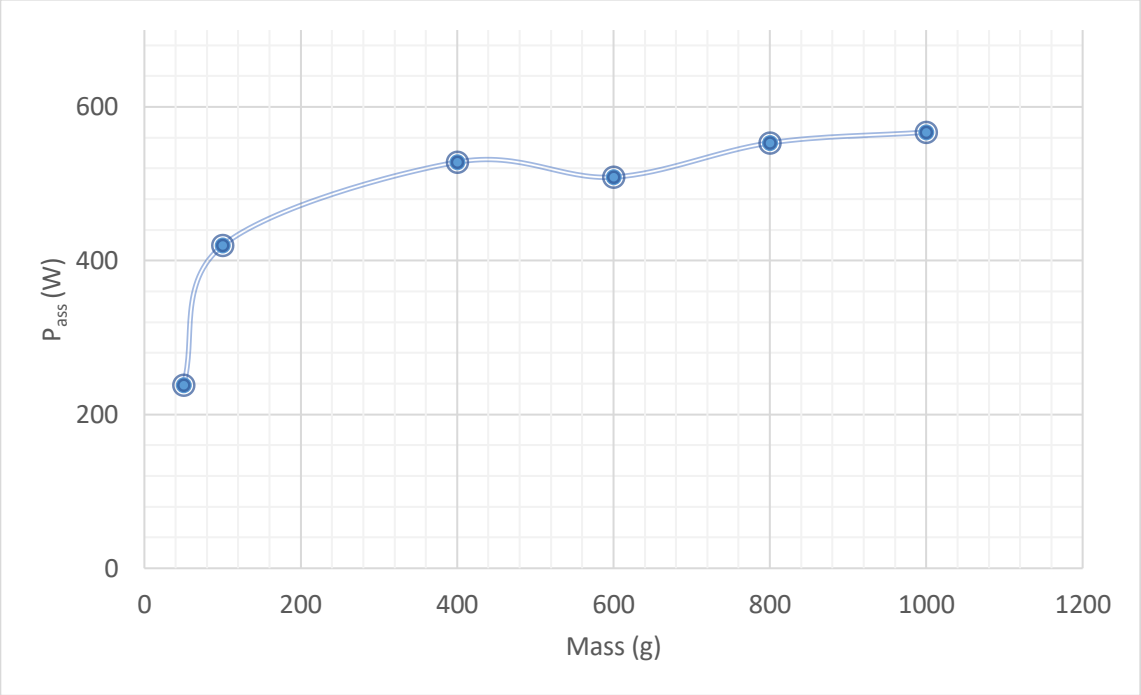

Figure 37 Power absorbed as the sample volume changes

As mentioned above, the probe method is based on a coaxial line ending abruptly at the tip that is in contact with the material being tested. The probe method is the easiest to use because it does not require a particular sample shape or special containers and allows measurements in a wide range of frequencies. The only flaw of the use of this method is that it requires perfect contact between the probe surface and the sample surface and if this is easily obtainable for liquid or fluid products, it is not possible for granular matrices with dimensions ranging from a few mm to a few cm in diameter.

To allow the perfect contact between the probe and the surface of the granular food products, they were grinded and then compressed to obtain cylindrical samples. To product each tablet, an amount of about 45 g of seeds was grinded and the flour was placed in a steel cylindrical holder used to compress the flour into tablets. In this way, tablets of density and

composition equal to the initial particles are obtained, but which can be easily placed in contact with the surface of the probe and then tested.

The samples were compressed on an over-the-counter hydraulic press to obtain a tablet with density equal to the true density of the seeds. For the valuation of the true density of the seeds, the liquid displacement method was used. Toluene ($C_6H_5CH_3$) was used as a displacement liquid due to its low tendency to permeate through the sample [28]. The seed density was determined by dividing the weight of randomly selected quantity of samples by the volume occupied by those seeds as measured with toluene in 50 ml pycnometers.

At last, the compressed sample was placed in ABS holder (ABS not warm up exposed to MW) to side the shape and to make more handling the samples during the heating process (figure 38).

Figure 38 Flaxseeds tablets in ABS holders

The ABS holder is especially designed to fit the steel holder (figure 39) for the tablet's extrusion. Dimensions of ABS holders are of 50 mm inner diameter and 36 mm in length.

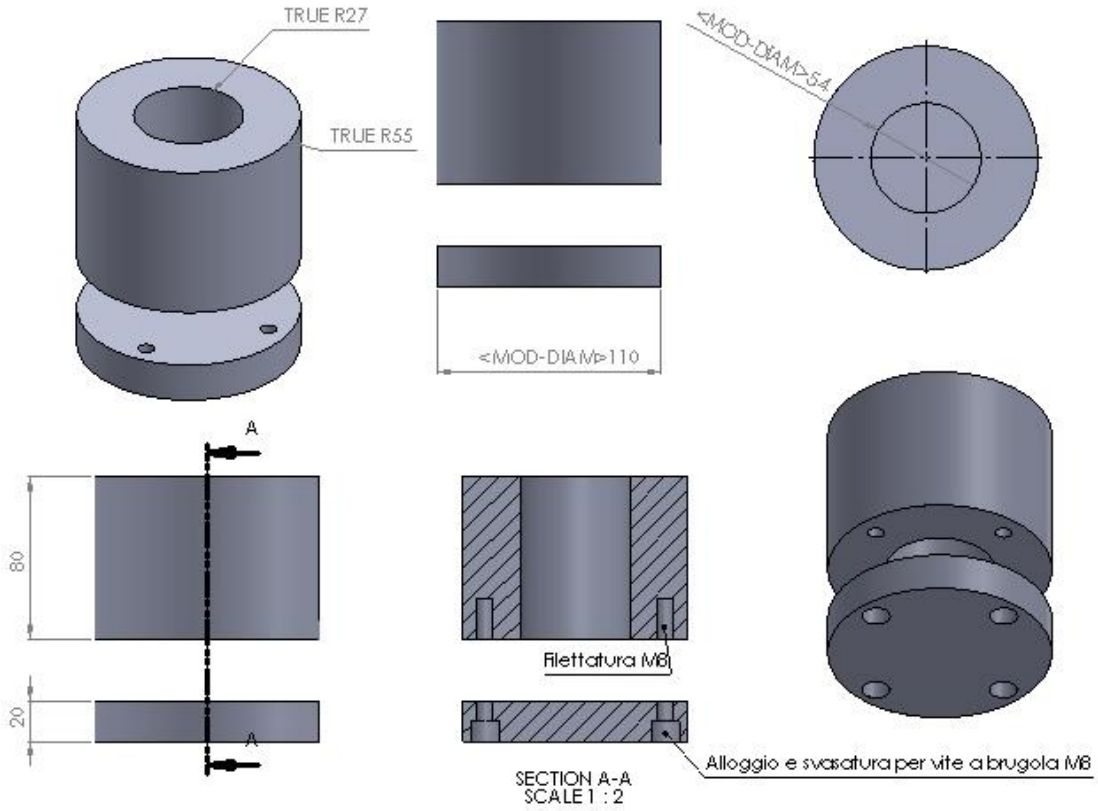

Figure 39 Steel cylindrical holder used to make the flour tablets

The correctness of the measurements of the dielectric properties on the samples thus prepared was verified by comparing these data with the temperature variations using equation (A-24).

For polymeric granular products, it is not possible to compact them due to the enormous pressures that would be needed to obtain a tablet of the desired density, so they have been ground to obtain a powder with a size of less than 300 µm. To be able to grind the polymer pellets, they have been previously cooled with liquid nitrogen, to make them more fragile. To obtain the desired particle size, the grinding residues were sifted several times and ground again. Polymer particles < 300 µm can be easily measured with the available probe, like previously shown in table 14. In literature, the pulverization method has already been used to measure the dielectric properties of polymers and other solids [35], [36], but never in such a wide range of frequencies as the one examined in this paper and never with the use of the high temperature coaxial probe.

The correctness of this protocol was confirmed by exploiting Orfeuil law, but it was not possible to directly measure the dielectric properties at various temperatures of the polymer

powder, due to the technological limit of the probe which cannot record too small values of ε". For this reason, it was decided to evaluate E^2 from equation (A-18) in the case of a becher containing 50 mL of water heated by microwave (equation (3)) and to consider it with a good approximation equal to the electric field that established inside a becher containing 50 g of polymer powder. In this way, the equation (A-21) can be rearranged and used to evaluate ε" of the polymer using equation (4) for a microwave heating of 10 seconds:

$$E^2 = \frac{P_w}{2\pi f \varepsilon_0 \varepsilon''_{r,w}} \qquad (3)$$

$$\varepsilon''_r = \frac{\rho_p \, c_{p,p} \, \Delta T_p}{2\pi f \varepsilon_0 E^2 \, dt} \qquad (4)$$

Where P_w is the power transferred to the volume of water, $\varepsilon''_{r,w}$ is the loss factor of the water at the frequency considered, that is 2.45 GHz, instead, ρ_p is the density, $c_{p,p}$ is the specific heat at constant pressure and ΔT_p is the temperature increase of the polymer powder.

The evaluation of P_w was illustrated at the beginning of this section.

For the tests with polymer pellets, an alternative protocol to the one described above was also sought, which would allow to made measurements without having to grind the particles. For this reason, many tests were carried out with the use of a liquid matrix in which it is possible to disperse the polymer pellets thus allowing the use of the high temperature probe. The liquids that were considered for this purpose were isopropanol and silicone oil, both having dielectric properties quite close to those of polymeric materials. From the data obtained from these tests, we then tried to derive an equation that would allow to calculate the value of the polymer loss factor. The results of these tests will be illustrated and commented later.

4.3 NUMERICAL MODELING SYSTEMS: FEM 3D

This paragraph presents the phases that led to the development of a model, using the FEM numerical simulation, for the radiofrequency heating of liquid products with applicators developed by Officine di Cartigliano, analysing and justifying the made choices. The mathematical modeling of the system is complex, because it is necessary to consider all the different physical phenomena that interact: electromagnetic field, heat transmission and fluid dynamics. For this purpose, it was decided to use COMSOL Multiphysics®, that is a

multipurpose and multi-physical finite element code. This type of FEM code is able to conduct a coupled electromagnetic-thermal analysis by solving the PDEs that model the physics involved and their interactions. Obtaining a model allows a deeper understanding of the project and the process under analysis, thanks to the simulation of a wide range of possible operating conditions and physical effects.

The model was built and validated on an existing component; the RF applicator made available by Officine di Cartigliano.

4.3.1 COMSOL MULTIPHYSICS®

COMSOL Multiphysics® is a simulation platform that incorporates all steps of the modeling workflow: from defining geometries, material properties and physics to describing specific phenomena, to resolution and post-processing. It is able to interface with other engineering and mathematics software, such as Matlab, Excel or AutoCAD.

The procedure required by the COMSOL Multiphysics® calculation code is divided into the following three sequential work phases:

1. Pre-processing - definition of the physical-mathematical model;
2. Numerical calculation - solution;
3. Post-processing - analysis of results.

Once the physical theory underlying the analysis is understood, numerical computation represents the phase that requires more resources, both from a computational point of view and in terms of time, given the complexity of the problem. The greater energy-intensive phase for the user is, instead, attributable to the first one, which can be further divided into the following sub-phases:

- Creation or acquisition of geometry: the pre-processor of the calculation code can both import a geometry coming from another software (generally CAD), and generate the geometry that is needed internally;
- Finite element discretization: the geometries, that is the integration subdomains for the differential equations, are discretized and divided into nodes connected to each other by elements whose behaviour is known through defined shape functions. The so-called mesh or calculation grid is obtained;

- Definition of materials: the materials for each subdomain of the computing domain must be defined, that is the schematizations or mathematical models of the materials and the related physical properties involved in the analysis;
- Physical settings: this category includes all the other settings necessary to completely define the "physics" of the problem, that is, all the quantities (scalar or vector) and the physical constants involved into the analysis. In the case of paired problems, these settings must be made for each considered physics. Comsol considers among the physical settings also the definition of the materials for each subdomain, the boundary conditions and the choice of the formulation of the elements, because Comsol is a non-dedicated environment but with a modeling open to any physical area. It also offers the possibility of defining functions for each vector or scalar quantity entering the problem, or the definition of new quantities and quantities that are obtained from the integration, on a chosen domain, of the main unknown variable obtained from the solution of the differential equations and not foreseen by default among the quantities resulting by the calculation;
- Boundary conditions: the constraints, contacts, interface conditions of the different subdomains, and more generally the conditions imposed on the unknown dependent variable (solution of the differential equation) are specified in order to obtain the particular solution desired on the boundary of a certain subdomain. This category also includes the initial conditions on the unknown variable;
- Physical couplings, choice of the solver and output quantities from the calculation: a multi-physical analysis can easily reach the limits posed by the available computational resources. A multiphysics calculation code therefore allows to set incomplete - that is, non-biunivocal - couplings between the various physical analyses in progress. That is, it is possible to neglect the influences (typically the weak ones, in order to not compromise the validity of the analysis) that a physical phenomenology has on the others. For example, it is possible to solve the equations of the harmonic electromagnetic field and in sequence solve the equations of the temperature field, neglecting the effects that the temperature distribution has on the electromagnetic properties. Each type of problem, therefore of the differential equation that governs it, must be faced with an adequate numerical solver among the different ones offered by

the code. To reduce the computational effort, it is finally necessary to correctly define the quantities that you want to obtain from the calculation.

As regarding the results analysis phase, this can be done using the tools that generally an FEM simulation environment makes available to the user. They range from purely numerical data in the form of printouts, to level maps on subdomains and contours, and to flow lines of the scalar or vector output fields. A very important tool are also the graphs that show the trend in space or time of a certain selected magnitude. In the case of Comsol, it is possible to analyse the quantities provided by default at the output of the solver, or those defined by the user and integrated on a selected domain by the code, as already mentioned in the description of the physical settings available. To validate the results of an FEM calculation, a convergence analysis is performed to verify that when the size of the grid elements is reduced, there is a convergent trend of the calculated quantities.

The computer used to perform the simulations is a FUJITSU Workstation CELSIUS R940, RAM 1024 GB, 2 Processors Intel® Xeon® CPU E5-2620 v4 @ 2.10 GHz.

4.3.2 RF APPLICATOR MODEL FOR LIQUIDS

The applicator geometry was created in 3D CAD (figure 40). It was necessary to implement a 3D simulation, even if very expensive, because the geometry does not present any symmetry. However, the CAD details useless for simulation purposes were removed, in order to reduce the computational cost.

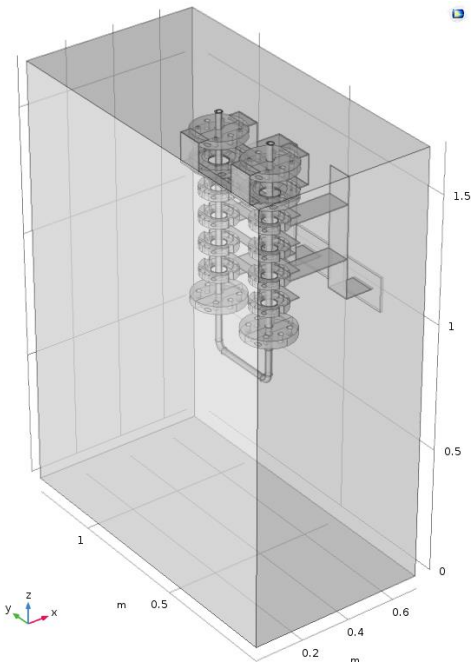

Figure 40 Model geometry, front view

4.3.2.1 RF APPLICATOR MODEL

The applicator was inserted inside a parallelepiped-shaped domain of dimensions equal to those of the air surrounding the applicator in its housing in the real system.

The electrode is powered through thin blades, drawn directly in COMSOL, connected to two ports that simulate the generator section. They are positioned at the end of the connecting plates, in the center of the two rectangular openings of the domain visible in figure 41:

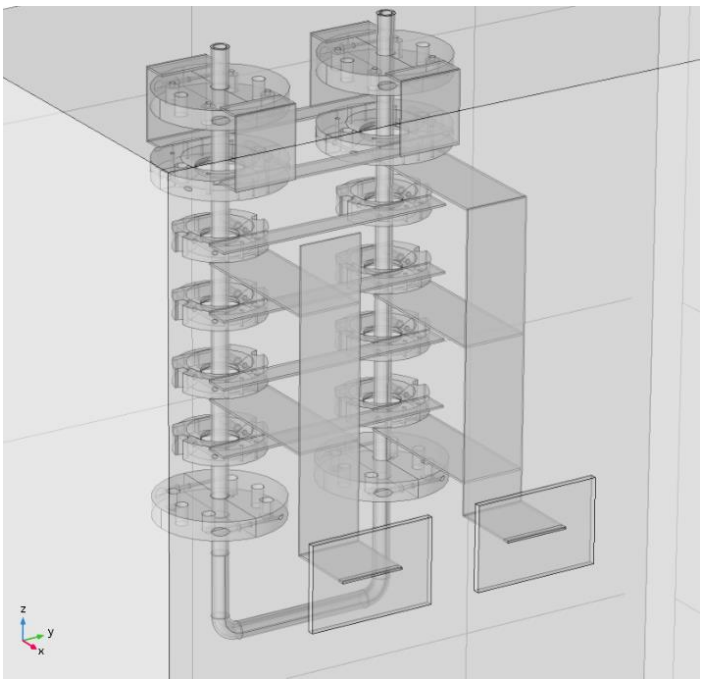

Figure 41 Model geometry, back view

In order to carry out the simulation it is necessary that each domain of the geometry be assigned a material whose specific properties are known. These were assigned as reported in table 17:

Table 17 Corresponding materials for each domain

Domain	**Material**	**Origin**
Electrodes	Aluminium	COMSOL Library
Parallelepiped	Air	COMSOL Library
Tube	Teflon	Literature
Volume inside the tube	Water/Milk	Literature
Volume around the doors	Air	COMSOL Library
Connecting plates	Aluminium	COMSOL Library
Surface	Material	Origin
Parallelepiped surface	Aluminium	COMSOL Library

The properties of the materials can be chosen from the library already present in the software or newly defined, as in this work happened for water, milk and Teflon. In particular, the properties of the materials necessary to solve the equations of physics in one particular domain cannot be omitted; it was, therefore, of fundamental importance to define the electrical properties in the whole domain, where the electromagnetic field, the thermal and fluid dynamics equations are solved and in the volume inside the tube where the heat transport, momentum and mass equations are solved. Among the electrical properties of materials, in the particular type of study under examination, electrical conductivity, a function of temperature and voltage, is of fundamental importance. Due to the absence of adequate measuring instruments, it was necessary to refer to the literature data for the products of interest, water and milk. At a preliminary stage, these were used as first attempt values in the simulation. The properties of water were developed starting from the "Water" material present in the COMSOL library, which refers to distilled water. The permittivity ε' was defined by the user, using a polynomial as a function of temperature:

$$\varepsilon' = -0.0008\,T^2 - 0.2436\,T + 84.652 \qquad (5)$$

Where *T* is the temperature in Celsius.

This polynomial was obtained through a regression in Excel of the measures referred to paragraph 4.1. The physical properties of milk have been developed through bibliographic research, instead the dielectrics properties were obtained, as for water, by regressing the measures presented in paragraph 4.1. In table 18 properties of milk in the form of polynomials as a function of temperature are reported [37]–[39]:

Table 18 Properties of milk as function of temperature

Property	Function
Thermal conductivity	$k = (326.58 + 1.0412\,T - 3.37 \times 10^{-3} T^{2})(4.6 \times 10^{-1} + 5.4 \times 10^{-1} X_{water}) 1.73 \cdot 10^{-3}$
Specific heat	$Cp = \sum CpiXi$ $c_{p_{lipids}} = 1984.2 + 1.4373\,T - 4.8008 \times 10^{-3} T^2$ $c_{p_{proteins}} = 2008.2 + 1.2089\,T - 1.3129 \times 10^{-3} T^2$ $c_{p_{carbs}} = 1548.8 + 1.9625\,T - 5.9399 \times 10^{-3} T^2$ $c_{p_{minerals}} = 1092.6 + 1.8896\,T - 3.6817 \times 10^{-3} T^2$ $c_{p_{water}} = 4176.2 - 0.0909\,T + 4.4731 \times 10^{-3} T^2$
Density	$\rho = (1040{,}7 - 2{,}665 \cdot 10^{-1} \cdot T - 2{,}3 \cdot 10^{-3} \cdot T^{2}) - \left[X_{fat} \cdot (1{,}011 + 9{,}76 \cdot 10^{-3} \cdot T - 4{,}81 \cdot 10^{-5} \cdot T^{2})\right]$

Viscosity	$\log \mu = A_0 + A_1 T + A_2 T^2 + (B_0 + B_1 T + B_2 T^2) S + (C_0 + C_1 T + C_2 T^2) S^2$
Permittivity	$\varepsilon' = 0{,}0004\, T^2 + 0{,}0108\, T + 85{,}609$

Where:

- k is the thermal conductivity (W/m·K);
- T is the temperature in Celsius;
- x_{water} is the mass fraction of water;
- c_p is the specific heat (J/kg·K);
- x_i represents the mass fraction of each constituent of milk (fats, proteins, carbohydrates, minerals and water);
- c_{pi} is the specific heat relating to the i-th constituent;
- ρ is the density (kg/m^3);
- x_{fat} is the mass fraction of lipids;
- μ is the viscosity (cP),
- S is the total solids content (% by mass);
- A_i, B_i and C_i are coefficients defined in the following table:

Table 19 Viscosity coefficients

Coefficient	Value
$\boldsymbol{A_0}$	0,249
$\boldsymbol{A_1}$	-0,013
$\boldsymbol{A_2}$	0,000052
$\boldsymbol{B_0}$	0,02549
$\boldsymbol{B_1}$	-0,000098
$\boldsymbol{B_2}$	0,0000004
$\boldsymbol{C_0}$	0,000543
$\boldsymbol{C_1}$	-0,0000139
$\boldsymbol{C_2}$	0,000000117

Teflon, an insulating polymeric material, inserted exclusively in the electromagnetic study of the problem, was simulated with the following parameters [40]:

Table 20 Teflon properties

Property	Expression
Relative permeability	$\mu = 1$
Electric conductibility	$\sigma = 10^{-16}\ S/m$
Permittivity	$\varepsilon = 2.3$

4.3.2.2 MESH CONSTRUCTION AND MODELING PARAMETERS

The mesh used was of the "User defined" type and particularized for three different areas:

- All domains
- Water/Milk
- Teflon

The elements of the mesh are of the unstructured tetrahedral type. For the water/milk domain and for the Teflon, the mesh was calibrated for fluid dynamics, for the rest of the domain it was calibrated for generic physics. The adequacy of the mesh used was assessed by monitoring speed and temperature on the volume of fluid inside the tube (both for water and for milk) and incident power flow through the surface around the fluid.

The mesh inside the volume of water or milk has been modified on the edges with the specific *Boundary layer* command (figure 42), in order to thicken it near the edges, where the greatest gradients are expected.

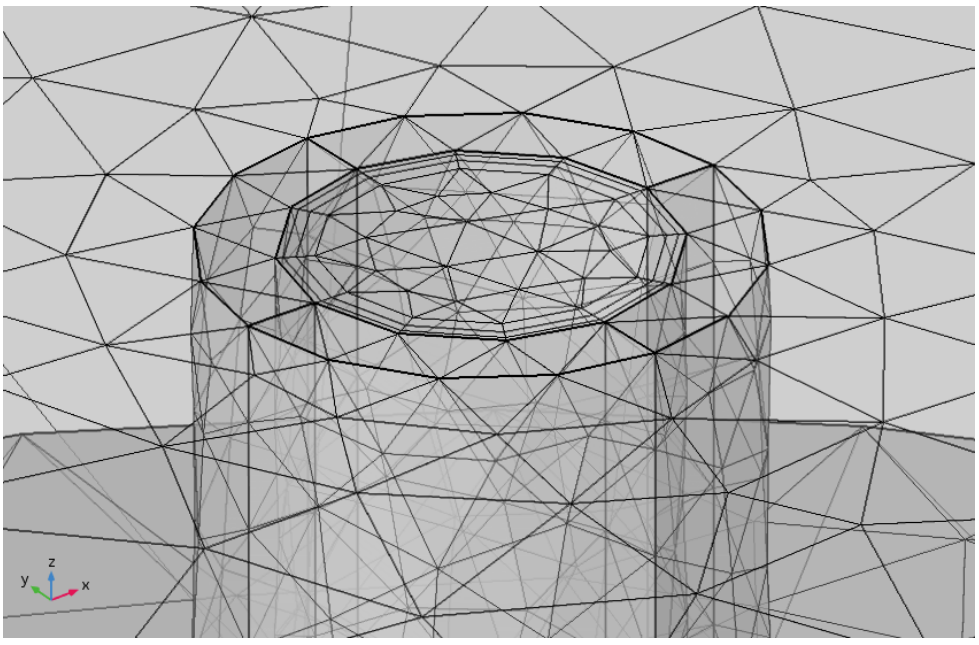

Figure 42 Detail of the boundary layer in the liquid volume

A *Normal* mesh was fixed in the entire geometry, particularized with a *Finer* in the Teflon domain, to avoid interpenetration effects between pipe and fluid that a *Normal* mesh would have entailed. The meshes in the water/milk domain, were subsequently thickened in order to allow a comparison to obtain a model with the most suitable mesh and the lowest possible computational cost. The comparison between two successive meshes was carried out using the *Join* command, which allows to compare the data of two different meshes by interpolating the results in the same points of the domain. The error between one mesh and another was evaluated relatively, according to the formula:

$$relative\ error = \frac{|data1 - data2|}{data1} \times 100 \qquad (6)$$

where *data1* and *data2* are the set of values of the solution calculated respectively with the more and less dense mesh in comparison. The values were compared on a plane that cuts the domain occupied by the fluid exactly in half, and then deepened on the entire volume of fluid, exporting the data regarding the error in an Excel sheet. As regards to the power flow, however, the integral on the surface external to the fluid was evaluated, highlighted in blue in figure 43.

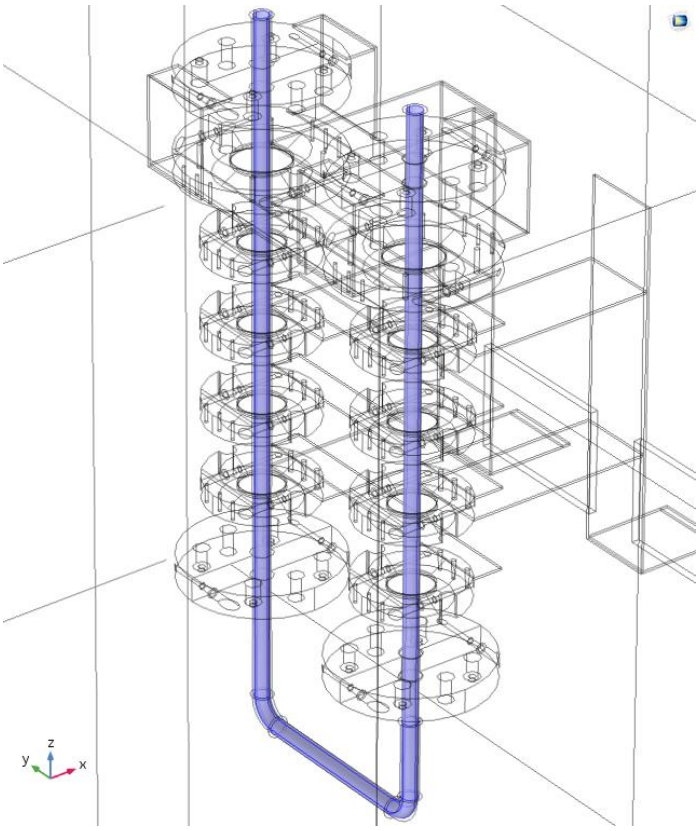

Figure 43 Power flow integration surface

An integral evaluation was chosen since the interest, in this case, is aimed exclusively at the power transferred to the fluid and not at the precise distributions of the electromagnetic quantities.

- Water domain

For the water domain, the investigated meshes were Normal, Fine, Finer and Extra Fine. The graphical results relating to speed and temperature are shown respectively in figure 44a and figure 44b. The study was carried out using a voltage of 7000 V and a conductivity of 0.03 S/m as input parameters.

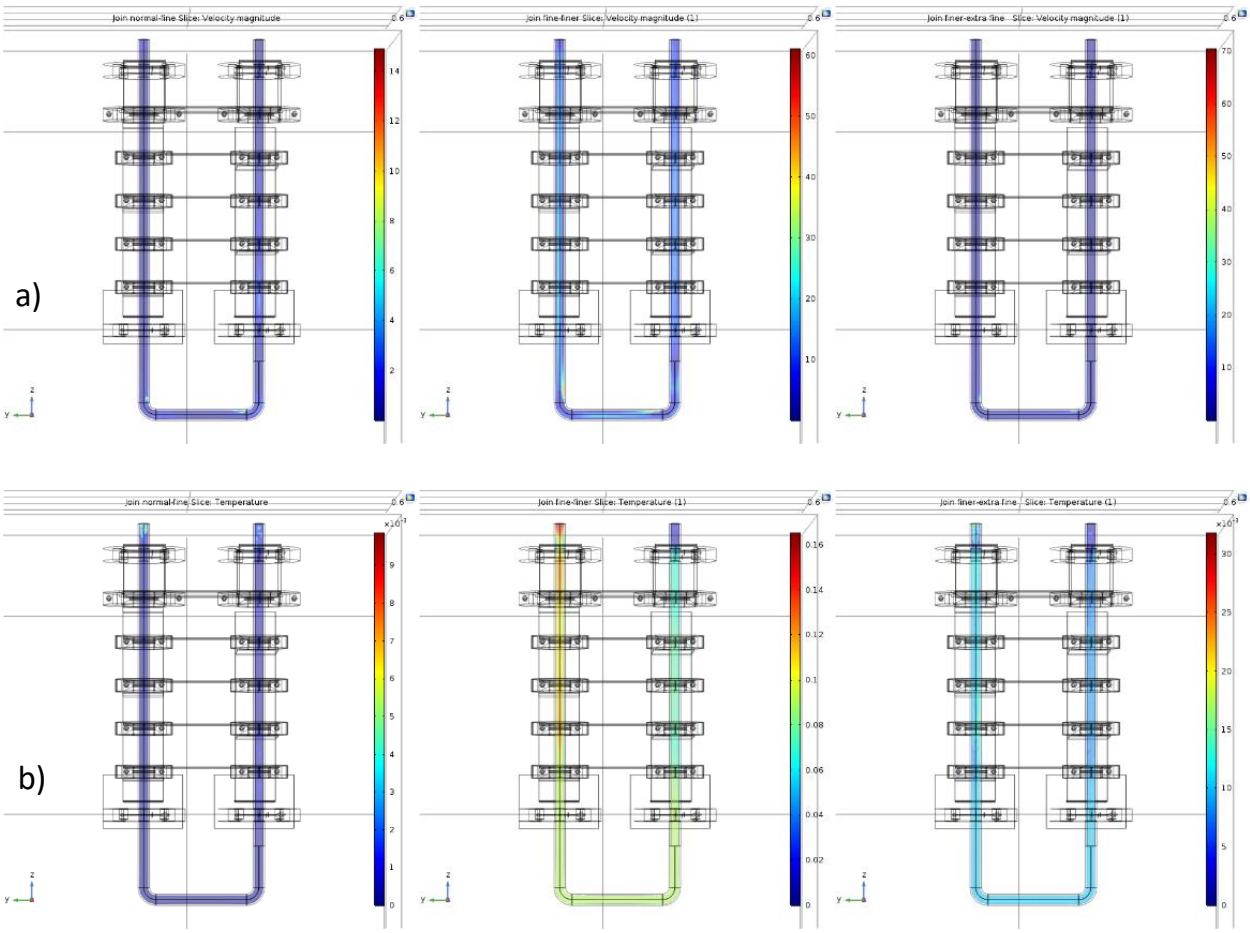

Figure 44 From left to right: Normal-Fine, Fine-Finer, Finer-Extra Fine meshes, a) speed comparison and b) temperature comparison for water

From the legend scale of values, it can be seen that the error between the meshes for the temperature is everywhere below 0.16%, for all three comparisons. The speed data, on the other hand, shows a greater error. To investigate further the analysis of the data, therefore, the speed values, relating to the entire volume inside the pipe, were exported to an Excel spreadsheet and organized into histograms in which the range of errors was divided into ten

classes (bin) for each of which the number was reported (figure 45).

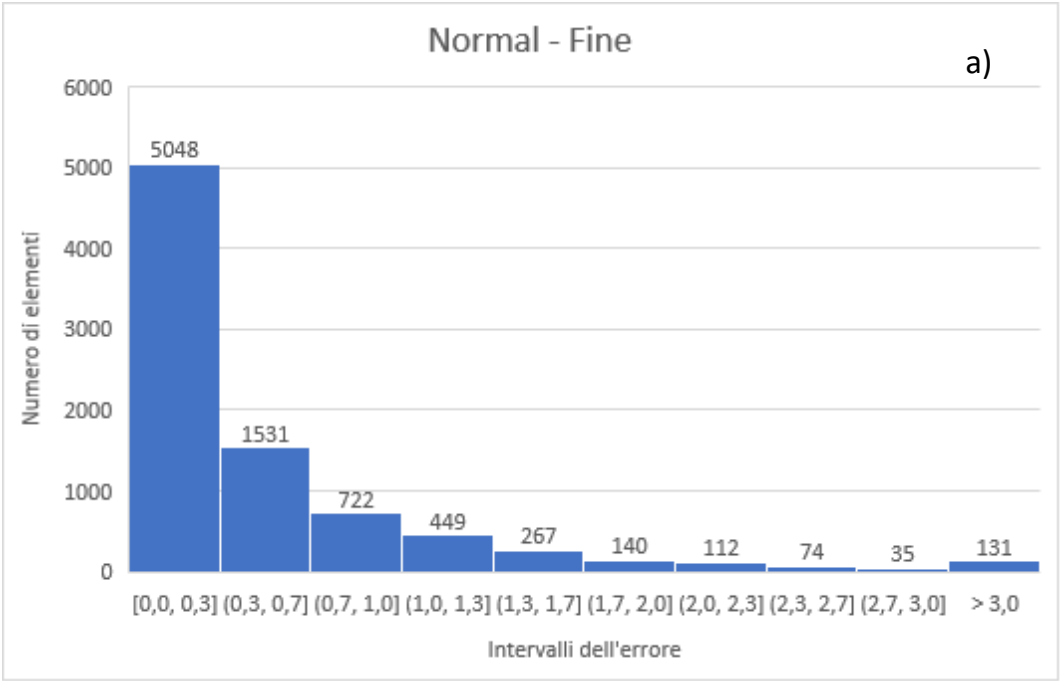

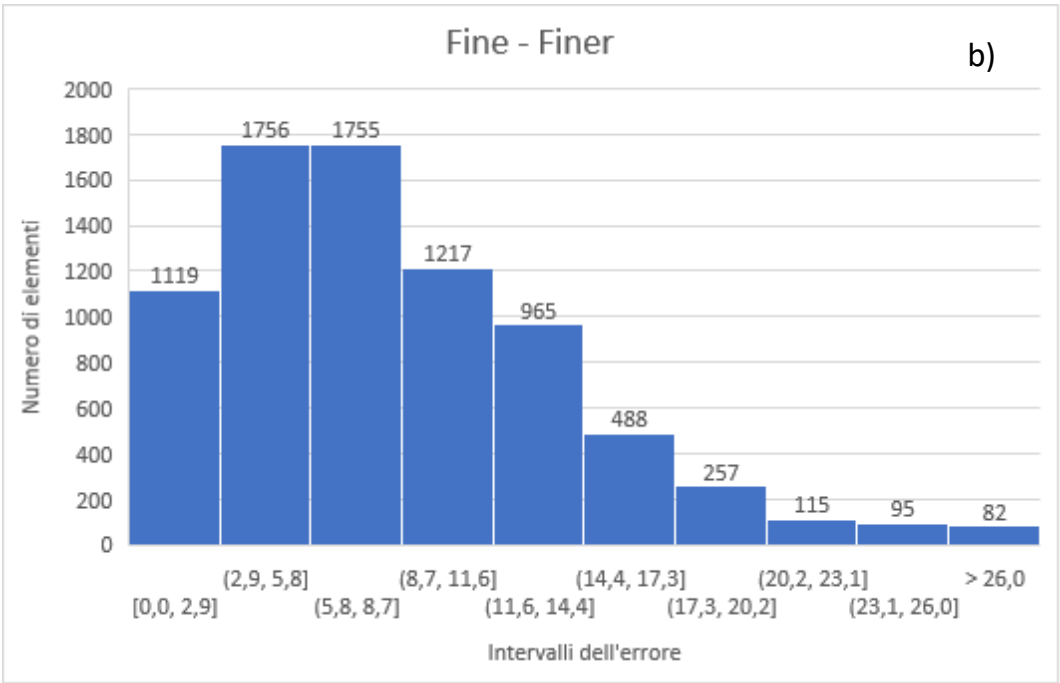

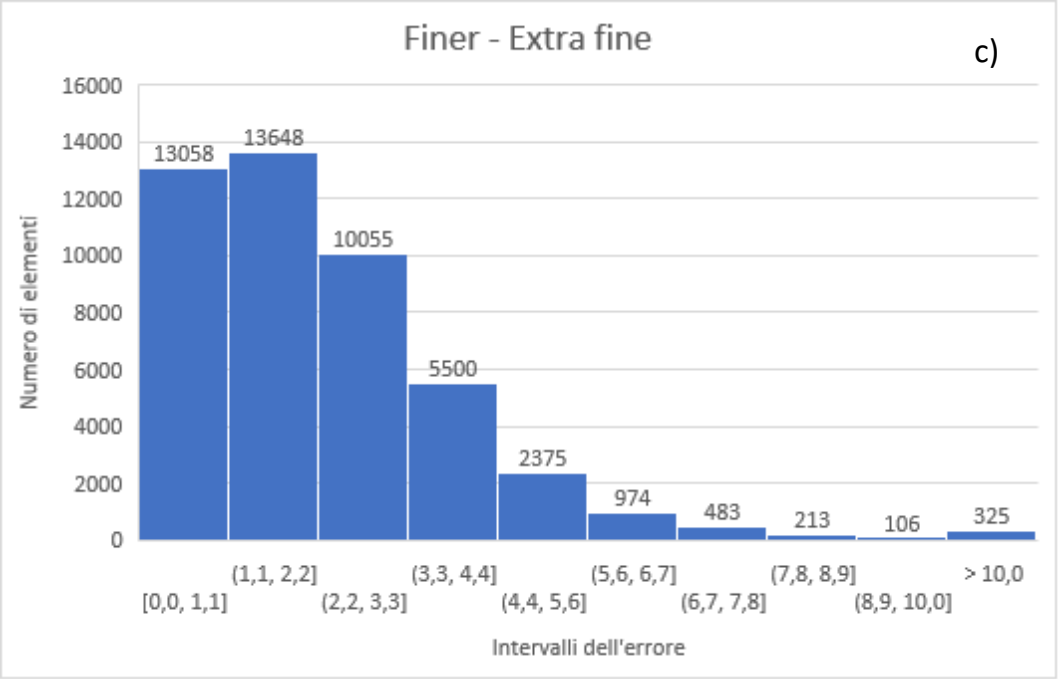

Figure 45 a) Error histograms between Normal and Fine meshes, b) Error histograms between Fine and Finest meshes, c) Error histograms between Finer and Extra fine meshes

From the graphs shown above it is possible to conclude that the mesh that guarantees an error of less than 10% in almost all the points of the volume of interest is the Finer one, even if it implies a rather high computational cost.

The evaluation of the integral of the electromagnetic power through the surface are reported in table 21 and reveal a relative error that follows the same trend as the previous evaluations:

Table 21 Electromagnetic power, integrated on the surface external to the water and relative errors

Mesh	Power (W)	Relative Error
Normal	2839.0	-
Fine	2839.3	0.01%
Finer	2963.2	4.18%
Extra Fine	2990.4	0.91%

Even for the reference parameter for electromagnetism, the results show a more than acceptable error. Having solved the problem with the k-ε model, which will be illustrated later, the system automatically implemented the wall functions, functions that ignore the flow field in the buffer region (the one near the walls) and analytically calculate a non-zero velocity at the walls. The parameter through which it is possible to evaluate if the domain in which the wall functions are calculated is too large is the *wall lift off in viscous units* (δ_w^+), which is plotted by default by the software and must be close to 11.06 in the majority of

points on the wall. From figure 46 it can be seen how the value of δ_w^+ is perfectly equal to 11.06 and that, therefore, there is no need to further refine the mesh close to the walls, confirming the goodness of the choice.

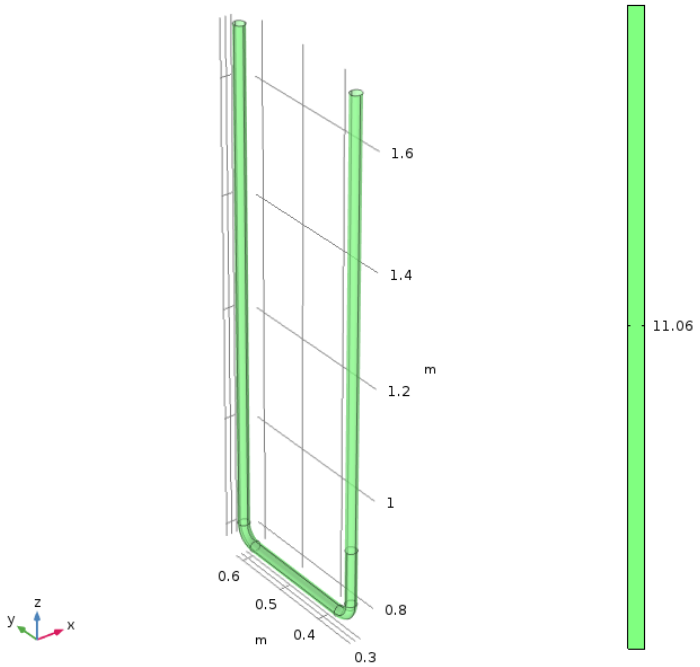

Figure 46 Wall lift off in viscous units for the Finer mesh

- Milk domain

When the material changes from water to milk, the mesh must be validated again. Similarly, to what has been done previously, the Normal, Fine, Finer and Extra Fine meshes have been investigated. The graphical results relating to speed and temperature are shown respectively in figure 47a and 47b. The study was carried out using a voltage of 5710 V and a conductivity of 0.076 S/m as input parameters.

a)

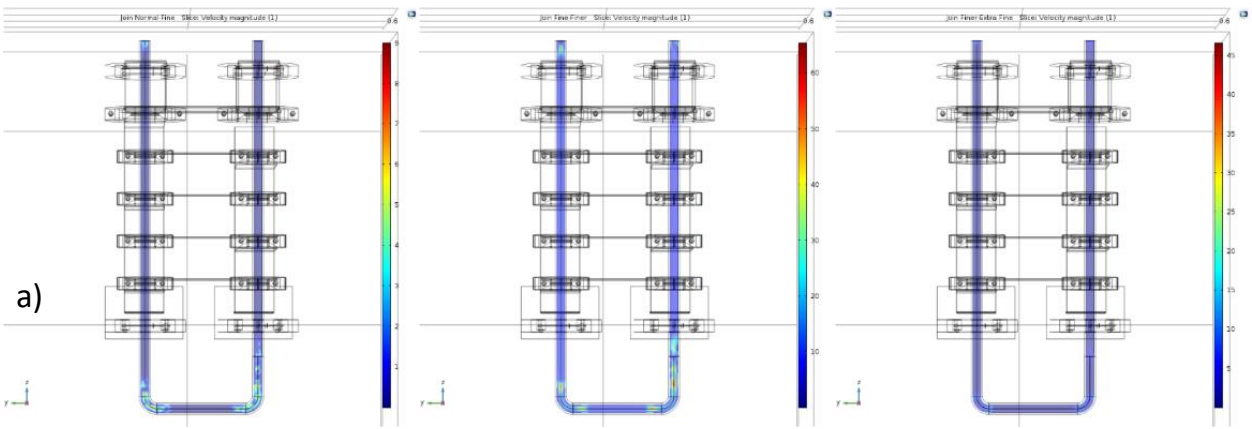

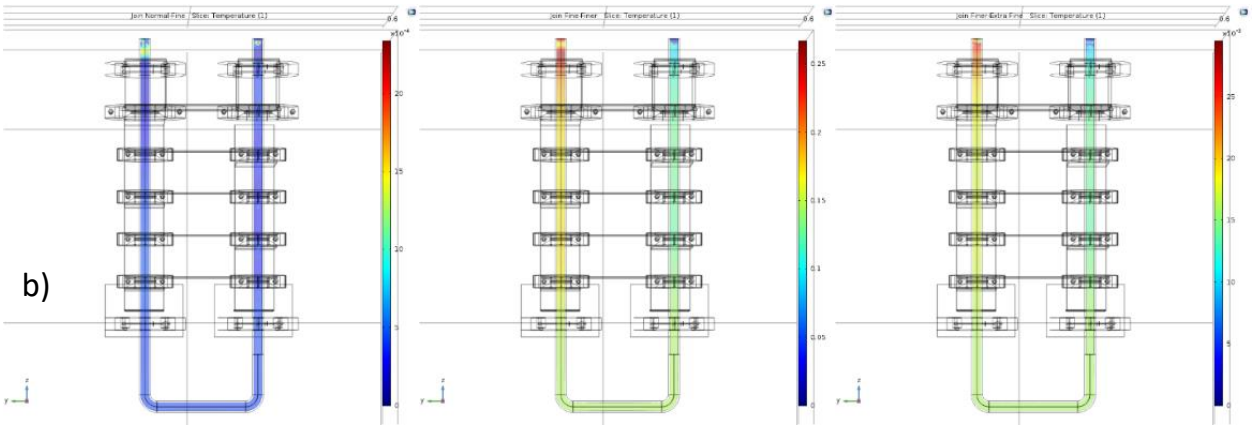

Figure 47 From left to right: Normal-Fine, Fine-Finer, Finer-Extra Fine meshes, a) speed comparison and b) temperature comparison for milk

From the scale of values of the legend it can be seen that the error between the meshes for the temperature is everywhere below 0.25%, for all three comparisons. The speed data, on the other hand, shows a greater error. Then, as previously done, the velocity values relating to the volume inside the pipe were exported to an Excel spreadsheet and organized into histograms in which the range of errors was divided into ten classes for each of which the number was reported (figure 48).

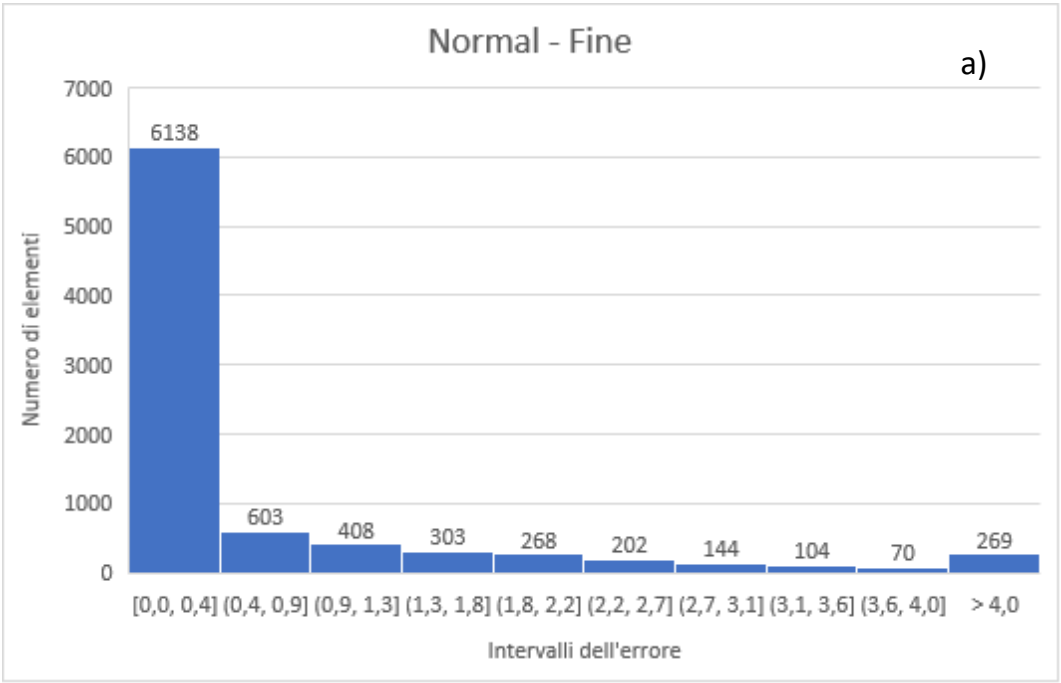

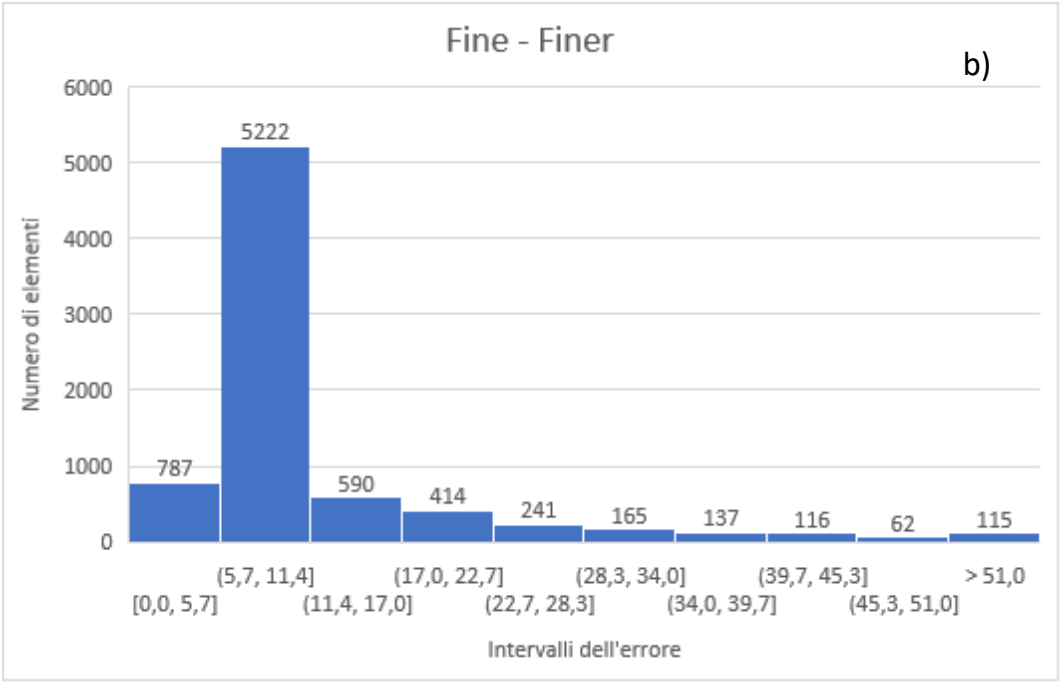

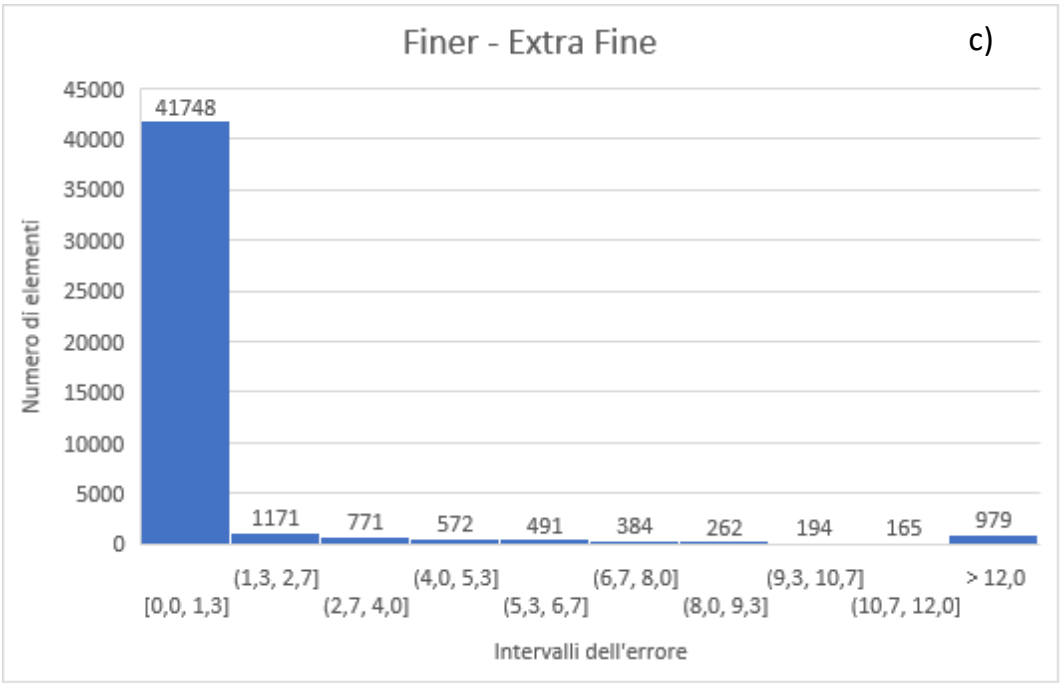

Figure 48 a) Error histograms between Normal and Fine meshes, b) Error histograms between Fine and Finest meshes, c) Error histograms between Finer and Extra fine meshes

From the graphs shown above it is possible to conclude that the mesh that guarantees an error lower than 1.3% in almost all the points of the volume of interest is the Finer one, even if it implies a rather high computational cost. The evaluation of the integral of the electromagnetic power through the surface reveals a relative error that follows the same trend as the previous evaluations, like shown in table 22:

Table 22 Electromagnetic power, integrated on the surface external to the milk and relative errors

Mesh	Power (W)	Relative Error
Normal	3586.7	-
Fine	3587.2	0.01%
Finer	3753.9	4.44%
Extra Fine	3790.5	0.97%

Even for the reference parameter for electromagnetism, the results show a more than acceptable error. Also in this case, just like for water, the *wall lift off in viscous units* (δ_w^+) was evaluated, which once again was close to 11.06 in most points of the wall.

As regarding the physics used, COMSOL is able to solve the differential equations typical of each physics, knowing the boundary conditions. A brief description of the choices made in this regard will be made below, while the solved equations, given the prolixity, will be presented in Appendix II.

The equations that model electromagnetic phenomena are implemented in COMSOL through the physics "Magnetic and Electric Fields (*mef*)"; the reference impedance value is 50 Ω. Maxwell's equations are valid on all domains; all edges, on the other hand, are assumed to be magnetically and electrically insulated by default. The first boundary condition chosen to model the system was the grounding of all aluminium edges, including those surrounding the two openings of the domain for the entry of the slats connected to the doors. The grounded edges are highlighted in blue in figure 49.

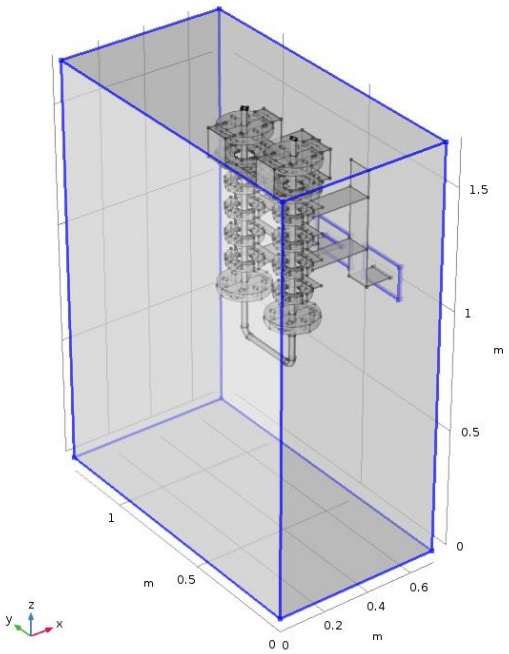

Figure 49 Grounded edges

The port on the right in figure 50, corresponding to the negative terminal in the real system, is also grounded (Grounded - GND), as a reference. The door on the left, on the other hand, is powered at the voltage value (High - HV), thanks to the imposition of the second boundary condition, called *concentrated door*.

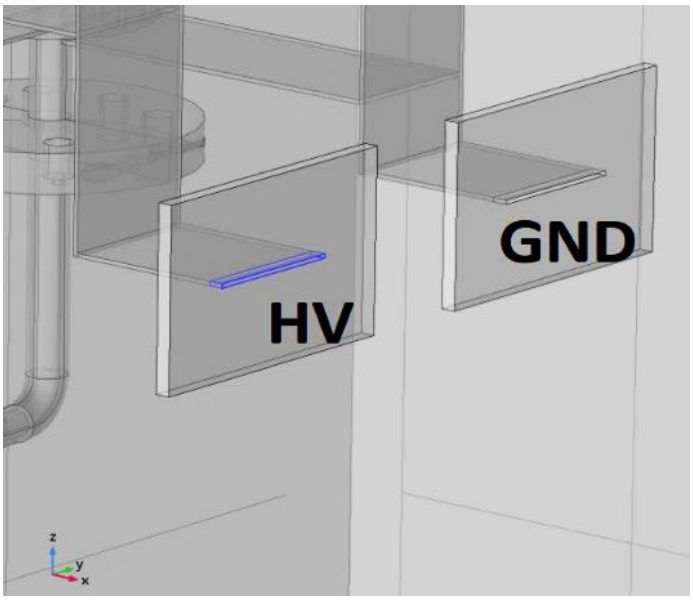

Figure 50 High Voltage port and Grounded port

The equations that model the liquid flow are implemented in COMSOL by the physics "*Turbulent Flow*, k-ε (*spf*)"; this physics relates only to the liquid domain. The choice of a turbulent modeling rather than a laminar one was made after the evaluation of the Reynolds number, using equation (7), for both liquids at the inlet of the tube. The values of the physical properties (table 23) were calculated at the inlet temperature (80°C) using the tables in the literature for water [41] and the polynomials referred to in paragraph 4.3.2.1 for milk. The speed was calculated using equation (8), knowing the flow rate (150 L/h) and the diameter of the circular section pipe (2 cm).

$$Re = \frac{\rho\, u\, d}{\mu} \qquad (7)$$

$$u = \frac{Q}{A} = \frac{Q}{\pi\frac{d^2}{4}} \qquad (8)$$

Table 23 Physical properties, velocity and Reynolds number for water and milk at a temperature of 80°C

Liquid	ρ, kg/m^3	μ, kg/ (m·s)	u (m/s)	Re
Water	971.6	$3.55 \cdot 10^{-4}$	128.93	$7.26 \cdot 10^{3}$
Milk	1004.6	$3.50 \cdot 10^{-4}$	133.31	$7.61 \cdot 10^{3}$

Since the physical properties vary negligibly in the used temperature ranges, the flow was assumed to be turbulent throughout the domain and, furthermore, since the process concerns liquids, it is permissible to assume the incompressible flow. The turbulence model used is the k-ε; it falls into the category of the two-equation model, as it adds two variables, precisely k and ε, and therefore two equations to the RANS (Reynolds Averaged Navier-Stokes), that is the Navier-Stokes equations averaged over time on a large interval with respect to a turbulent oscillation but small with respect to the variability of the physical phenomenon over time.

The mass and momentum balance equations of the model hold in all domains; all the contours are assumed by default to be similar to a wall. The first boundary condition chosen to model the system was the inlet of liquid, in mass terms, through the surface highlighted in blue and with an arrow entering in figure 51 and the second concerns the outlet condition through the surface highlighted with an outgoing arrow in the same figure.

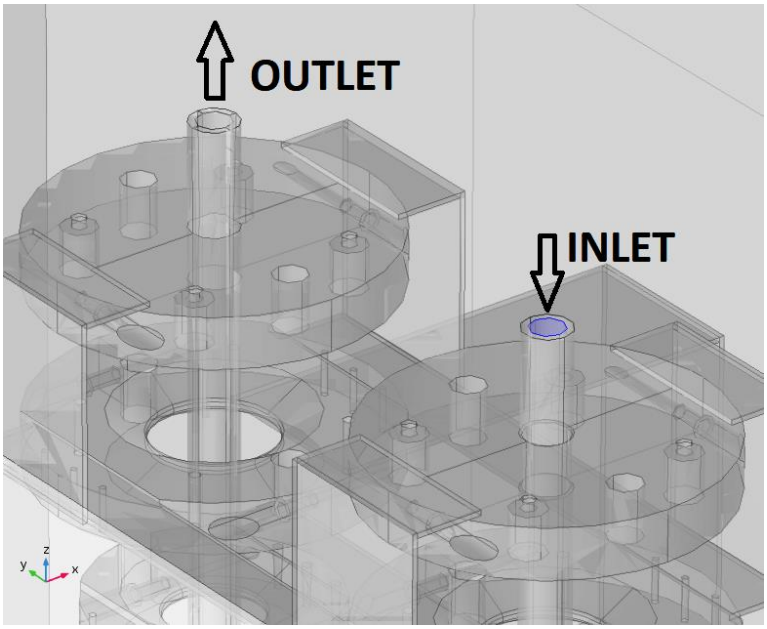

Figure 51 Liquid flow inlet and outlet

The heat exchange equations are implemented in COMSOL by the physics "*Heat transmission in fluids* (*ht*)"; this also relates only to the liquid domain. The energy balance is resolved in the whole domain of physics and by default, all contours are thermally insulated. There are two boundary conditions that override this condition: the temperature on the inlet surface, set at 80°C (figure 52) and the outgoing temperature flow on the outlet surface, similar to what was done for the turbulent flow.

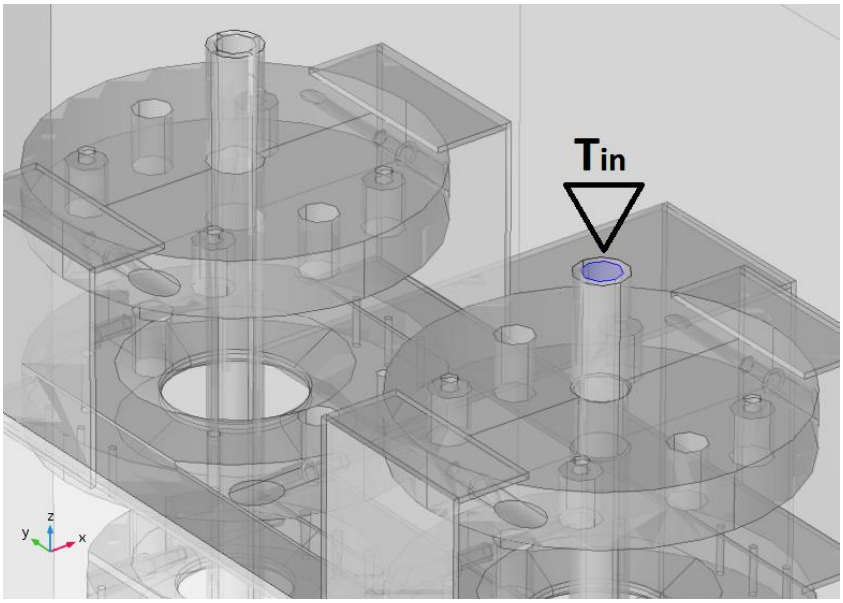

Figure 52 Surface of fluid inlet temperature set

COMSOL is able to couple the three physics presented in the previous paragraphs into two multiphysics:

- *Electromagnetic heating* (*emh*) – that is the energy transfer to the fluid thanks to electromagnetic fields;
- *Non-isothermal flow* (*nift*) – fluid that flows at a non-constant temperature.

The resolution of the balance equations takes place with the finite element method. For physics Magnetic and Electric Fields, the resolution was calculated in the frequency domain, set at 27.12 MHz; for the physics Heat Transmission in fluids and Turbulent Flow, and for the two multiphysics Electromagnetic Heating and Non-isothermal Flow it was calculated in the time domain.

The validation of the model was performed by comparing the results of the simulations with the heating of the samples, that are water and milk, obtained with the use of the experimental RF treatment system.

4.4 EXPERIMENTAL SYSTEM

The plant on which the experimental tests were conducted for the validation of the FEM model is a "Radio frequency sterilizer for liquid and formulated products", capable of delivering up to 45 kW of power. This plant is located in the Test Room of the Radio Frequency

Division - Food Sector (figure 53) at Officine di Cartigliano. It is inserted within a line dedicated to liquid treatment as follows:

- Pasteurizer
- RF unit
- Aseptic packaging machine

Figure 53 The RF pasteurization plant in the testing room of the Officine di Cartigliano

The pasteurization unit before the RF treatment has a dual purpose: to bring the product up to temperature before the thermal jump carried out with radiofrequency and to cool the milk out of the RF section, before sending it to the packaging machine which allows fill sterile bags aseptically with the product. The tests are carried out with this layout and not with the RF heating only because it is close to the real operation of a pasteurization plant.

The inlet flow enters the line and first passes through the pasteurizer from which it exits to pass through the RF applicator tube. After heating, RF performs the thermal stop and the product is subsequently cooled and sent to packaging.

4.4.1 PASTEURIZER

The pasteurization plant is a pilot plant for low viscosity liquids, adaptable to the specific product to be treated. The technical specifications are shown in table 24:

Table 24 Pasteurizer technical specifications

Manufacturer	SANOVO Technology Italia
Electric power supply	3 × 400V - 50 Hz
Installed power	~12 KW
Maximum working pressure	10 bar
Maximum working temperature	100°C
Compressed air consumption	Max 20 L/min at P = 7 - 10 bar
Steam Consumption	Max 1000 L/h - Inlet Pressure 0.5 - 3 bar
Frozen Water Consumption	Max 1200 L/h 0/+1°C - Inlet Pressure ~2 - 3 bar

The whole system can be managed on the screen using the WinCC management software. However, it is also possible to use the physical buttons on the outside of the electrical panel. The liquid is withdrawn by a compressed air pump and sent inside a 25-liter hermetic tank. Inside this tank it is possible to measure the conductivity of the product and the level of the liquid, which allows to manage emptying and filling on the screen. The tank is at atmospheric pressure and is equipped with a side outlet to prevent overflow. The liquid is drawn from this tank using two separately controllable pumps: a centrifugal pump, which guarantees high flow rates, and a volumetric pump, which is able to treat higher viscosity products. They push the liquid into the section where the heat exchanges take place.

There is a first pre-heating phase in the heat recovery section, in which the cold product exchanges heat by passing through two series of tube-in-tube exchangers counter-current with the hot one leaving the thermal stop. The exchange is therefore indirect and the service fluid used is water. After this pre-heating, the product is pushed inside the homogenizer. Finally, the product passes through a tube and shell exchanger where it exchanges with the hot water present on the shell side. Hot water is produced in the same pasteurizer using an additional counter-current tube exchanger in which the water exchanges with steam produced by a special boiler. The water temperature of the shell is of fundamental importance for controlling the temperature of the product. The next step is the radiofrequency heating, in which the product passes through the applicator and is heated rapidly and volumetrically thanks to the interaction with the electric field.

Outside the RF section, the product passes through the insulated pipes dedicated to the thermal holding. These can be modulated in length, directly correlated to the travel time, from a minimum of 6.48 seconds to a maximum of 70.69 seconds, so as to be able to process products that require different dwell times. Downstream of the holding, the product is first

pre-cooled, as mentioned before, in the heat recovery exchangers, and then cooled with icy water in order to block the proliferation of any thermophilic bacteria that may have survived the pasteurization. This is also a counter-current tube-in-tube exchanger, which uses cold water produced by a special chiller as an exchange fluid. The parts of the system presented are indicated in red in figure 54:

Figure 54 Pasteurization plant

4.4.2 RF SYSTEM

The RF section is the block in which the applicator and the radiofrequency generator circuit are housed. The structure and the components of this section have been fully described in paragraph 1.2.1.

The power supply, the generator and the applicator are located inside three steel compartments that act as a mechanical support, as a screen for electromagnetic fields towards the external environment and as a closure of the electrical circuit to earth.

The RF section is managed by PLC and can be controlled by an external touch screen embedded in one of the lateral steel panels, at the height of the power supply block.

4.4.3 PACKAGING MACHINE

The last part of the plant is dedicated to aseptic packaging in sterile bags or in 25-liter drums through a packaging machine whose technical specifications are shown in table 25:

Table 25 Packaging machine technical specifications

Manufacturer	Boema S.p.A.
Electric power supply	3 × 400V - 50 Hz
Installed power	~1 KW

The machine, shown in figure 55, uses steam and hot water as a service fluid, for washing and for the sterilization.

Figure 55 Aseptic packaging machine

Sterility is guaranteed by the constant presence of steam in the head of the packaging machine; where the temperature drops below the necessary threshold, the safety devices prevent the packaging from continuing until the temperature conditions are re-established for a certain period of time.

The packaging machine can also be managed on the video, using a touch screen installed on the side of the machine itself.

4.4.4 EXPERIMENTAL TESTS

The experimental tests on the product of interest were carried out, after the development with water, on raw milk. It was taken from a local producer, transported at a temperature of 4°C in a steel tank to the test room of the Officine di Cartigliano and immediately treated. The milk test consisted of three main phases:

- Preparation;
- Production;
- Wash.

The first and third phases are part of the sanitation processes, in order to control and prevent those factors that affect the quality and safety of products.

Production is the phase in which the product enters, is processed and sent to the packaging machine where it will be bagged. The main stages are:

1. *VAT Empty* - the collection tank is emptied with water that was used for washing and at the same time the circuit goes into an open cycle;
2. *PHE Line Filling* - the milk is pumped into the filling tray of the pasteurizer and after enters the circulation, pushing the water still present in the pipes;
3. *Real Production* - the production becomes effective after all the water has been pushed out of the milk. The pasteurizer works at full capacity;
4. *VAT Empty* - after production, the tank is emptied of milk and filled with water for the subsequent washing;
5. *Production Recovery* - the water in the tray pushes the milk still present in the pipes outside the system;
6. *Rinsing* - a first rinse is carried out with system water.

The final washing removes the possible incrustations typical of a dairy establishment, such as those deriving from the denaturation of proteins, from the polymerization of fats, the caramelization of sugars.

4.4.4.1 ENERGY BALANCE

The energy balance was calculated collecting data from the video interface of the RF machine. The modifiable parameter for controlling the temperature of the product outside the RF

section is the voltage. It depends on the power delivered by the machine and on the anode current to the triode. From the on-screen management software of the machine, controlled by PLC, it is possible to view these values and choose whether to work by setting a desired value of power to be delivered to the product or temperature of the product at the outlet.

From the data read on the screen it is possible to trace all the information necessary for the complete energy balance. The input voltage to the applicator is calculated as:

$$V = \frac{P}{I} \qquad (9)$$

Where *V* is the voltage that is supplied at the input to the electrode, *P* is the power and *I* is the anode current. The power and the anode current can be read directly from the PLC. However, only a portion of the power will be transferred to the product in the form of heat, while the other will be dissipated in losses:

$$P_p = \dot{m}\, c_p\, \Delta T \qquad (10)$$

Where P_p is the power transferred to the product, $\dot{m}$ is the mass flow rate, c_p is the specific heat and ΔT is the temperature difference between the fluid inlet and outlet. The power dissipated in loss, called no-load power, can be evaluated by difference:

$$P_v = P - P_p \qquad (11)$$

Where P_v is the no-load power.

In addition to the thermal balance and the evaluation of efficiency, thanks to the preliminary tests with water, all the pasteurizer holdings were analysed, in order to evaluate the quality of the thermal insulation.

4.4.4.2 PRELIMINARY TEST WITH WATER

The preliminary test involved heating the water in the pasteurizer up to a temperature of 80°C, which is the inlet temperature in the RF section. The values shown in table 26 were chosen as the set point for the T_{out}^{RF} , as they fall within the typical ranges of a pasteurization. These temperatures were reached over time with the same order in which they were reported, in fact, the temperature was first increased and then decreased with a step of 5°C.

Table 26 RF outlet temperatures and ΔT with water

Test	T_{in}^{RF}	T_{out}^{RF}	$\Delta T = T_{out}^{RF} - T_{in}^{RF}$
1	80°C	90°C	10°C
2	80°C	95°C	15°C
3	80°C	100°C	20°C
4	80°C	105°C	25°C
5	80°C	110°C	30°C
6	80°C	105°C	25°C
7	80°C	100°C	20°C
8	80°C	95°C	15°C
9	80°C	90°C	10°C

4.4.4.3 RAW MILK TEST

The test for the milk heating in the pasteurizer was conducted at two different temperatures: 80°C and 75°C, inlet milk temperatures to the RF section. The value of 95°C was chosen as the set point for the T_{out}^{RF} . As reported in table 27, the test was first carried out starting from 80°C and then from 75°C.

Table 27 RF outlet temperatures and ΔT with water

Test	T_{in}^{RF}	T_{out}^{RF}	$\Delta T = T_{out}^{RF} - T_{in}^{RF}$
1	80°C	95°C	15°C
2	75°C	95°C	20°C

The average residence time inside the applicator tube was estimated at 16.88 seconds while the holding time was 15 seconds. The product was packaged at a temperature of 6°C.

The points of the test with raw milk are less numerous than those with water, because making a temperature drop in a continuous process is particularly onerous when working with the real product. Changing the outlet temperature means changing the working point of the system; to complete this operation it is necessary to wait for a transient, during which the liquid flow rate is not valid as a sample and is lost. Furthermore, after the transitory, it is necessary to wait for the processed fluid at the desired working point to push out the product that is inside the tubes before the packaging machine.

5. RESULTS

5.1 DEVELOPMENT OF TEST PROTOCOLS AND IMPEDANCE MEASUREMENTS

The next paragraphs illustrate the results deriving from the development of measurement protocols for the different types of materials analysed and the data relating to their dielectric properties. The measurements were carried out in triplicate and consequently, the results are reported as the average of the made measurements.

5.1.1 LIQUID MATERIALS

The results of the impedance tests carried out on food liquids using the continuous laboratory scale treatment system illustrated in paragraph 4.2.1 will be shown below.

5.1.1.1 RAW MILK

Impedance measurements on raw milk were carried out using the continuous system at two different voltages to the power supply of the pump, corresponding to two different flow rates. The temperatures at which the measurement was carried out are 25, 50 and 70°C. The results at 27 MHz and 2.45 GHz are reported in table 28:

Table 28 Dielectric properties of raw milk at different temperatures at 27 MHz

T	Q=300 L/h				Q=500 L/h			
	27 MHz		2.45 GHz		27 MHz		2.45 GHz	
	ε'	ε''	ε'	ε''	ε'	ε''	ε'	ε''
25°C	85.69	334.07	68.21	14.45	85.72	333.88	68.22	14.45
50°C	86.63	544.18	62.00	18.57	86.47	535.62	62.26	18.37
70°C	87.59	680.21	58.11	21.78	87.36	670.40	58.35	21.53

The results reported above are of the same order of magnitude as those already present in the literature [22], but given the different compositions of raw milk analysed, there are differences between the values. In order to perform a regression, the results of the two flow rates were averaged and arranged on a plane to obtain a polynomial trend line of order two. In figure 56 regressions' results are shown.

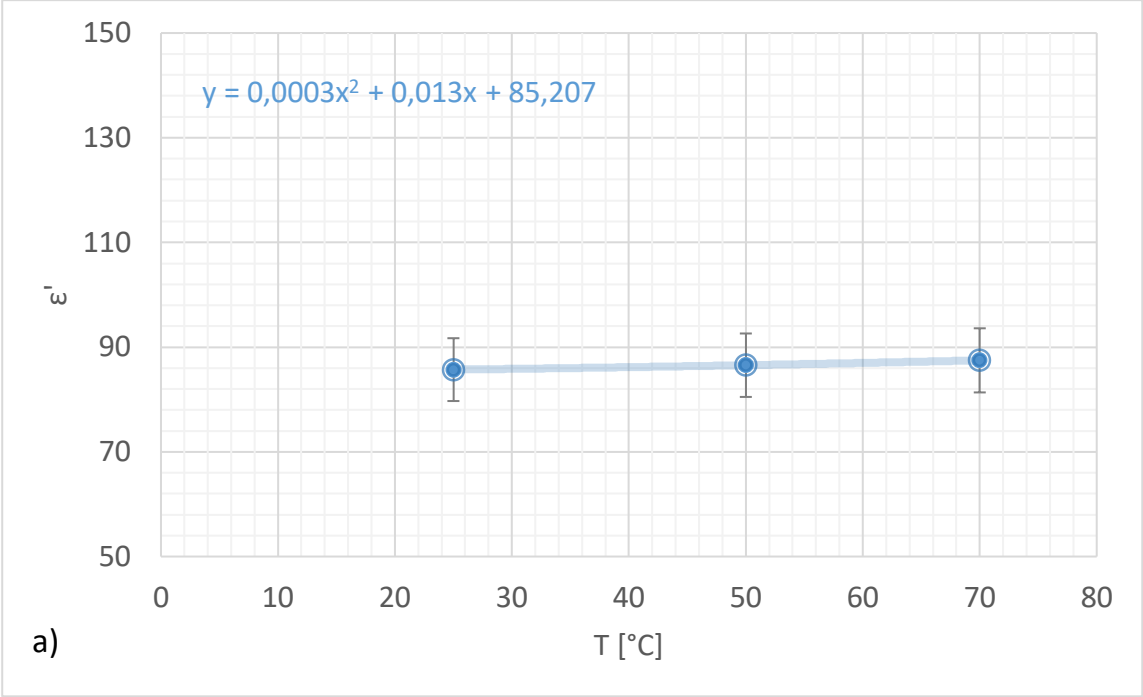

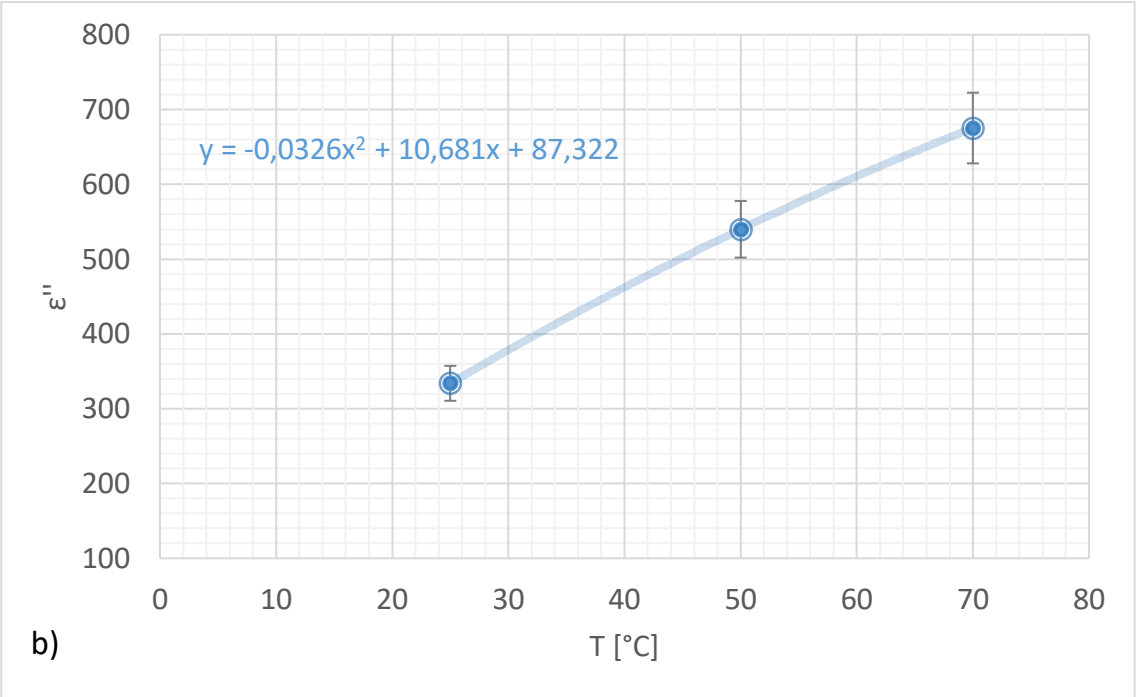

Figure 56 Dielectric properties of raw milk behaviour with temperature at 27 MHz a) ε' and b) ε''

Regression on ε’ at 27 MHz, parametric in temperature, was used in the definition of the properties of materials in COMSOL.

Also for the dielectric properties at 2.45 GHz, regressions are performed and their results are shown in figure 57:

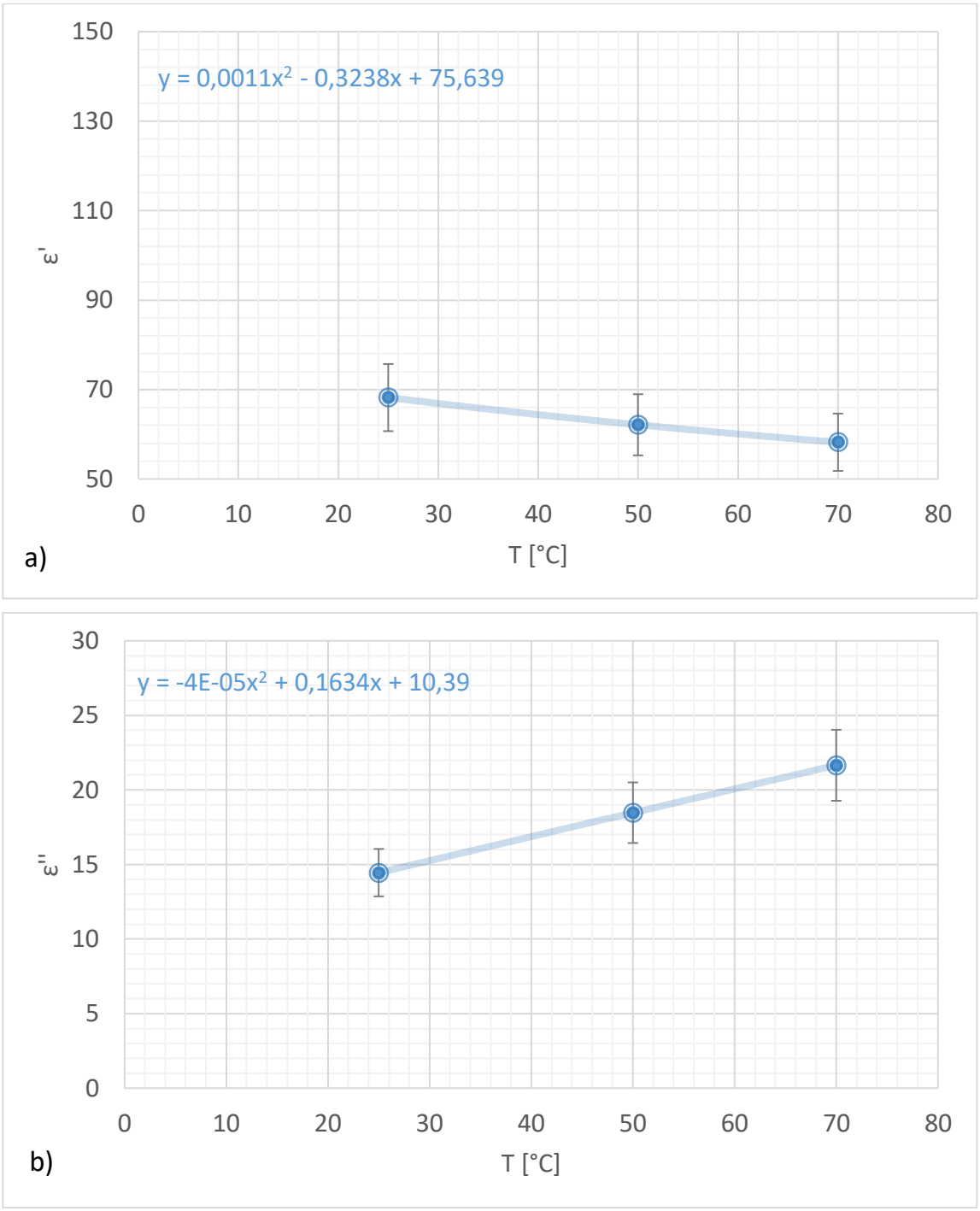

Figure 57 Dielectric properties of raw milk behaviour with temperature at 2.45 GHz a) ε' and b) ε''

5.1.1.2 ALMOND MILK

The two almond milk samples were also analysed using the continuous processing system (section 4.2.1) and they were heated up to a temperature of 135°C. In table 29 the results of both almond and organic almond milk at 27 MHz and 2.45 GHz are shown:

Table 29 Dielectric properties of almond and organic almond milk at different temperatures at 27 MHz and 2.45 GHz

T	Almond milk				Organic almond milk			
	27 MHz		2.45 GHz		27 MHz		2.45 GHz	
	ε'	ε''	ε'	ε''	ε'	ε''	ε'	ε''
30°C	76.16	53.71	68.24	10.34	77.85	46.09	71.44	10.08
50°C	73.08	78.96	64.00	6.99	68.78	70.69	66.21	6.26
80°C	62.27	118.42	57.32	4.98	62.19	98.80	59.61	4.52
100°C	58.55	141.49	53.16	4.48	57.07	117.63	54.79	3.86
120°C	54.86	163.81	48.10	4.18	53.40	132.83	50.98	3.49
135°C	53.03	198.89	45.14	4.34	51.02	144.59	47.99	3.30

As can be seen from the values shown in table 30, the dielectric constant, in the two types of milk considered, tends to decrease with increasing temperature and no significant differences are observed in the values of ε' in both cases. As reported in the literature, in fact, the dielectric constant decreases with increasing temperature. Furthermore, the loss factor, in both cases, tends to increase with the temperature. This is in accordance with what is reported in the literature, as ε'' increases with increasing temperature in the radio frequency range. There are some slight differences in the loss factor values. This could be due to the different chemical composition of the two products. In fact, in almond milk there are emulsifiers, which are absent in organic almond milk. These emulsifiers are polar molecules and, as such, could lead to an increase in the loss factor of the product.

There are no data in the literature with which to compare these results, but given the composition of the samples, they appear to be very plausible.

Since the values of the dielectric properties for the two samples are, on the whole, very similar to each other, it was decided to average the measurements between the two types of almond milk and thus derive a single regression function common to both. The polynomial trend lines at 27 MHz are shown in figure 58:

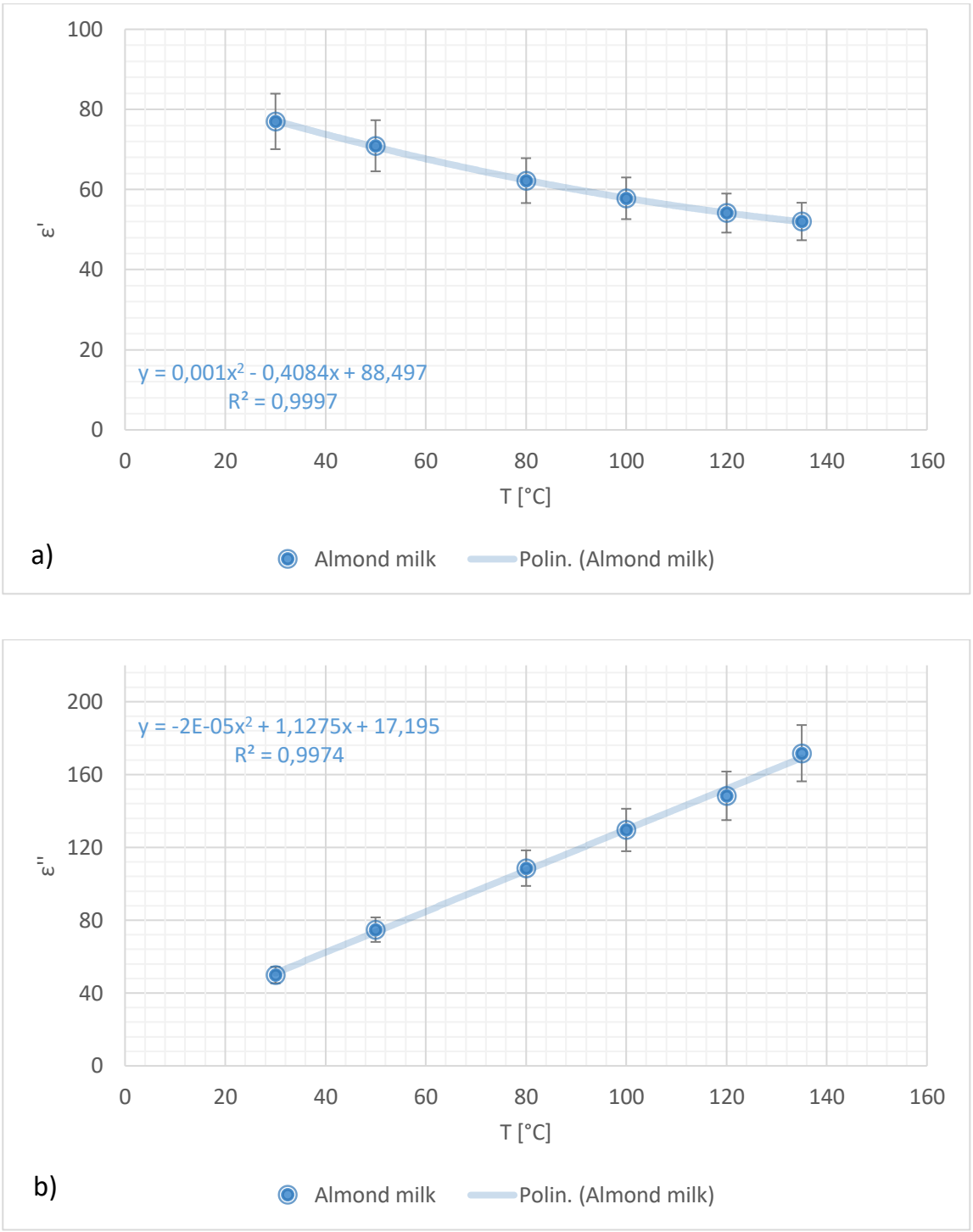

Figure 58 Dielectric properties of almond milk behaviours with temperature at 27 MHz a) ε' and b) ε''

The regressions are performed in the same way at the frequency of 2.45 GHz. The results are shown in figure 59:

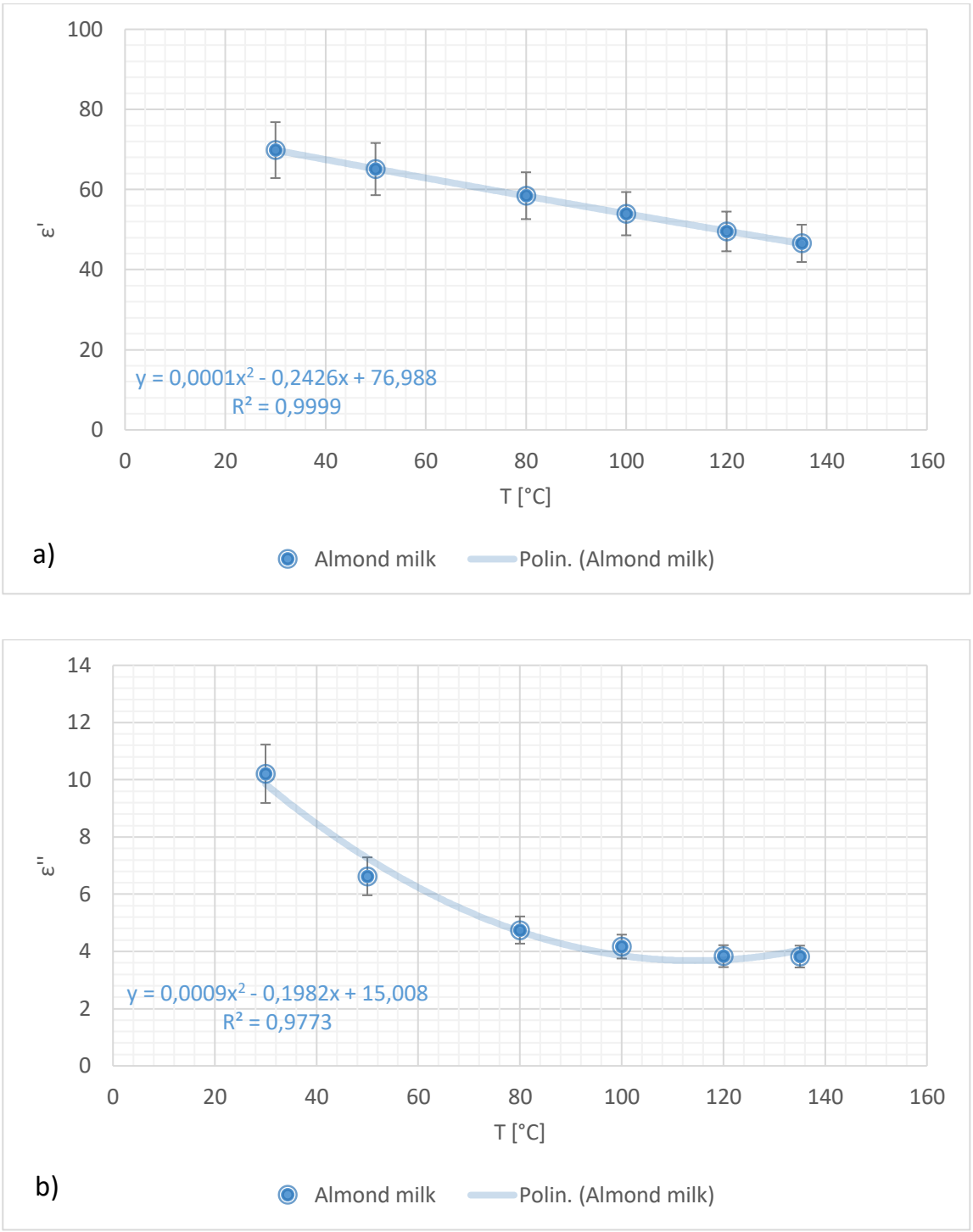

Figure 59 Dielectric properties of almond milk behaviours with temperature at 2.45 GHz a) ε' and b) ε''

5.1.1.3 FRUIT JUICES

The three types of fruit juices, cranberry, pomegranate and pear juice, were also tested with the continuous system and heated up to a temperature of 85°C. The dielectric properties of the samples are shown in the following table:

Table 30 Dielectric properties of cranberry, pomegranate and pear juices at different temperatures at 27 MHz and 2.45 GHz

T	Cranberry				Pomegranate				Pear			
	27 MHz		2.45 GHz		27 MHz		2.45 GHz		27 MHz		2.45 GHz	
	ε'	ε''	ε'	ε''	ε'	ε''	ε'	ε''	ε'	ε''	ε'	ε''
25°C	78.5	81.0	70.9	12.2	80.9	125.8	72.2	12.2	79.5	93.0	72.0	12.3
35°C	77.1	87.4	70.0	10.9	79.6	144.1	70.8	10.9	78.0	106.5	70.6	10.7
50°C	74.5	106.8	67.3	8.9	76.2	177.9	67.0	8.9	76.8	119.0	69.4	9.7
65°C	73.2	117.9	65.9	8.0	74.8	216.8	64.6	7.9	75.6	130.4	68.0	8.8
75°C	72.9	124.3	65.3	7.9	72.6	241.0	61.6	7.3	71.9	173.7	63.2	7.0
85°C	72.2	130.7	64.5	7.7	70.8	261.2	59.3	7.1	69.3	191.3	60.1	6.5

As can be seen from the above data, the dielectric constant values for the three types of juices are practically the same for both radiofrequency and microwave. As for the loss factor, however, there are more differences between the values at 27 MHz, while those at 2.45 GHz are very similar to each other. In the literature [23] there are data only regarding pear juice and these are in agreement with those shown in table 30.

Given the diversity of the values of ε'' at 27 MHz, it was preferred to obtain a specific regression for each type of juice at this frequency, while an average was made between the three juices for the values of ε'. The results of the regressions are shown in the following figures:

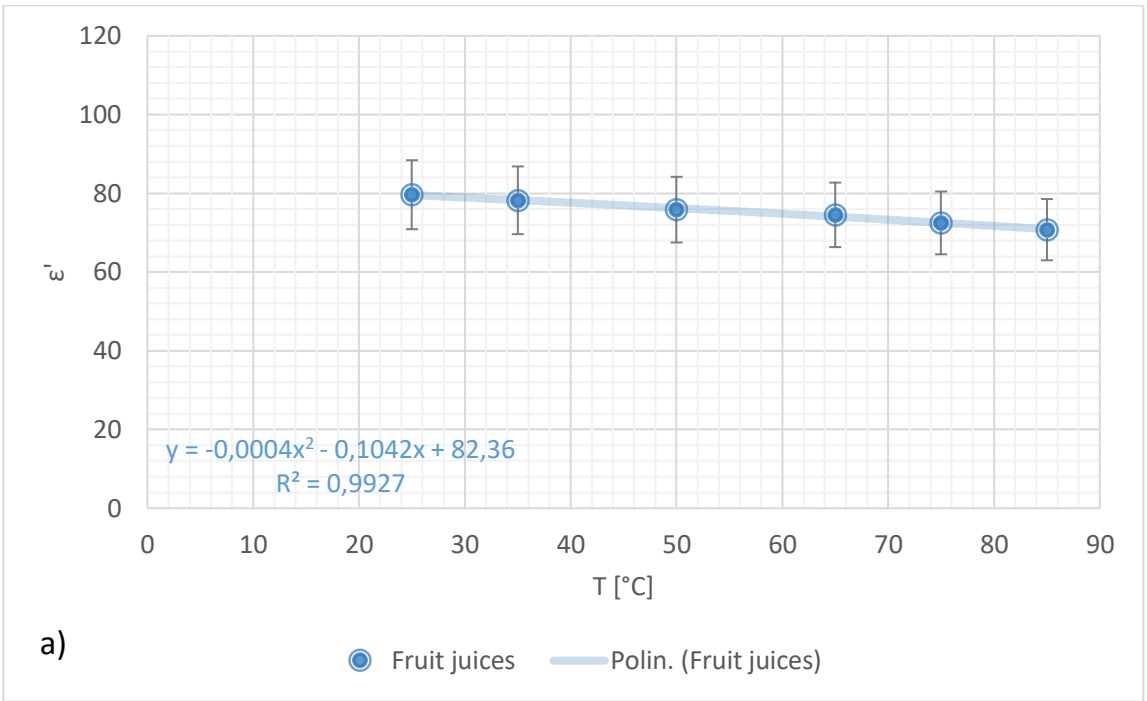

a)

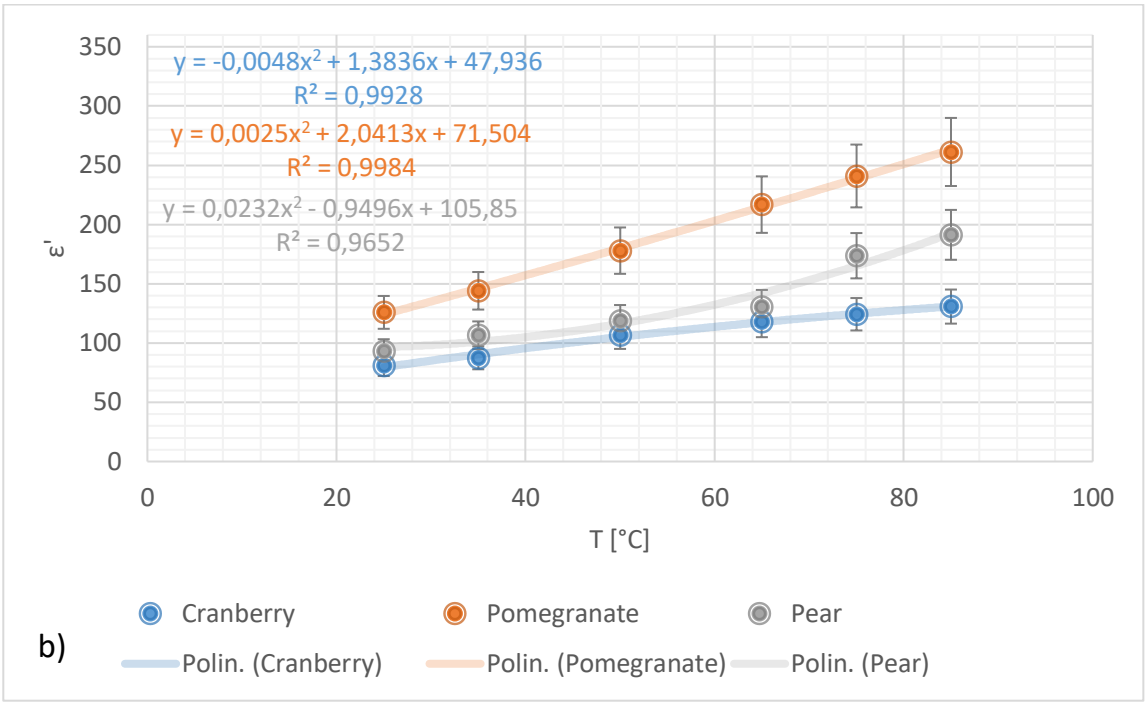

Figure 60 Dielectric properties of fruit juices behaviours with temperature at 27 MHz a) ε' and b) ε''

For the regressions at 2.45 GHz, the average of the values for both the dielectric constant and the loss factor of the three sample types was evaluated. The results of the regressions are shown in figure 61:

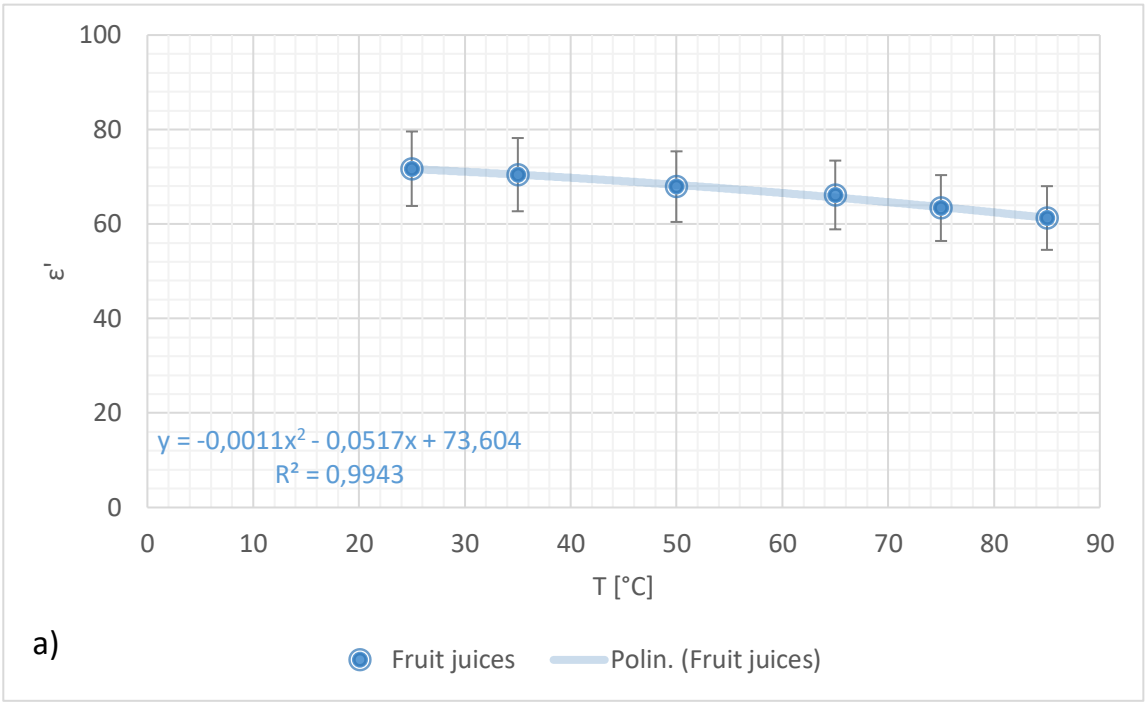

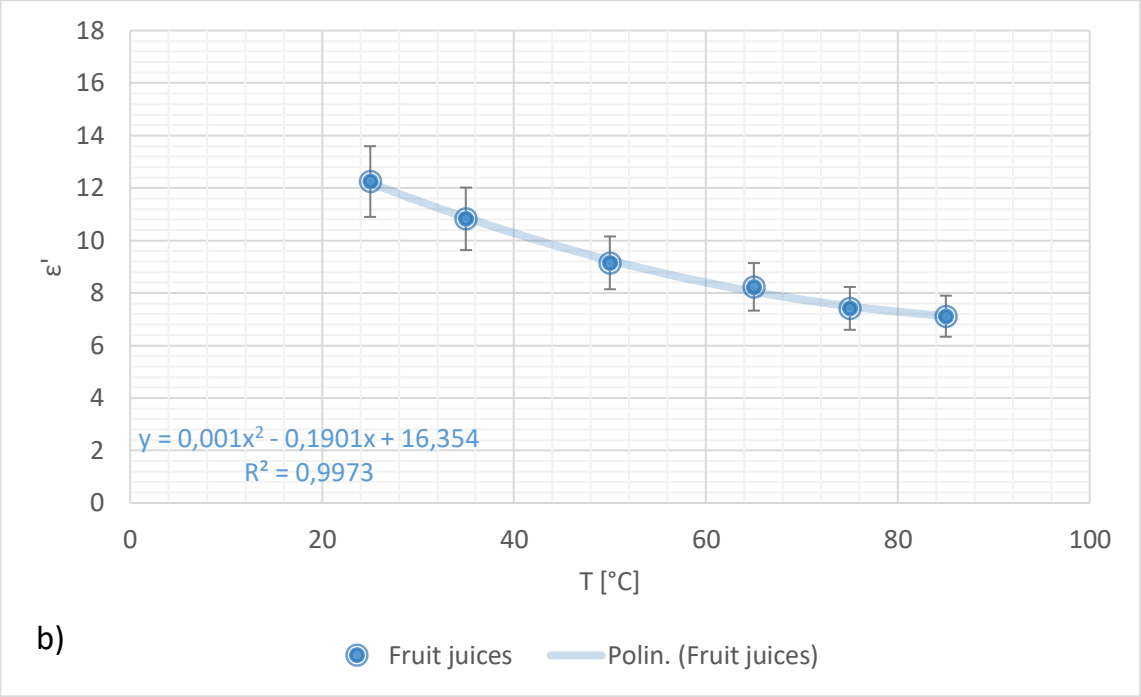

Figure 61 Dielectric properties of fruit juices behaviours with temperature at 2.45 GHz a) ε' and b) ε''

5.1.2 FLUID MATERIALS

The results of the impedance tests carried out on food fluids using the static laboratory scale treatment system illustrated in paragraph 4.2.2 will be shown below. Since the heating took place with the use of a microwave oven, it was not possible to exceed 90°C, both for the handling of the sample and for the start of the boiling of the same.

5.1.2.1 PUREES

Two types of fruit purees, strawberry and peach purees, with and without pieces were heating using the Whirlpool Extra Space microwave oven. The warm-up occurred at 10 second intervals and at each step temperatures and dielectric properties were measured. The tests results at 27 MHz and 2.45 GHz are shown respectively in tables 31 and 32:

Table 31 Dielectric properties of strawberry and peach purees with and without pieces at different temperatures at 27 MHz

T	Strawberry		Strawberry with pieces		Peach		Peach with Pieces	
	ε'	ε''	ε'	ε''	ε'	ε''	ε'	ε''
28°C	95.24	261.63	98.30	362.63	96.72	321.18	94.05	260.87
51°C	96.26	346.60	96.92	437.08	98.10	380.96	91.98	295.98
71°C	100.84	410.67	90.64	497.99	100.06	455.33	85.64	358.79
85°C	94.35	426.16	74.11	414.64	103.38	531.87	81.18	342.16

Table 32 Dielectric properties of strawberry and peach purees with and without pieces at different temperatures at 2.45 GHz

T	Strawberry		Strawberry with pieces		Peach		Peach with Pieces	
	ε'	ε''	ε'	ε''	ε'	ε''	ε'	ε''
28°C	72.9	13.1	70.9	13.7	71.6	14.2	67.5	13.3
51°C	69.8	11.6	64.2	12.1	69.6	13.2	60.3	11.0
71°C	67.3	11.3	56.4	11.2	66.3	12.4	46.3	8.3
85°C	64.2	11.3	50.0	10.2	64.0	12.6	52.0	9.5

In the literature only the data of strawberry puree in the microwave range have been found [42], and there is much agreement with the values obtained from the experimental tests, so also the radiofrequency results are considered plausible. For the peach puree we can compare the tests results with the dielectric values of the peach at microwave frequency [43] and also in this case there is a good agreement. As is evident from the data shown, the dielectric properties appear to be very similar between the two types of purees and the presence of the pieces does not seem to affect them either at radio frequencies or in microwaves.

For this reason, the regressions were performed by averaging the values on the analysed samples. The results at 27 MHz are shown in the following graphs:

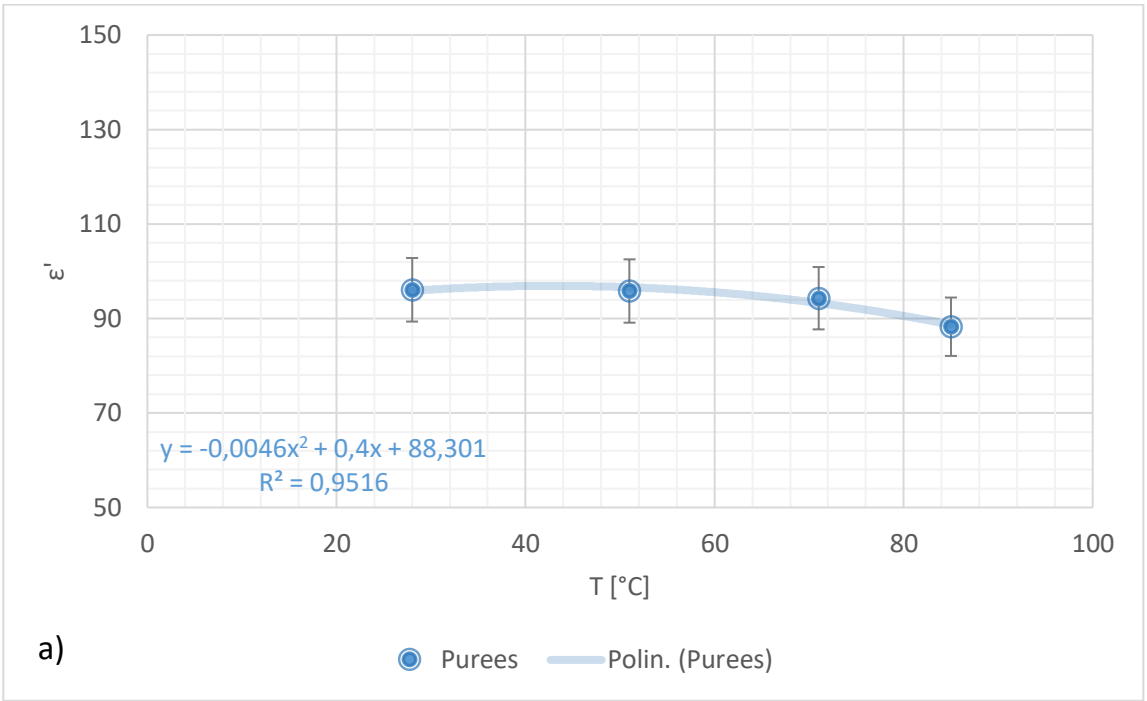

a)

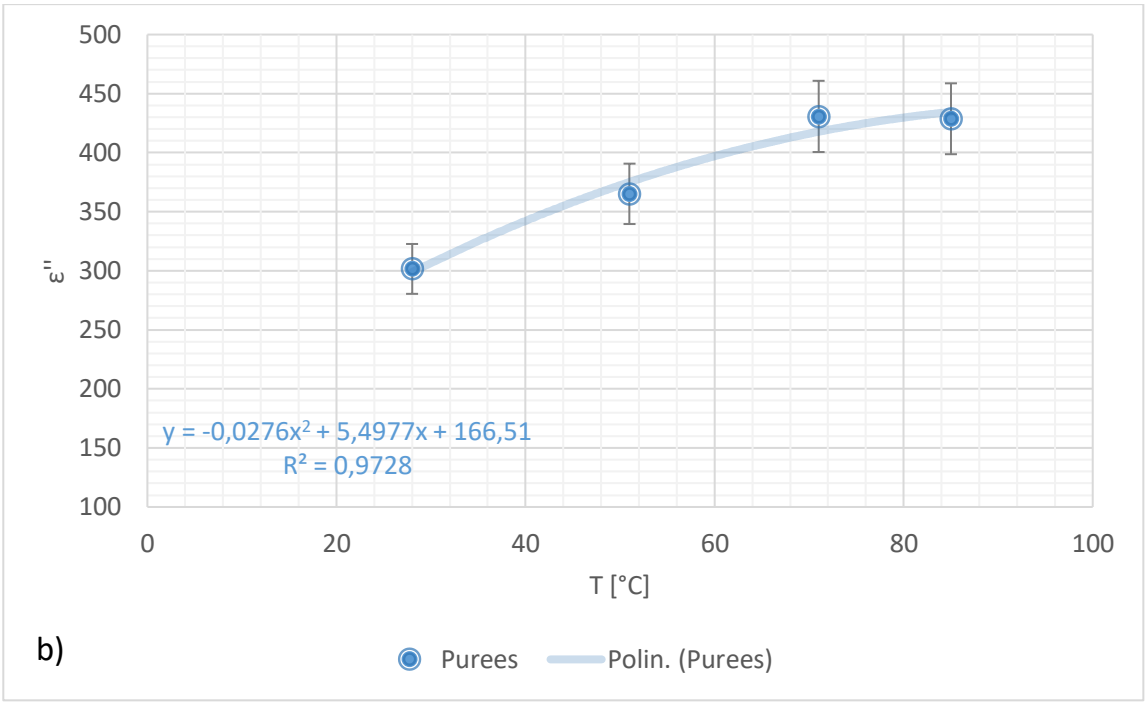

Figure 62 Dielectric properties of fruit purees behaviours with temperature at 27 MHz a) ε' and b) ε''

The regressions are performed in the same way at the frequency of 2.45 GHz. The results are shown in figure 63:

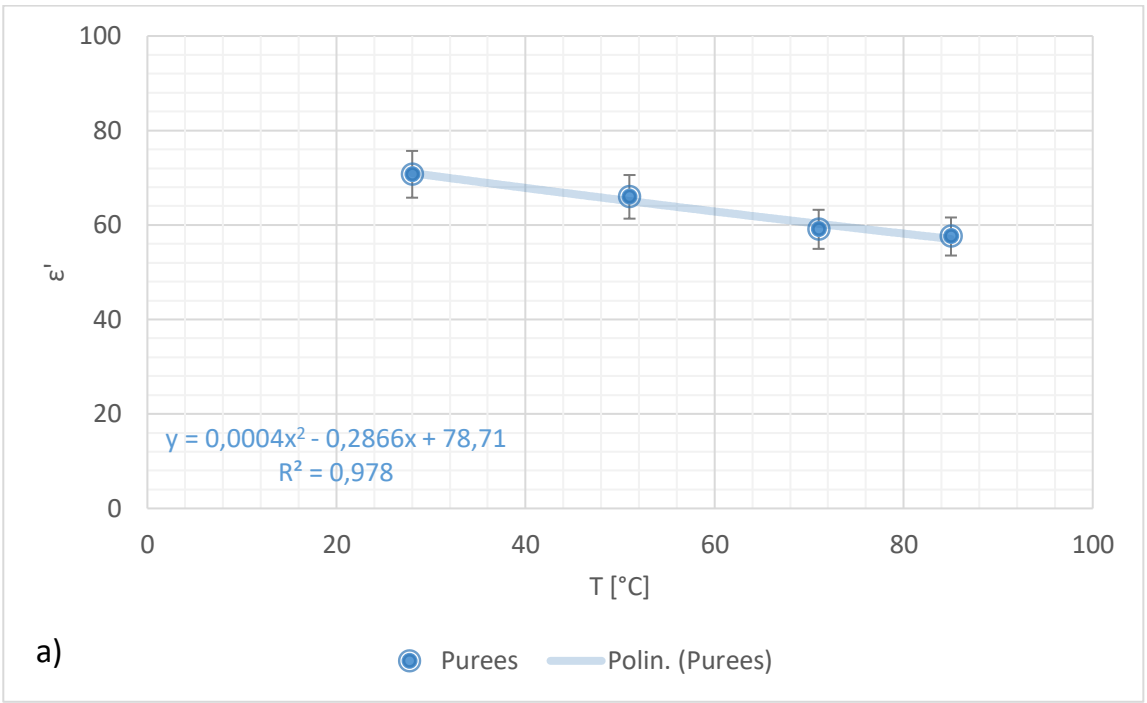

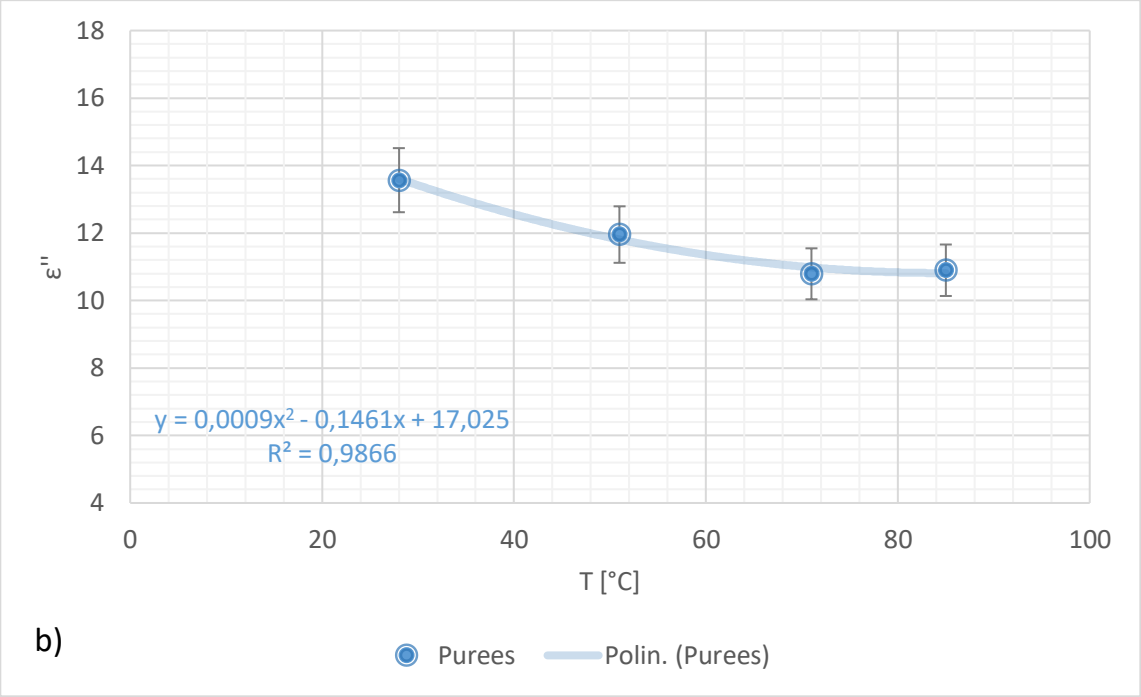

Figure 63 Dielectric properties of fruit purees behaviours with temperature at 2.45 GHz a) ε' and b) ε''

5.1.2.2 ICE CREAM PREPARATIONS

Ten types of ice cream preparations were tested using the laboratory static system. For some samples, there was no possible to exceed 75°C due to the alcohol content. The tests results at 27 MHz and 2.45 GHz are shown from tables 33 to 36:

Table 33 Dielectric constants of ice cream preparations at different temperatures at 27 MHz

T	Black Cherry	Fig	Straw-berry	Wild Straw-berries	Wild Berry	Pine-apple Jelly	Toffee Milk topping	Bourbon Vanilla	VQS Straw-berry	Eggnog
	ε'									
10°C	49.57	38.21	48.03	53.70	53.54	60.41	48.42	40.85	54.46	40.34
30°C	48.37	40.71	46.54	48.81	51.73	54.63	47.81	37.09	56.10	43.03
50°C	39.81	38.54	42.01	47.17	51.96	52.89	47.33	36.71	55.51	38.74
75°C	48.48	38.17	41.25	40.77	49.50	52.04	47.34	35.68	54.44	33.26
90°C	46.00	36.70	36.89	40.11	41.19	48.92	32.49	32.33	53.26	-

Table 34 Loss factors of ice cream preparations at different temperatures at 27 MHz

T	Black Cherry	Fig	Straw-berry	Wild Straw-berries	Wild Berry	Pine-apple Jelly	Toffee Milk topping	Bourbon Vanilla	VQS Straw-berry	Eggnog
	ε''									
10°C	8.54	9.41	7.05	8.50	8.85	11.62	10.01	6.24	12.44	8.90
30°C	8.75	9.62	6.30	6.96	8.75	6.07	8.66	5.09	14.28	10.13
50°C	6.88	9.20	5.82	7.08	9.83	5.93	8.81	5.30	16.97	10.77
75°C	8.75	9.89	5.68	6.66	9.89	6.23	9.57	6.04	21.75	12.41
90°C	9.96	11.41	5.88	9.76	11.49	6.76	8.74	5.68	29.14	-

Table 35 Dielectric constants of ice cream preparations at different temperatures at 2.45 GHz

T	Black Cherry	Fig	Straw-berry	Wild Straw-berries	Wild Berry	Pine-apple Jelly	Toffee Milk topping	Bourbon Vanilla	VQS Straw-berry	Eggnog
	ε'									
10°C	22.65	15.67	22.57	28.71	27.24	39.21	25.90	19.78	31.77	19.27
30°C	26.64	17.94	23.62	25.02	28.29	32.41	24.86	20.85	34.69	22.40
50°C	21.68	18.28	22.50	27.54	31.50	33.09	26.37	24.41	36.69	22.20
75°C	28.68	19.55	24.43	25.06	30.89	35.43	28.56	20.89	38.65	20.45
90°C	29.43	20.31	22.23	27.95	27.12	35.20	21.71	19.88	39.38	-

Table 36 Loss factors of ice cream preparations at different temperatures at 2.45 GHz

T	Black Cherry	Fig	Straw-berry	Wild Straw-berries	Wild Berry	Pine-apple Jelly	Toffee Milk topping	Bourbon Vanilla	VQS Straw-berry	Eggnog
	ε''									
10°C	12.29	8.12	11.58	13.90	14.13	15.03	12.02	10.17	14.67	10.66
30°C	12.18	8.98	11.43	12.57	13.75	14.69	11.82	9.22	15.01	11.55
50°C	9.98	8.56	9.91	12.29	13.69	14.07	11.74	8.91	14.43	10.12
75°C	12.32	8.60	9.65	10.37	12.89	13.43	11.63	8.09	13.38	8.01
90°C	11.16	8.18	8.06	9.33	9.88	11.89	7.26	7.23	12.03	-

There are no data in literature on the dielectric properties of ice cream preparations with which compare the obtained data. As is evident by observing the above data, the dielectric constant and the loss factor are quite similar between the various types of ice cream preparations, both in the radio frequency and microwave ranges. Only the ε'' values of the VQS strawberry at 27 MHz deviate from the general trend. For this reason, carrying out the regressions, to identify the trend of the loss factor at 27 MHz, it was decided to average the values excluding the VQS strawberry, while for all the other trends, it was decided to include

it. The results of the performed regressions are shown in the following graphs:

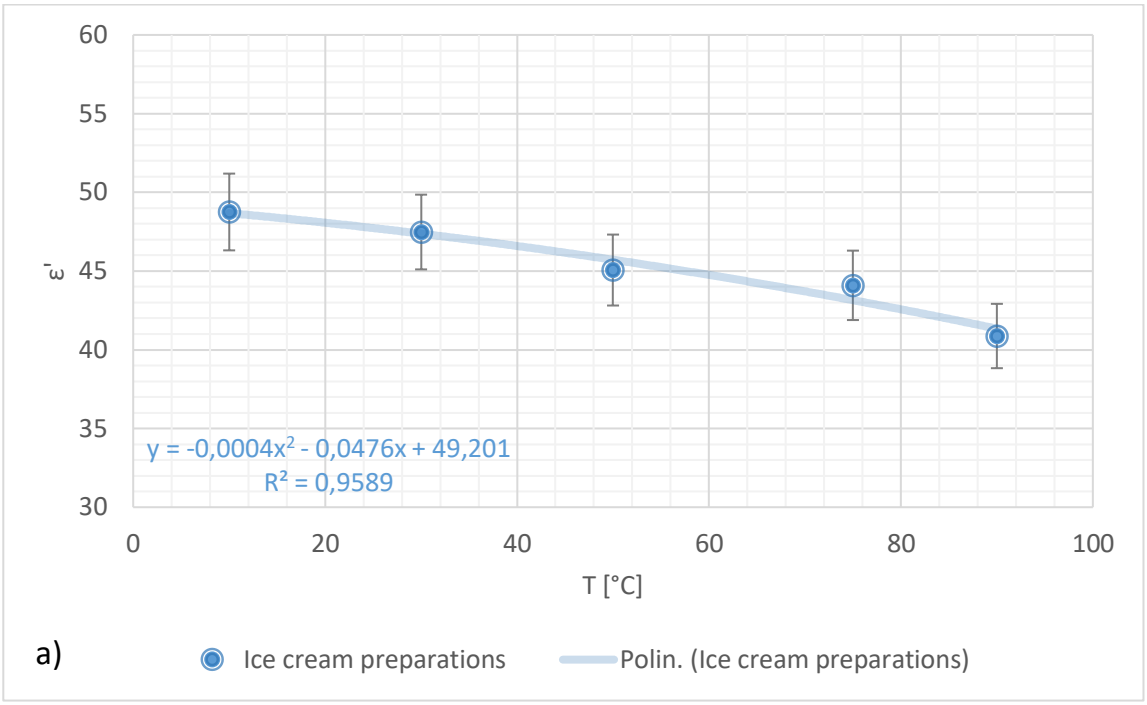

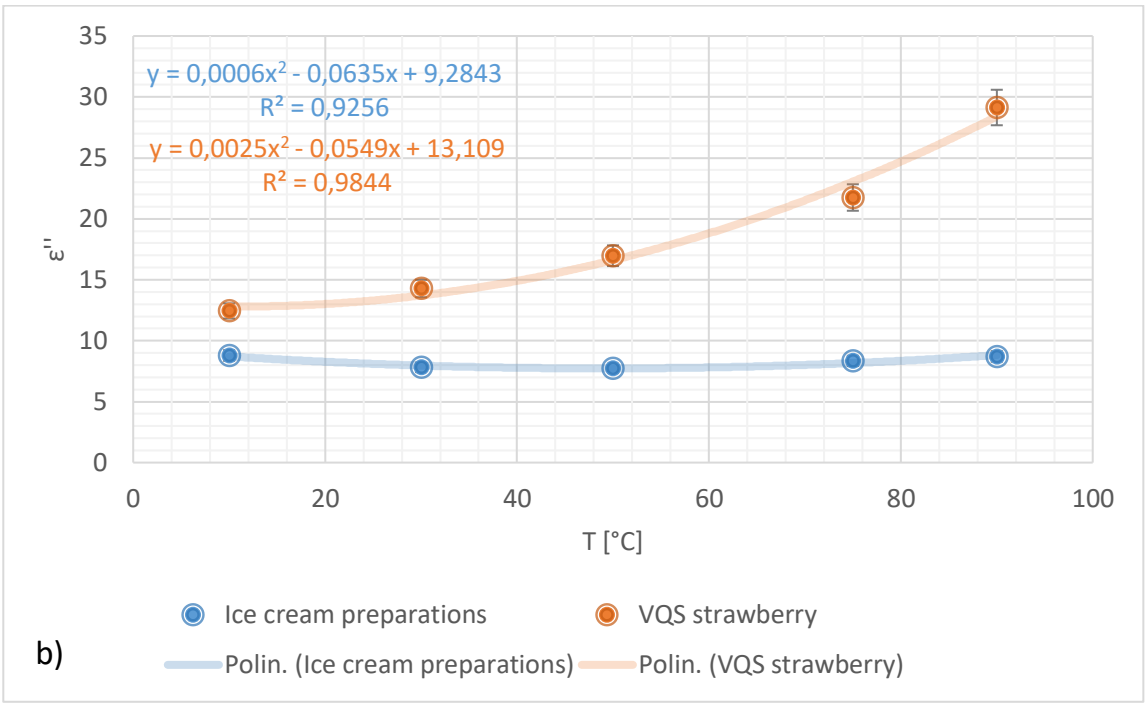

Figure 64 Dielectric properties of ice cream preparations behaviours with temperature at 27 MHz a) ε' and b) ε''

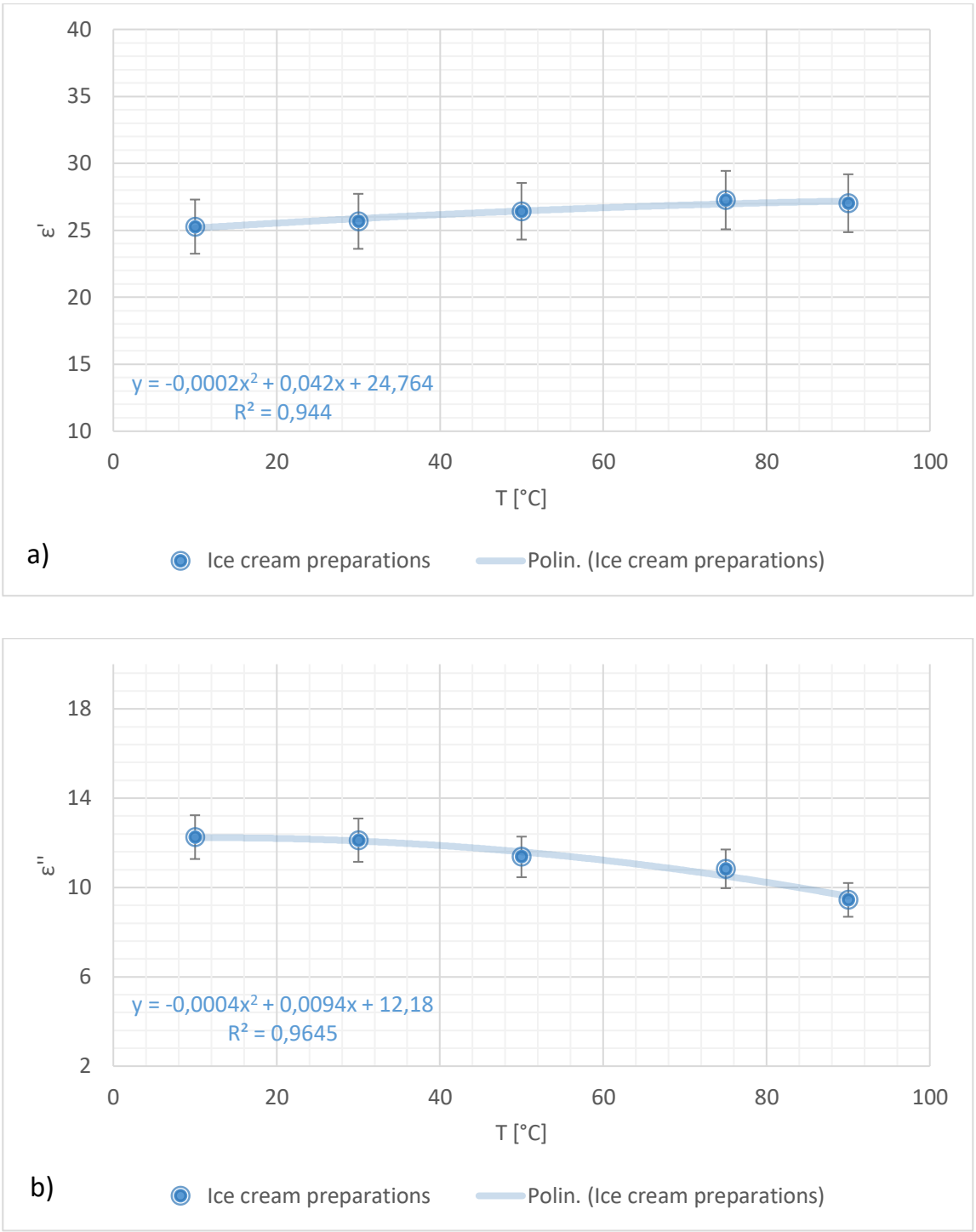

Figure 65 Dielectric properties of ice cream preparations behaviours with temperature at 2.45 GHz a) ε' and b) ε''

5.1.3 SOLID FOOD MATERIALS

The results of the impedance tests carried out on solid food products using the static laboratory scale treatment system illustrated in paragraph 4.2.2 will be shown below. As already mentioned, to allow perfect contact between the surface of the probe and the surface of the samples, the seeds examined were ground and compressed in order to obtain a tablet

of the same composition and density as the seeds. The tablets were heated at 10 seconds steps and at each step temperatures and dielectric properties were measured. The maximum reached temperature for both the materials not exceeded 50°C to avoid water evaporation. To validate the measurements made on the tablets, a thermal approach was also adopted (figure 66) which aims to compare the data obtained with the use of the impedance analyser with those calculable from the thermal increase according to equation (A-24).

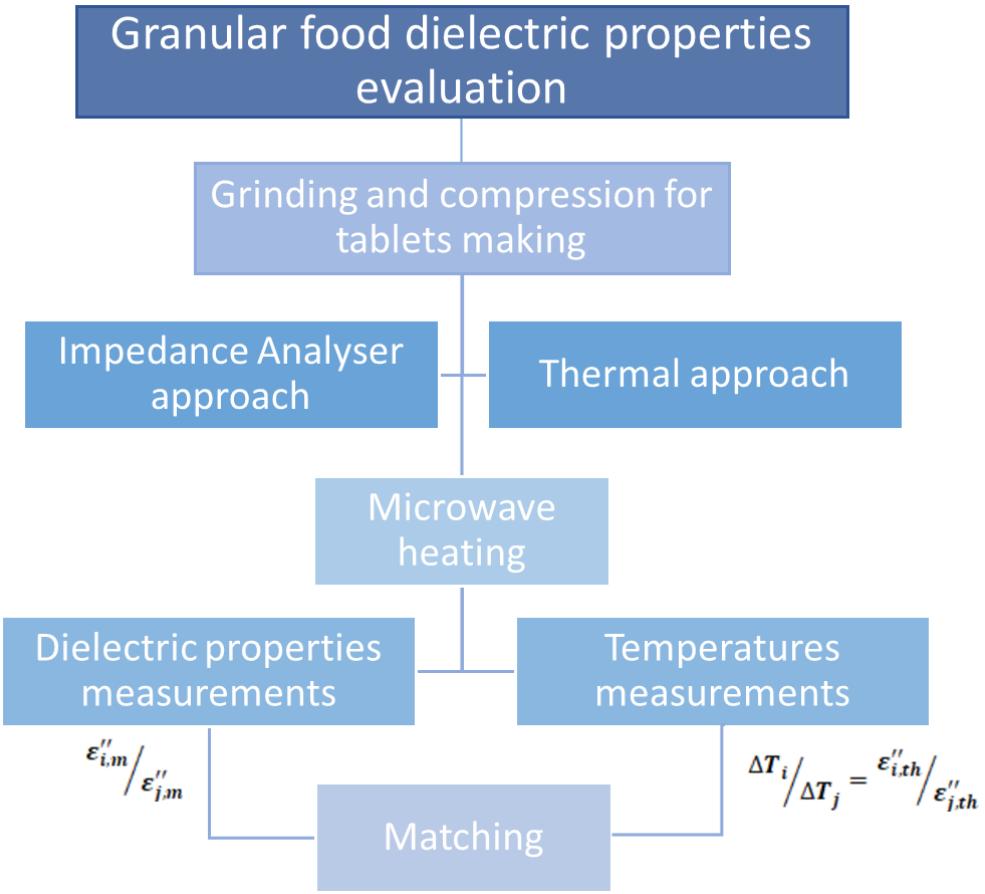

Figure 66 Used methods to measure the dielectric properties of granular foods

If the results obtained from the two approaches are in agreement, the correctness of the measurements made with the tablets is verified. Of course, since the heating takes place with a microwave oven, only the values of the dielectric properties at 2.45 GHz were taken into consideration for the validation.

5.1.3.1 SUNFLOWER SEEDS

For sunflower tablets four heating were performed and the temperature increasing grows gradually at each step from 27°C to 46°C. In figure 67 the trends of the dielectric properties with temperatures are shown:

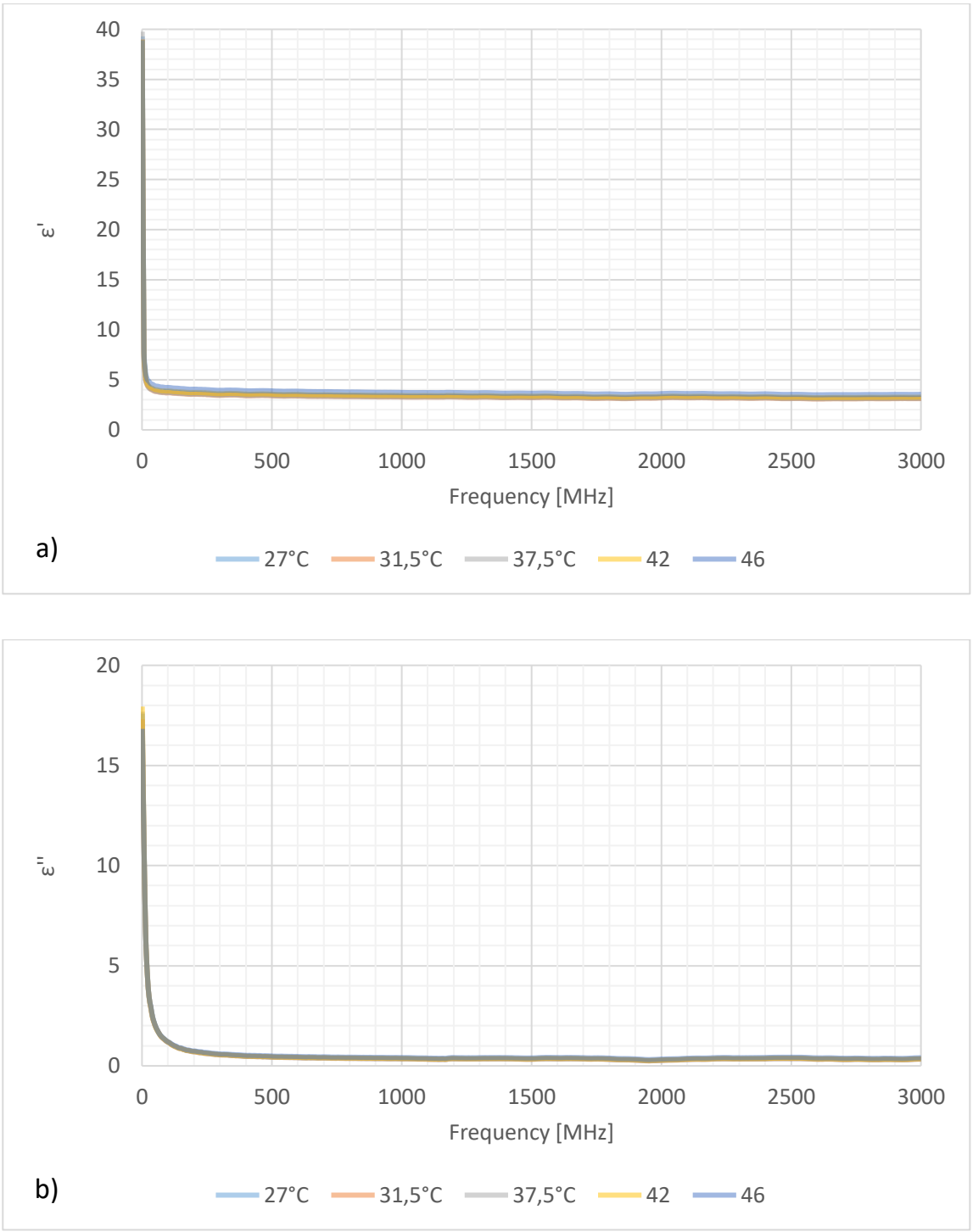

Figure 67 Dielectric properties sunflower seeds tablets behaviours with temperature in radiofrequency and microwave ranges a) ε' and b) ε''

In order to evaluate the dielectric properties using the thermal increases due to microwave heating, in table 37 the temperatures reached after every step and the valuation of the temperature variations ratio are shown:

Table 37 Temperature variations for sunflower seeds

Temperature	ΔT	$\Delta T_i / \Delta T_j = \varepsilon''_{i,th} / \varepsilon''_{j,th}$
27.0°C	-	-
31.5°C	4.2	-
37.5°C	4.8	0.875
42°C	5.05	0.9505
46 °C	5.4	0.935

At the same time, dielectric constant and the loss factor at 27 MHz and 2.45 GHz and also loss factors ratio at 2.45 GHz of compressed sunflower seeds after every MW heating step were measured and the results are summarized in table 38:

Table 38 Dielectric properties at 27 MHz and 2.45 GHz and loss factor variations at 2.45 GHz of sunflower seeds

Temperature	27 MHz		2.45 GHz			
	ε'_m	ε''_m	ε'_m	ε''_m	$\overline{\varepsilon''_m}$	$\varepsilon''_{i,m} / \varepsilon''_{j,m}$
27.0°C	4.2940	3.4419	3.2000	0.3705	-	-
31.2	4.2300	3.4500	3.1400	0.3630	0.3667	-
36.0	4.1752	3.4613	3.1574	0.3667	0.3648	1.005
41.05	4.3673	3.4315	3.2707	0.3875	0.3771	0.967
46.4	4.8328	3.4513	3.5579	0.4312	0.4093	0.921

The dielectric constant slightly increases with the temperature, while the loss factor is almost constant both in radiofrequency and microwave ranges. In the literature, data were found in a much lower frequency range than that analysed [27], so it was not possible to make comparisons with the obtained results.

In table 39 the loss factor ratios obtained through the two methods are shown.

Table 39 Loss factor ratio comparison for sunflower seeds

$\Delta T_i / \Delta T_j = \varepsilon''_{i,th} / \varepsilon''_{j,th}$	$\varepsilon''_{i,m} / \varepsilon''_{j,m}$	% E
0.875	1.005	14.857
0.9505	0.967	1.736
0.935	0.921	1.497

Except for the first results of the sunflower seeds, the values obtained with the two methods

are very close and the errors between them are lower than 2%.

Regressions were also performed for sunflower seeds in order to determine the temperature dependence of the dielectric properties, but at 27 MHz the evaluations were carried out only for ε', while ε'' was considered constant with the temperature and equal to 3.45. The results of the regression at 27 MHz are shown in the figure 68:

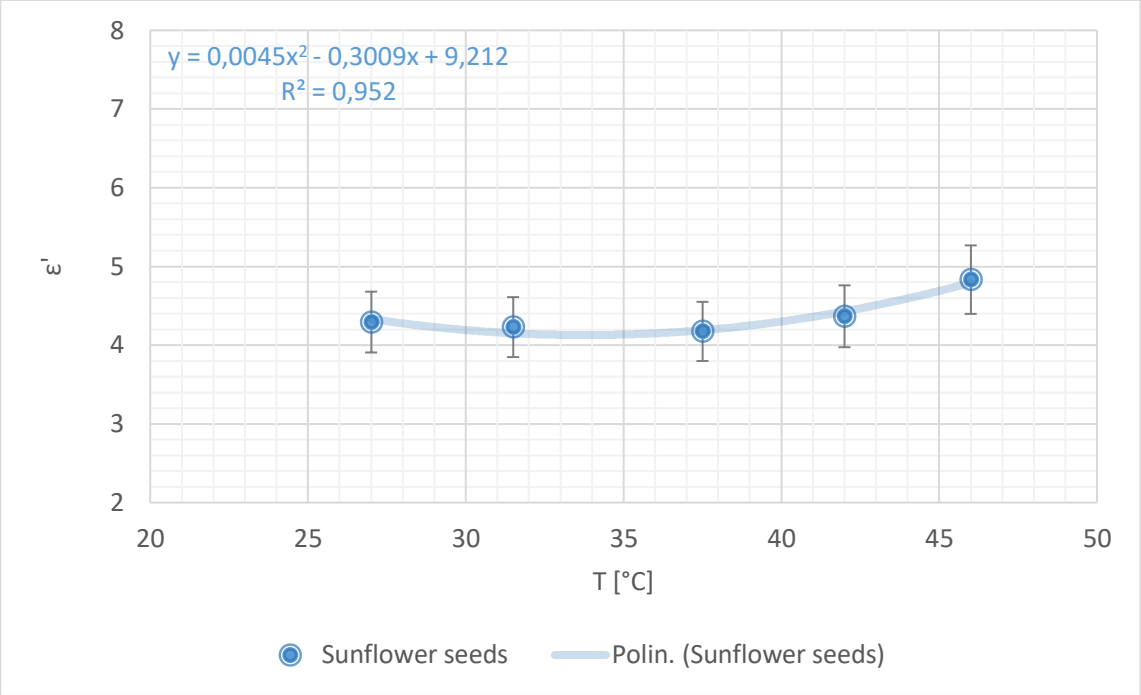

Figure 68 Dielectric constant of sunflower seeds behaviour with temperature at 27 MHz

At the frequency of 2.45 GHz, however, the regressions were performed for both ε' and ε'' and the results are shown in the following graph:

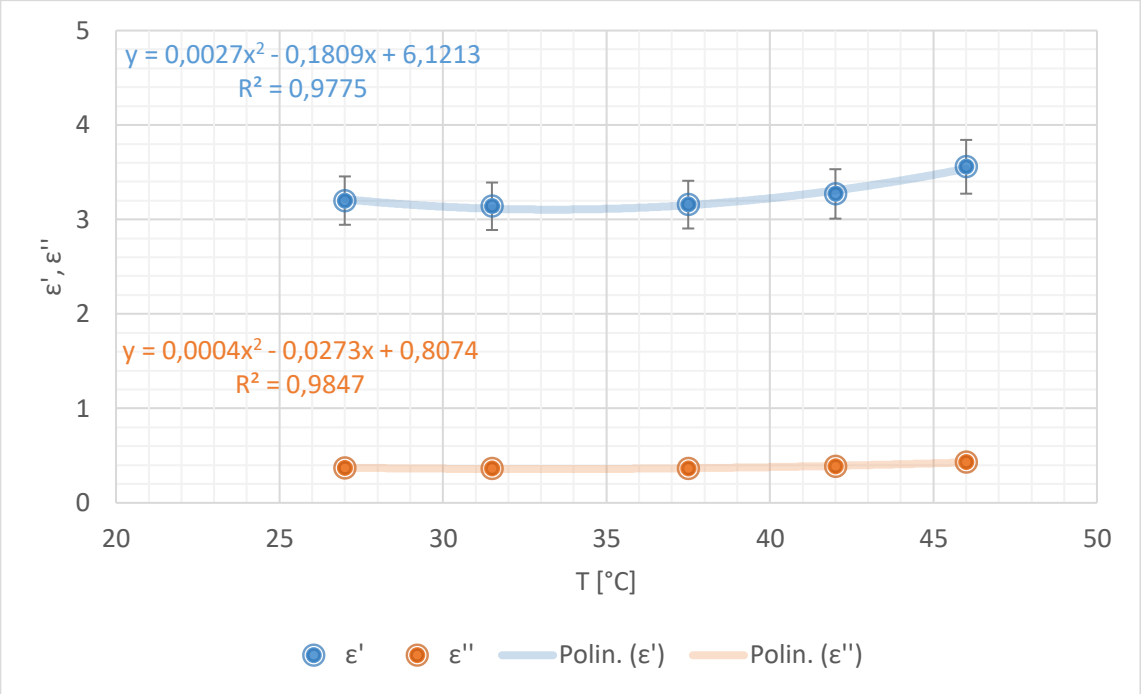

Figure 69 Dielectric properties of sunflower seeds behaviour with temperature at 2.45 GHz

5.1.3.2 FLAX SEEDS

For flax seeds tablets only two heating were performed due to the rapid temperature increase from 27°C to 46.5°C. In figure 70 the trends of the dielectric properties with temperatures are shown:

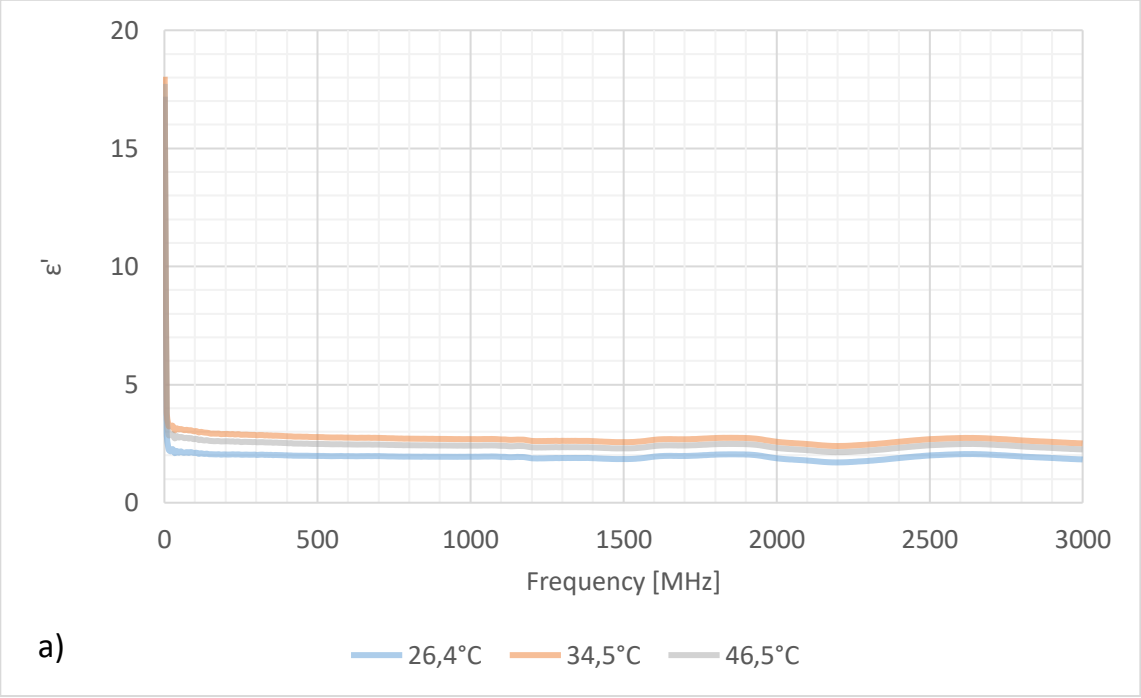

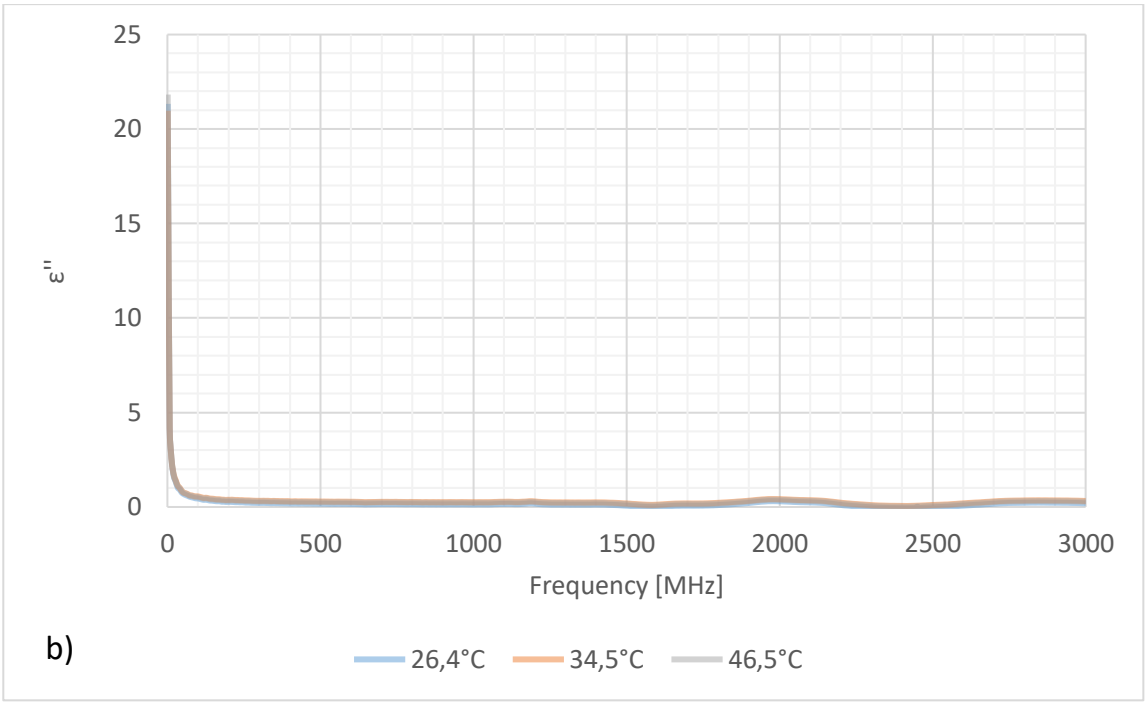

Figure 70 Dielectric properties flax seeds tablets behaviours with temperature in radiofrequency and microwave ranges a) ε' and b) ε''

For the dielectric properties' evaluation using the thermal approach, in table 40 the temperatures reached after every step and the valuation of the temperature variations ratio are shown:

Table 40 Temperature variations for flax seeds

Temperature	ΔT	$\Delta T_i / \Delta T_j = \varepsilon''_{i,th} / \varepsilon''_{j,th}$
26.4°C	-	-
34.5°C	8.1	-
46.5°C	12.0	0.675

Also in this case, at the same time, dielectric constant and the loss factor at 27 MHz and 2.45 GHz and also loss factors ratio at 2.45 GHz of compressed flax seeds after every MW heating step data are collected and the results are summarized in table 41:

Table 41 Dielectric properties at 27 MHz and 2.45 GHz and loss factor variations at 2.45 GHz of flax seeds

Temperature	27 MHz		2.45 GHz			
	ε'_m	ε''_m	ε'_m	ε''_m	$\overline{\varepsilon''_m}$	$\varepsilon''_{i,m} / \varepsilon''_{j,m}$
26.4°C	2.2690	1.3560	1.9500	0.0011	-	-
34.5°C	3.2540	1.4160	2.6390	0.069	0.03505	-
46.5°C	2.8890	1.3370	2.3800	0.032	0.0505	0.694

For flaxseeds, both the dielectric constant and the loss factor show an almost constant behaviour both in radiofrequency and microwave ranges. In literature there are data on the dielectric properties of flaxseeds at about 10 MHz [25] and these values are very similar to those obtained at radiofrequency.

In table 42 the loss factor ratios obtained through the two methods are shown.

Table 42 Loss factor ratio comparison for flax seeds

$\Delta T_i / \Delta T_j = \varepsilon''_{i,th} / \varepsilon''_{j,th}$	$\varepsilon''_{i,m} / \varepsilon''_{j,m}$	% E
0.675	0.694	2.814

the values obtained with the two methods are very close and the error between them is lower than 3%, this demonstrates the correctness of the measurements made using the tablets.

Also for flax seeds, regression were performed for ε' and ε'' both at 27 MHz and 2.45 GHz and results are show in the following graphs:

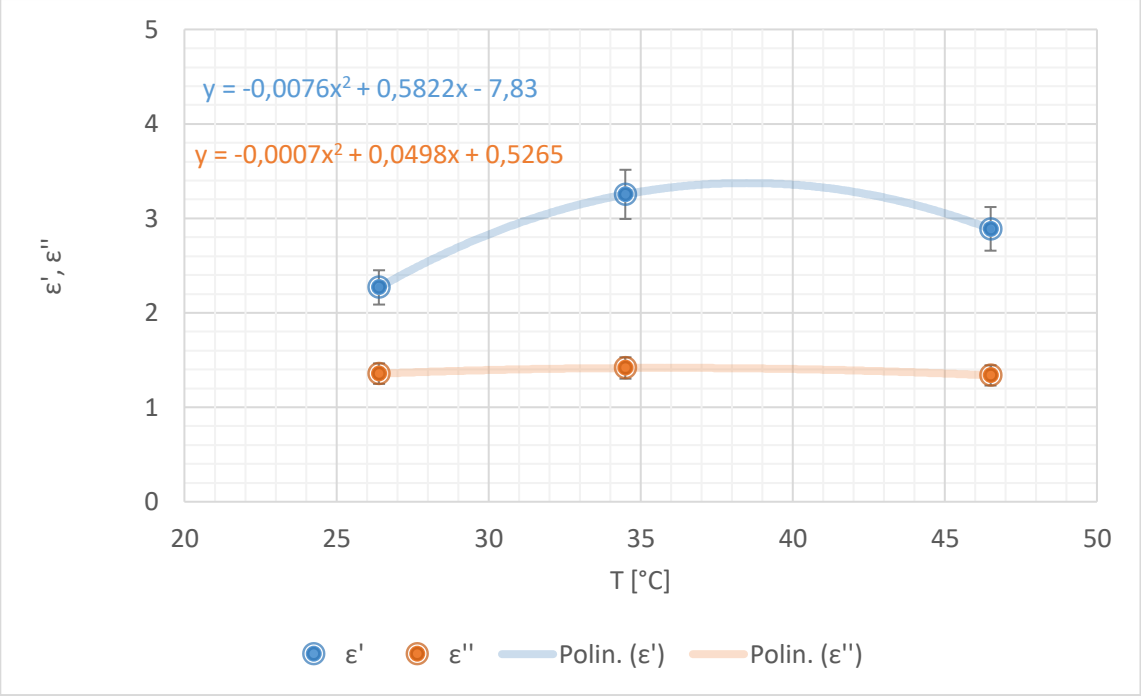

Figure 71 Dielectric properties of flax seeds behaviour with temperature at 27 MHz

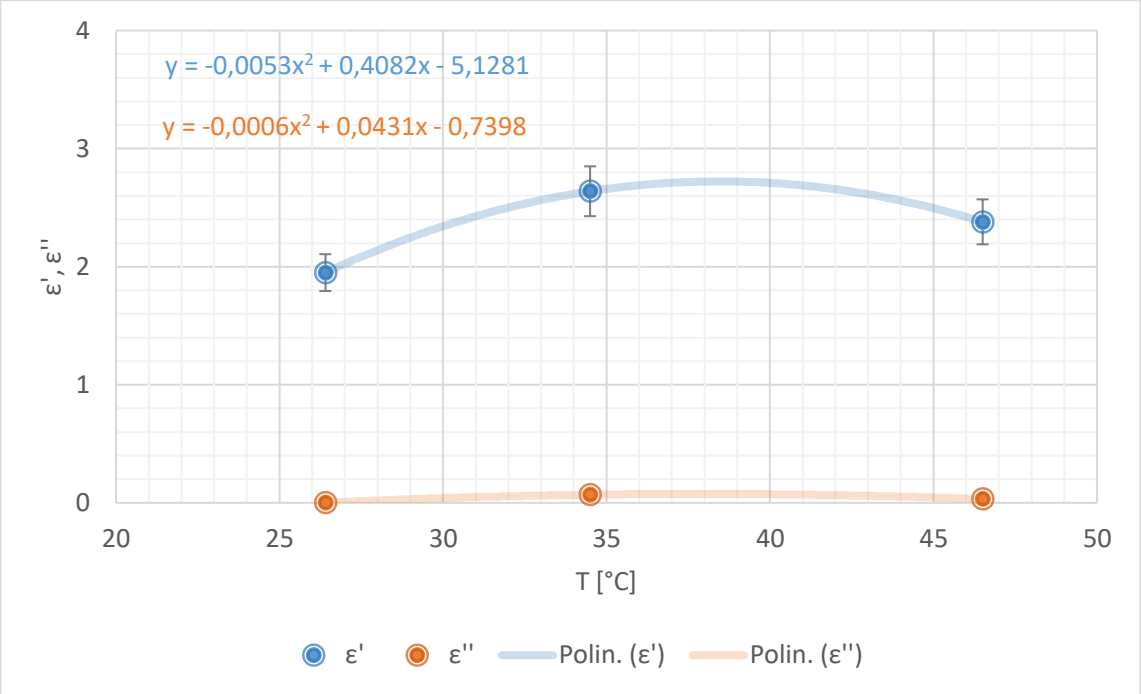

Figure 72 Dielectric properties of flax seeds behaviour with temperature at 2.45 GHz

5.1.4 SOLID POLYMER MATERIALS

The results of the impedance tests carried out on solid polymer products using the static laboratory scale treatment system illustrated in paragraph 4.2.2 will be shown below. As already mentioned, to allow perfect contact between the surface of the probe and the surface of the samples, the polymer pellets were ground until a particle size < 300 µm is obtained. As the polymer powder could not be compacted, due to the enormous pressures required to achieve the desired density, it was measured without further handling.

To validate this measurement protocol, equation (4) was used heating the sample for 10 seconds using the microwave oven. Unfortunately, it was not possible to carry out more than one heating on the polymers examined, since the values of ε'' are very little and decreasing with the temperature, it was impossible to read the ε'' values with the probe because they were too small to be detected. In fact, like shown in figure 73, already at room temperature oscillations are visible in the measurement of the dielectric properties which are more pronounced in the radiofrequency range than in the microwaves one and which are much more marked for the loss factor in the whole frequency range rather than for the dielectric constant.

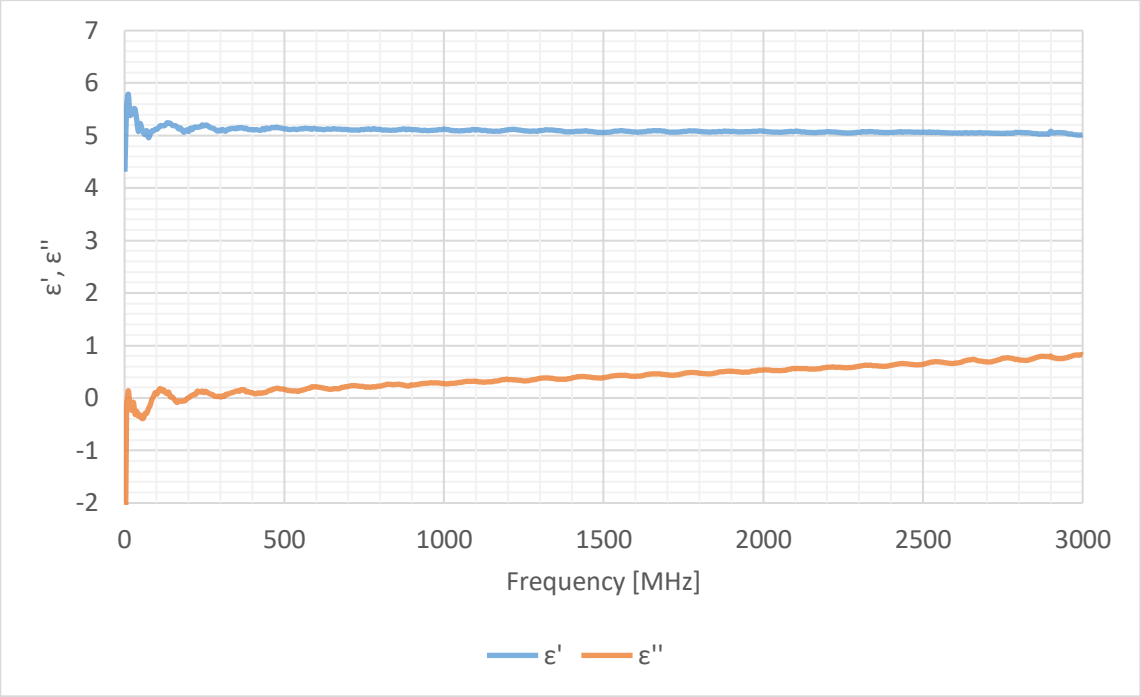

Figure 73 Dielectric properties of nylon 6,6 powder behaviour in the range of frequency between 1 MHz and 3 GHz

These oscillations are attributable to two main reasons: the first is that in the radio frequency range is very close to the lower measurement limit of the probe and therefore are inertia errors at low frequencies. Secondly, the values to be measured are so low to be of the same order of magnitude or much more likely of 2 or 3 orders of size inferior to the recommended value of measurability of $\tan \delta > 0.05$ (table 14).

As a demonstration of what has just been said, we tried to carry out the measurements in a narrower range of frequencies and in particular between 1 and 500 MHz, increasing the amount of points considered for the measurement. The graph obtained from this test is the following:

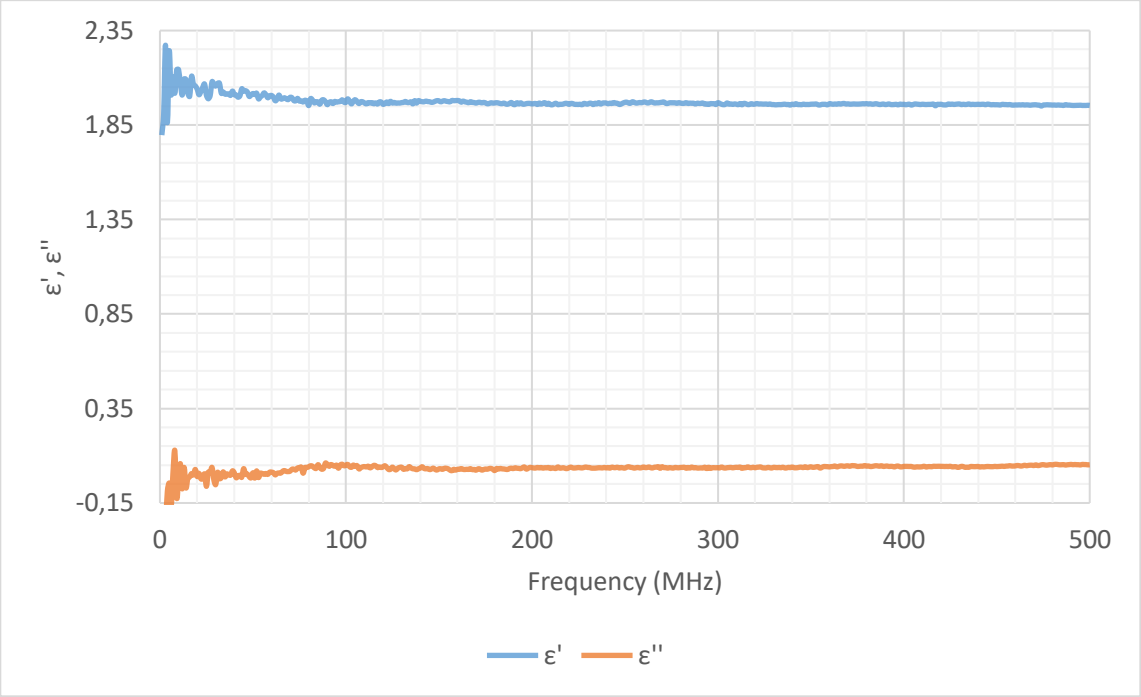

Figure 74 Dielectric properties of nylon 6,6 powder behaviour in the range of frequency between 1 and 500 MHz

As is evident from figure 74, the greatest oscillations occur in the first section of the curves, up to about 150 MHz, both as regards the dielectric constant and the loss factor, and subsequently decrease in intensity. The most pronounced oscillations, however, occur precisely in correspondence with the 1-50 MHz range and this makes it impossible to correctly determine the parameters at the reference frequency of 27 MHz and in particular for the loss factor, whose values oscillate between negative and positive values.

For these reasons, the microwave measurement data was first confirmed with the use of the equations seen in paragraph 4.2.2 and then a measurement protocol was investigated that would allow an easier and error-free determination of the dielectric parameters for this type of materials.

As regards the validation of the measurements carried out in the microwave range, equation (4) was used, but in this formula the value of E^2 is unknown, which was calculated using equation (3), knowing the power value in the case of a becher containing 50 mL of water heated by microwave, like shown in paragraph 4.2.2, and considering it equal to the electric field that established inside a becher containing 50 g of polymer powder with a good approximation. For the evaluation of E^2, the used data are shown in table 43:

Table 43 Values used to calculate E^2

Property	Value
P_w	238 W
f	2.45 GHz
ε_0	8.854 10^{-12} F/m
$\varepsilon''_{r,w}$	12

The value of ε''_w is evaluated by dielectric properties tests on water made during the impedance analyser setup. From the calculations, E^2 results equal to 3.88 10^6 V^2/m^2. For the evaluation of ε'' for Nylon 6.6, the used data are shown in table 44:

Table 44 Values used to calculate E^2

Property	Value
ρ_n	649.8 Kg/m^3
f	2.45 GHz
ε_0	8.854 10^{-12} F/m
$c_{p,n}$	0.969 KJ/Kg K

The values of ρ_n, $c_{p,n}$ were calculated for a nylon powder with a vacuum degree equal to 43% starting from the density and specific heat values of the nylon reported in the literature. In table 45 the comparison between the dielectric properties' measurements on nylon powder and the calculations is shown:

Table 45 Loss factor comparison for nylon 6,6

Temperature	2.45 GHz					
	ΔT	ε''_{calc}	ε'_m	ε''_m	$\overline{\varepsilon''_m}$	% E
25°C	-	-	5.061	0.658	-	-
29.9°C	4.9	0.583	5.064	0.640	0.649	10.17

Since the error between the two data is approximately 10%, it can be assumed that there is agreement between the ε'' thermally calculated value and the measured one, so the measurement protocol for the microwave range can be considered correct.

Unfortunately, like previously said, the use of this protocol is limited to microwaves only, because in the radio frequency range the values undergo too many oscillations and the technological limits of the high temperature probe do not allow to determine a univocal and correct value of the dielectric properties.

As already anticipated, we have tried to provide an alternative protocol that used a continuous medium that could guarantee a measurement of the dielectric parameters even with particles greater than 300. In this way, not only the grinding phase is avoided, but makes easier for operators to determine the characteristics of interest. For this reason, measurements were made by immersing the 2mm nylon 6,6 spheres in a liquid that allowed the probe to come into perfect contact with the sample surface. From the loss factor measured in this way, an attempt was made to derive a corrective factor that would allow us to derive the ε'' nylon value with the use of an equation such as:

$$\varepsilon''_{mix} = \alpha\, \nu_1 \varepsilon''_n + \nu_2 \varepsilon''_l \qquad (12)$$

Where ε''_{mix} is the loss factor of solid-liquid mixture, ε''_n and ε''_l the nylon and the liquid loss factors respectively, while v_1 and v_2 are the volumetric fractions of the respective components and are such that $v_1 + v_2 = 1$ and α is the corrective factor.

In this case two liquids were used and in particular isopropanol and silicone oil. Isopropanol is better coupled with the electric field, so its dielectric properties, even if not very high, are well readable with the high temperature probe. Silicone oil, on the other hand, has very low dielectric properties and much closer to those of polymers in general. In the following graphs, dielectric properties of isopropanol and silicon oil in all radiofrequency and microwave ranges, are shown, to better view the differences between them.

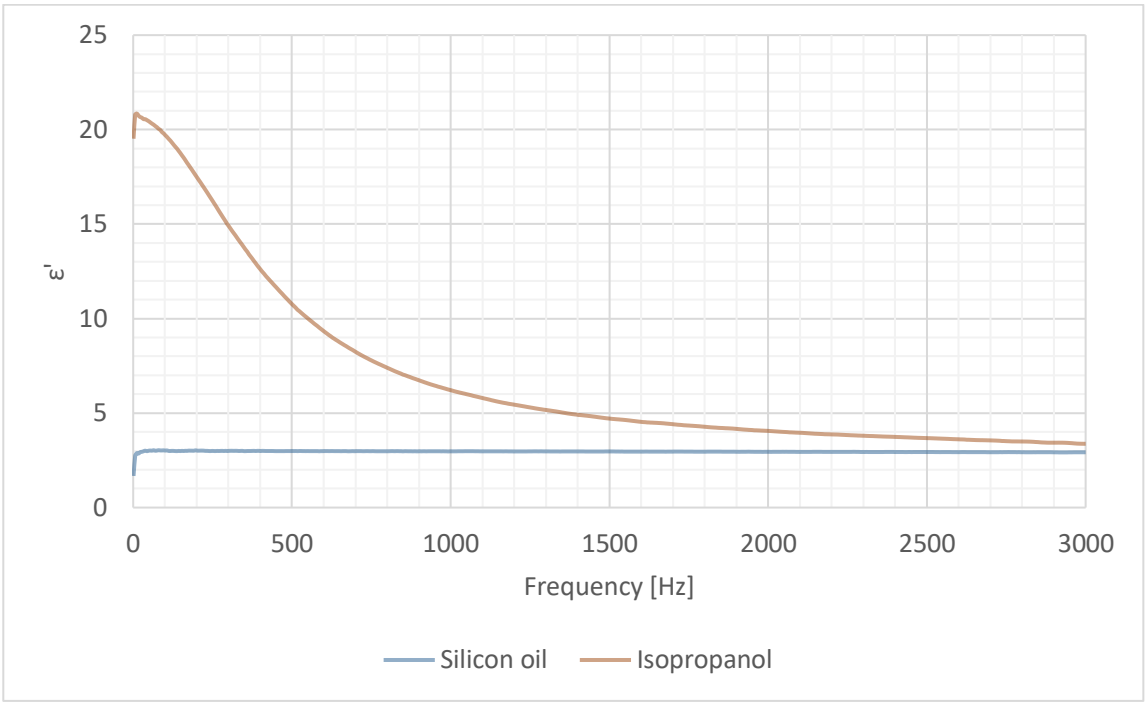

Figure 75 Dielectric constant of silicon oil (blue line) and isopropanol (orange line)

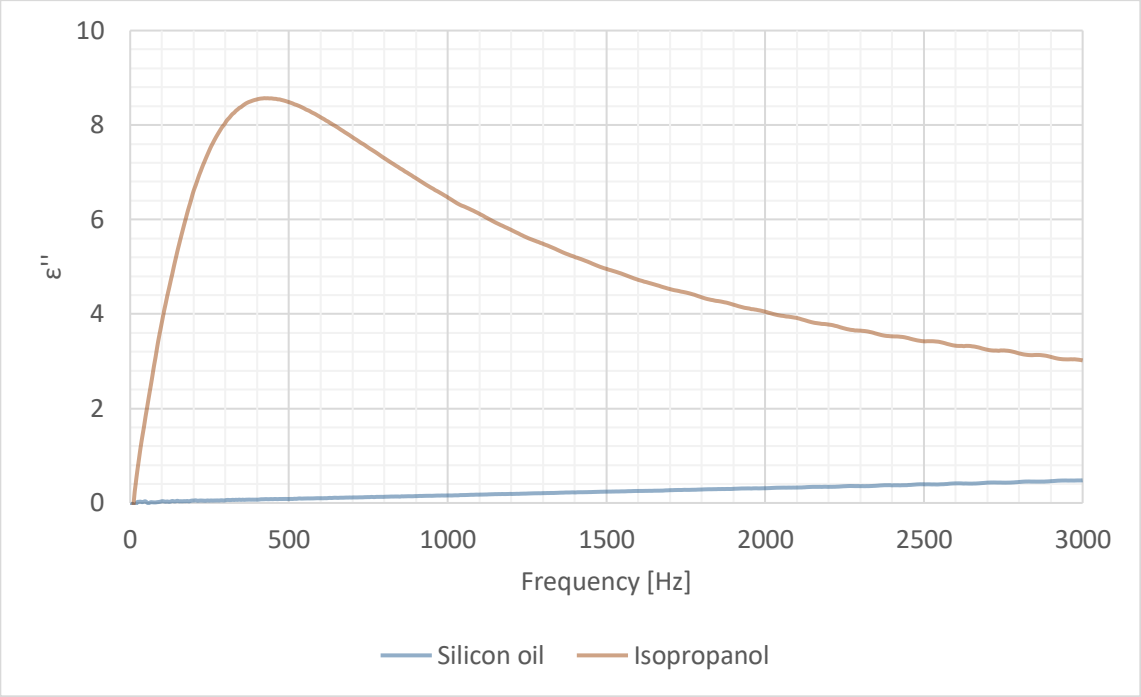

Figure 76 Loss factor of silicon oil (blue line) and isopropanol (orange line)

The table 46 shows the loss factor values of the mixture measured with each of the two examined liquids and the calculation of the correction factor α, such as to return a value of ε_n'' = 0.649, as measured previously. The v_1 value was measured equal to 0.44.

Table 46 Corrective factors evaluation

Liquid	**2.45 GHz**		
	$\boldsymbol{\varepsilon''_{mix}}$	$\boldsymbol{\varepsilon''_{l}}$	**α**
Isopropanol	0.024	3.95	2.87
Silicon oil	0.336	0.283	0.62

As is evident, the correction factor increases with the improvement of the coupling of the liquid with the electromagnetic field, this is because the better the coupling, the more the loss factor of the liquid affects the overall mixture loss factor value. Of course, the correction factor, in addition to being specific for the type of liquid used, is also specific for the frequency at which the loss factor is evaluated.

5.2 SIMULATIONS AND EXPERIMENTAL TESTS

The results presented below come from the simulation of the real RF applicator model and the experimental tests. The simulations, like the experimental tests, were carried out at different values of the applicator input voltage. To validate the model, the value of the electrical conductivity of the two materials was suitably varied.

The input parameters to the computer were the voltage applied to the gate and the conductivity of the material; those at the outlet were the temperature difference between the inlet and outlet fluid and the power transferred to the product. The outlet fluid temperature was evaluated by averaging the temperatures of the points belonging to the outlet surface. The power assessments were carried out by calculating the integral of the electromagnetic volumetric loss density within the milk volume, highlighted in pink in figure 77:

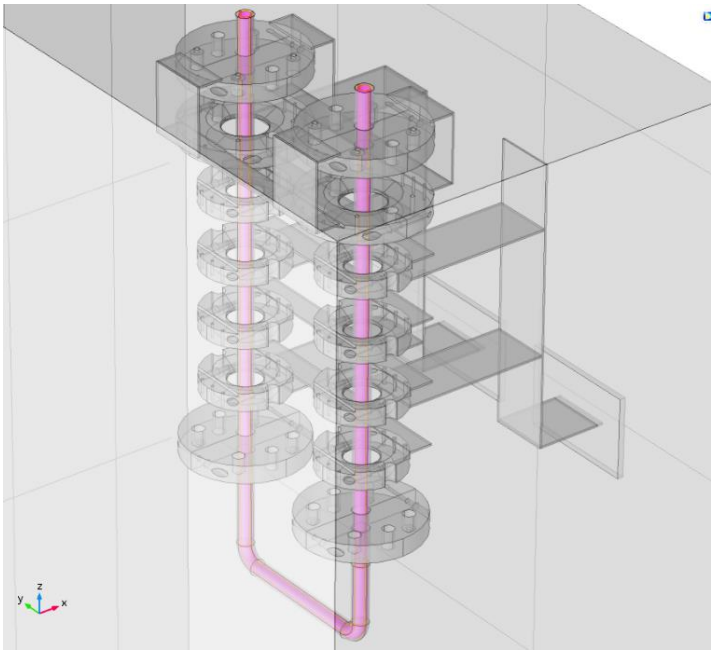

Figure 77 Volume of the tube occupied by the fluid

5.2.1 SIMULATION WITH WATER

Preliminarily, the range in which to frame the problem was investigated through first attempt values of electrical conductivity, setting a minimum and maximum value. The simulations were therefore carried out keeping the conductivity constant first at σ_{min} = 0.029 S/m and then at σ_{max} = 0.057 S/m; both cases had a voltage ranging from 6500 to 9000 V with a step

of 500 V. The results are shown for the power in figure 78a and for the temperature difference in figure 78b.

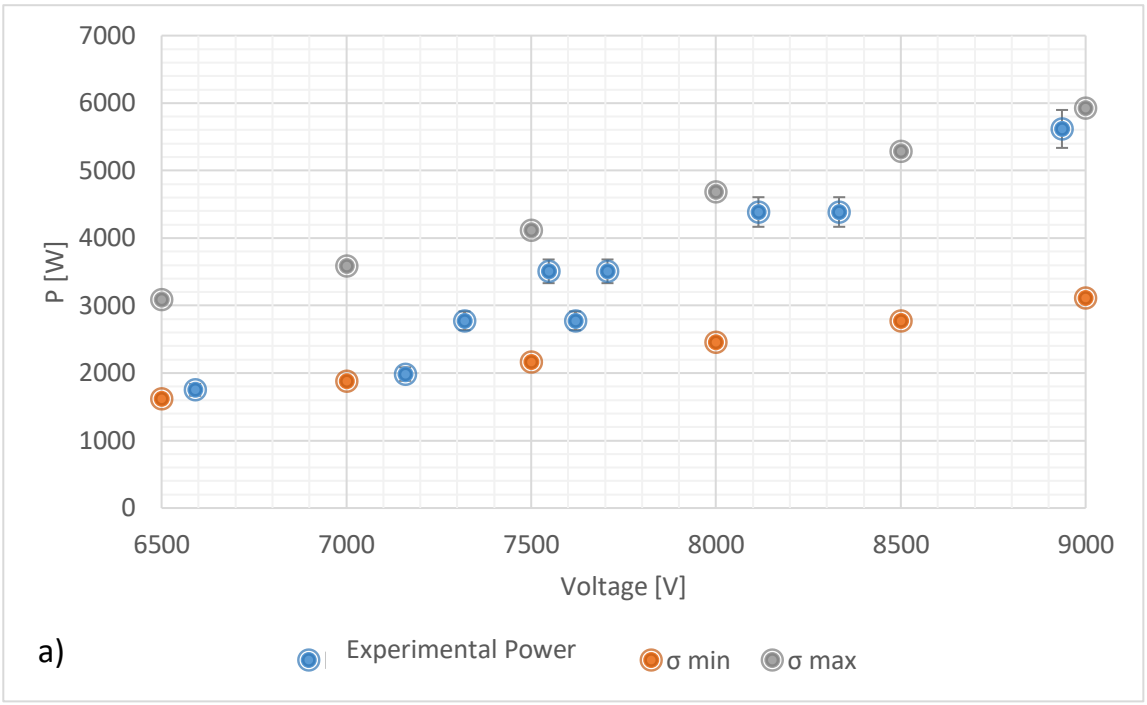

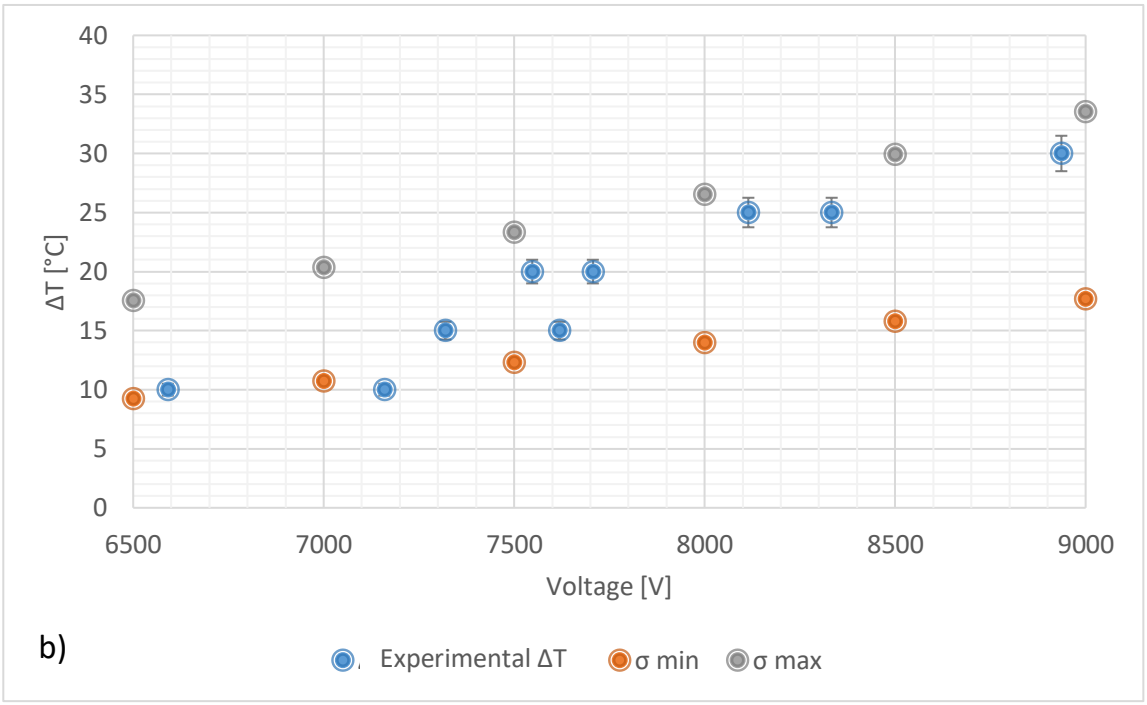

Figure 78 Trend of the a) power transferred and b) temperature differences in the experimental tests and in the simulations at σ_{min} and σ_{max}, as a function of the applicator voltage

As can be appreciated from the figures above, the minimum and maximum electrical conductivity chosen values well delimit the area of the plane in which the values found in the

tests are located.

In order to have a simulation as faithful as possible to reality, it was decided to deepen the study focusing on the voltage range in which the behaviour of the machine can be assimilated to a straight line with a unique slope; that is between 7000 and 9000 V. From this range a straight line was extrapolated using a linear regression, which was compared with the linear regressions of the points obtained from the simulation (figure 79):

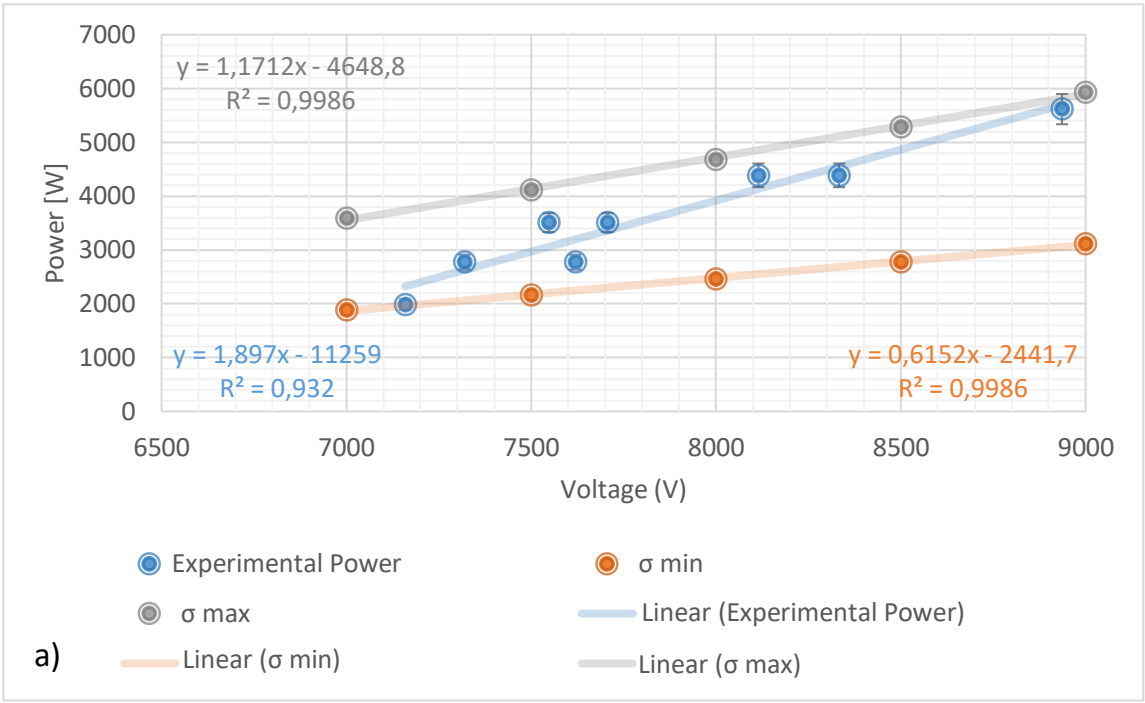

a)

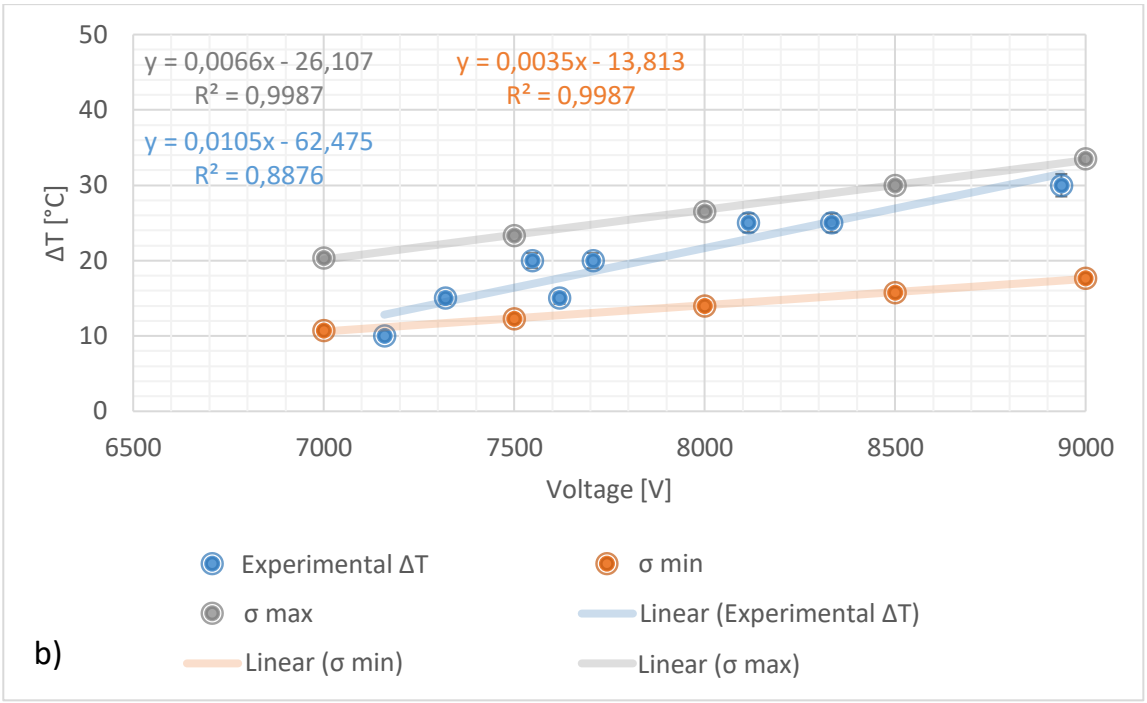

Figure 79 Regressions of the a) power transferred and b) temperature differences in the experimental tests and in the simulations at σ_{min} and σ_{max}, as a function of the applicator voltage

The three equations relating to power and the three relating to temperature obtained from the regression, were evaluated at voltages from 7000 to 9000 V with steps of 500 V. The data sets thus obtained were interpolated according to the equations:

$$\frac{P|_{\sigma_{max}} - P|_{\sigma_{min}}}{P|_{\sigma_{max}} - P_{regr}} = \frac{\sigma_{max} - \sigma_{min}}{\sigma_{max} - \sigma_{int|P}} \qquad (13)$$

$$\frac{\Delta T|_{\sigma_{max}} - \Delta T|_{\sigma_{min}}}{\Delta T|_{\sigma_{max}} - \Delta T_{regr}} = \frac{\sigma_{max} - \sigma_{min}}{\sigma_{max} - \sigma_{int|T}} \qquad (14)$$

Where is it :

- $P|_{\sigma_{max}}$ and $\Delta T|_{\sigma_{max}}$ are respectively the power and the temperature evaluated through the regressions relative to σ_{max};
- $P|_{\sigma_{min}}$ and $\Delta T|_{\sigma_{min}}$ are the power and temperature evaluated through regressions relative to σ_{min};
- P_{regr} and ΔT_{regr} are the power and temperature evaluated through the regressions related to the experimental tests;
- $\sigma_{int|P}$ and $\sigma_{int|T}$ are respectively the electrical conductivities obtained from the interpolation using equations (13) and (14).

Using the linear interpolation procedure, therefore, the electrical conductivity values have been obtained which are presumed to better approximate the real behaviour of the machine when the voltage varies, one weighted on the power, ($\sigma_{int|P}$) and the other on temperature ($\sigma_{int|T}$). The values shown in table 47, used as input parameters for the simulation, are the arithmetic average of the two weights:

Table 47 Couples of input parameters obtained by interpolation and used in simulation, and corresponding temperature

Conductivity (S/m)	Voltage (V)	Temperature (°C)
0.031	7000	91.0
0.04	7500	96.3
0.046	8000	101.5
0.051	8500	106.8
0.055	9000	112.0

Furthermore, to each conductivity-voltage couple corresponds a determined thermal increase and, therefore, a determined outlet temperature. The correlation between electrical conductivity and temperature and between electrical conductivity and voltage are shown in figure 80. Through a polynomial regression of order two, the two equations that represent the trend of conductivity as a function of temperature and voltage respectively were obtained.

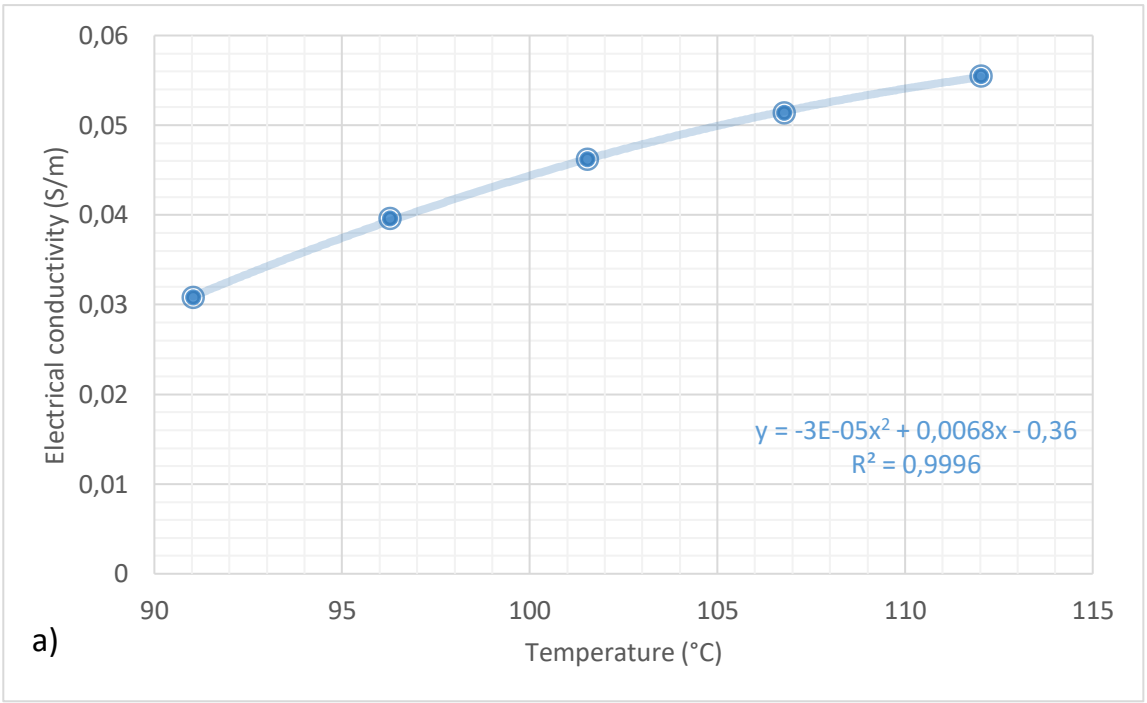

a)

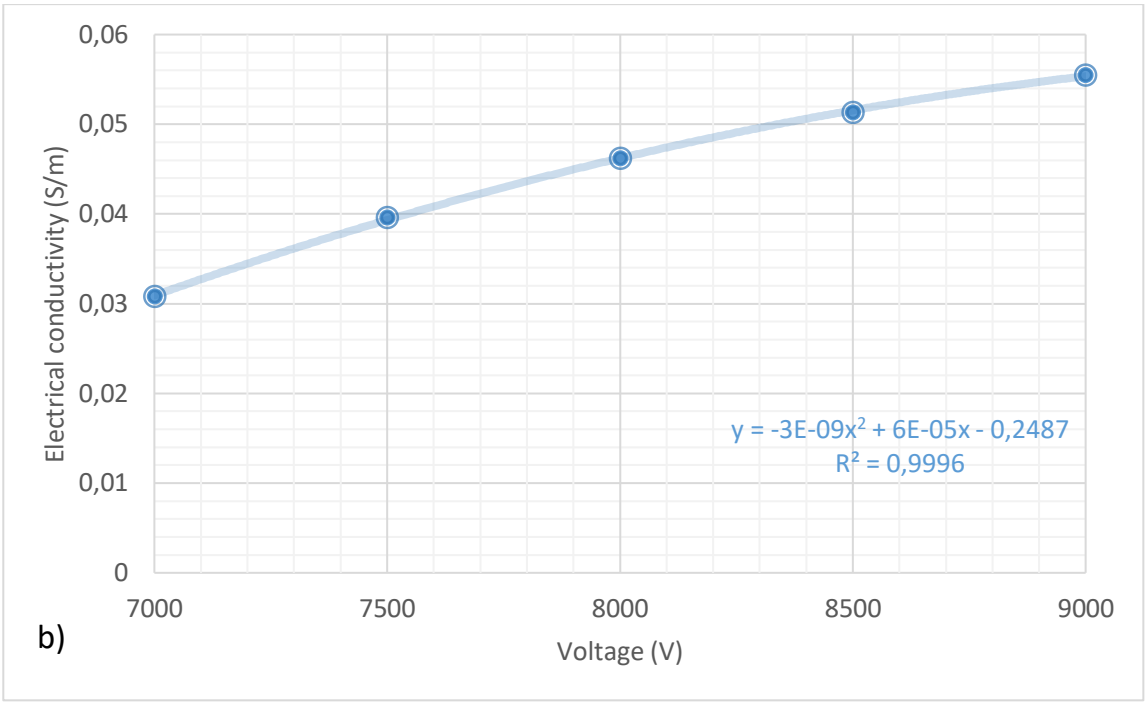

Figure 80 Regressions of thermal conductivity as a function of a) temperature and e) voltage

COMSOL allows to view the quantities of interest more immediately, plotting them directly on the geometry. As an example, the trends of the temperature (figure 81a) and of the electric potential (figure 81b) are shown in the case of the simulation at 6500 V and 0.029 S/m:

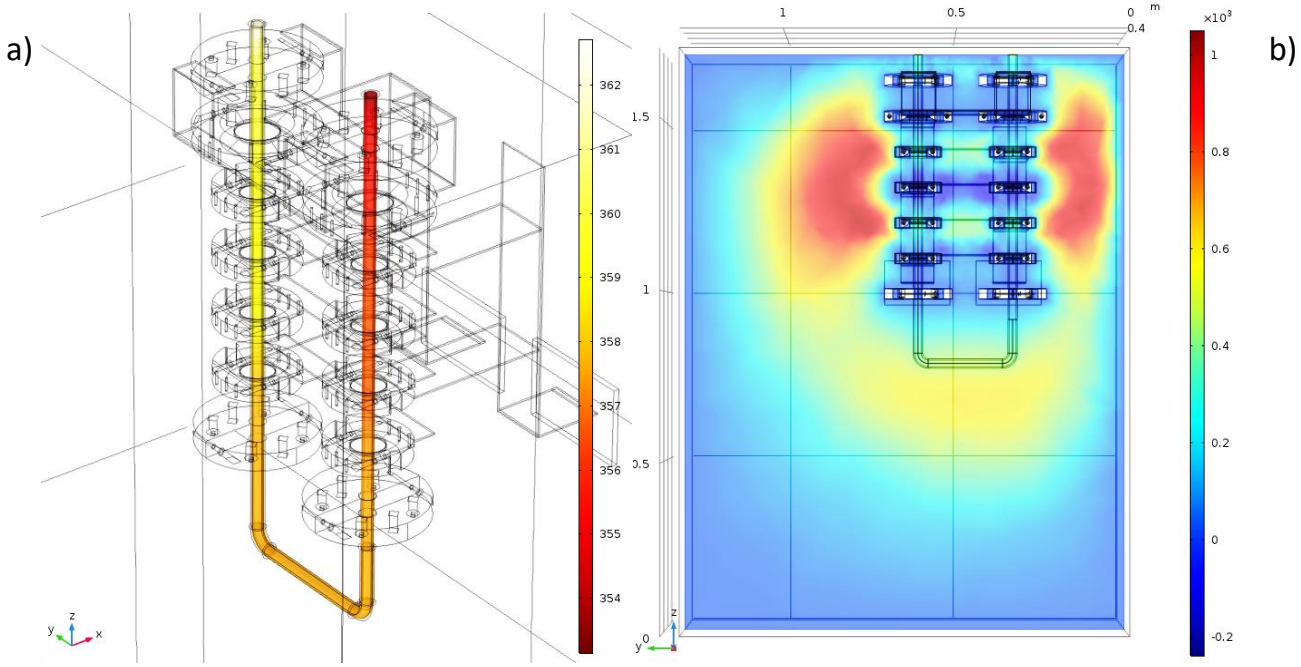

Figure 81 Trend of a) the temperature inside the applicator tube and b) the electric potential inside the domain

5.2.2 SIMULATION WITH MILK

As with water, milk also required a preliminary investigation of the first attempt values of electrical conductivity. The chosen maximum and minimum values are equal to σ_{min} = 0.065 S/m and σ_{max} = 0.08 S/m. Also in this case, the model was simulated for each of the two conductivity values with a voltage ranging from 5000 to 6500 V with a step of 500 V and regressions were made to determine the functions with voltage and temperature (figure 82).

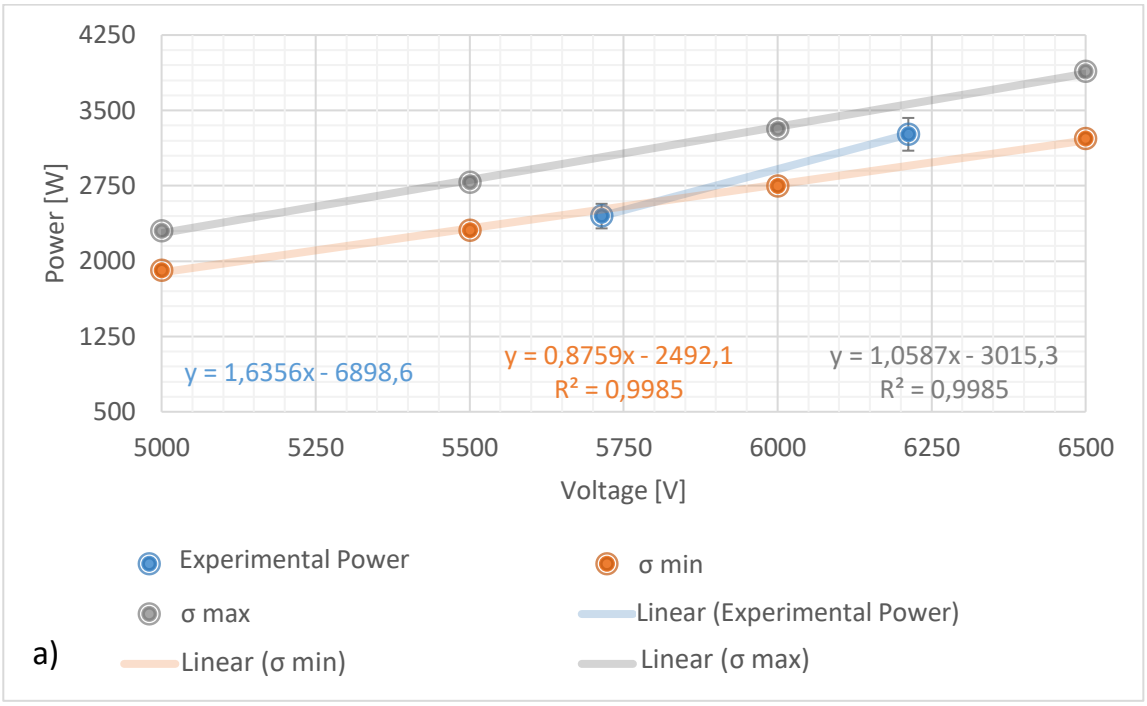

a)

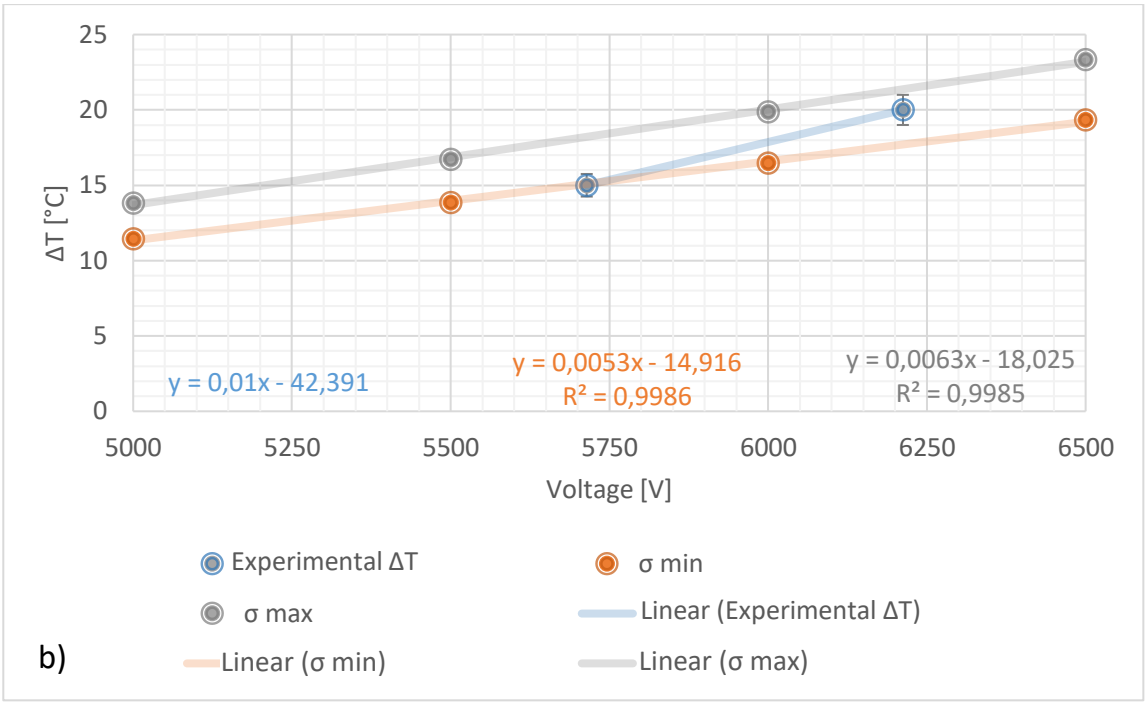

Figure 82 Regressions of the a) power transferred and b) temperature differences in the experimental tests and in the simulations at σ_{min} and σ_{max}, as a function of the applicator voltage

The obtained data were interpolated with the same methods used for water with equations (13) and (14) to evaluate the electrical conductivity values which are presumed to better approximate the real behaviour of the machine when the voltage varies, one weighted on the power, ($\sigma_{int|P}$) and the other on the temperature ($\sigma_{int|T}$). The values shown in table 48, used as input parameters for the simulation, are the arithmetic average of the two weights:

Table 48 Couples of input parameters obtained by interpolation and used in simulation, and corresponding temperature

Conductivity (S/m)	Voltage (V)	Temperature (°C)
0.056	5500	92.6
0.069	6000	97.6
0.078	6500	102.6

Also in this case, the trend of electrical conductivity with temperature and voltage was evaluated, as shown in figure 83.

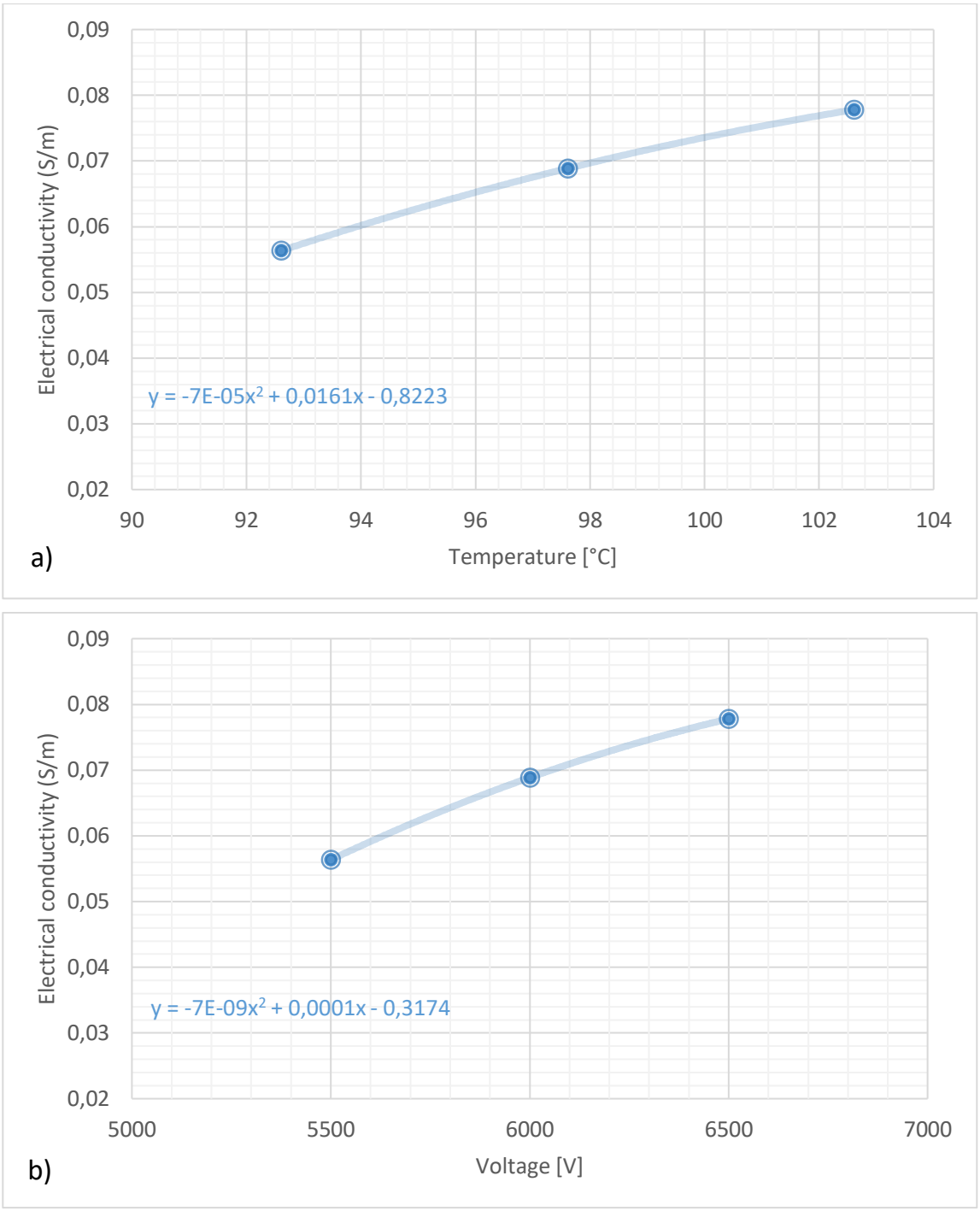

Figure 83 Regressions of thermal conductivity as a function of a) temperature and e) voltage

Also for milk, it is possible to view the temperature and electrical potential trends in the system:

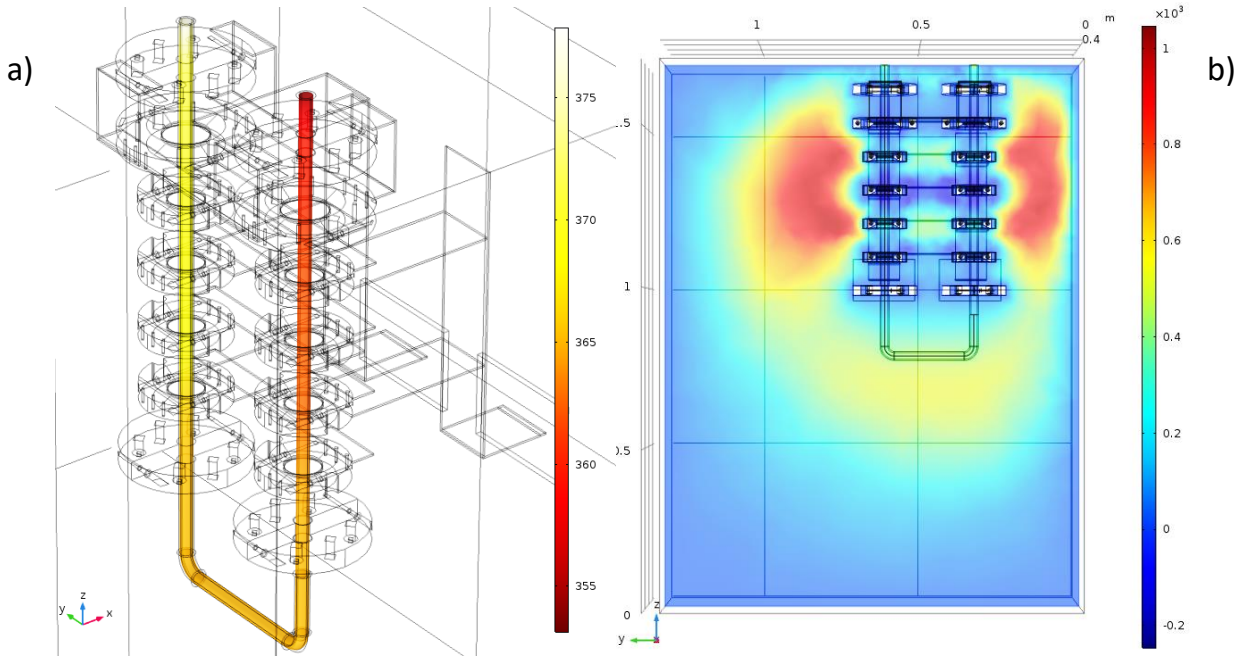

Figure 84 Trend of a) the temperature inside the applicator tube and b) the electric potential inside the domain

5.2.3 RESULTS OF EXPERIMENTAL TESTS

Below are the results obtained from the experimental tests with the RF machine both for the preliminary tests with water and those on the milk product.

5.2.3.1 PRELIMINARY TESTS

The values of the most important physical quantities corresponding to the desired work points were taken from the machine panel, as reported in table 49:

Table 49 RF machine data

Test	Power (W)	Anodic Current (A)
1	6300	0.88
2	7100	0.97
3	8000	1.06
4	9900	1.22
5	12600	1.41
6	10500	1.26
7	8400	1.09
8	8000	1.05
9	5800	0.88

As is evident from the above data, the working points are not unique with the same temperature difference. This is due to internal hysteresis in the machine.

Using equation (9) it is possible to calculate the voltage supplied to the applicator. Since the thermal difference, the average specific heat and the flow rate instant by instant, are known from equation (10) it is possible to calculate the power supplied to the product. Finally, thanks to equation (11) it is possible to calculate the no-load power and therefore calculate the percentage of no-load power and power to the product, as reported in table 50:

Table 50 RF machine data processing

Voltage (v)	ΔT	$\overline{c_p}$ (j/Kg K)	Q (L/h)	P_p (W)	P_v (W)	% P_p	% P_v
7159	10	4203	170	1985	4315	31.50%	68.5%
7320	15	4161.03	160	2774	4326	39.10%	60.9%
7547	20	4209.06	150	3508	4492	43.80%	56.2%
8115	25	4211.03	150	4386	5514	44.30%	55.7%
8936	30	4212.99	160	5617	6983	44.60%	55.4%
8333	25	4211.03	150	4386	6114	41.80%	58.2%
7706	20	4209.06	150	3508	4892	41.80%	58.2%
7619	15	4161.03	160	2774	5226	34.70%	65.3%
6591	10	4203	150	1751	4049	30.20%	69.8%

From the table it is clear that the no-load power is high in percentage terms, but decreases as the temperature difference increases. This is due to the fact that the machine does not work at full capacity since for such low flow rates, typical of a pilot plant, it is oversized.

The experimental results were reported on a graph as a function of the voltage applied by the electrode. It has been chosen to monitor the power transferred to the product and the temperature difference, like shown in figure 85:

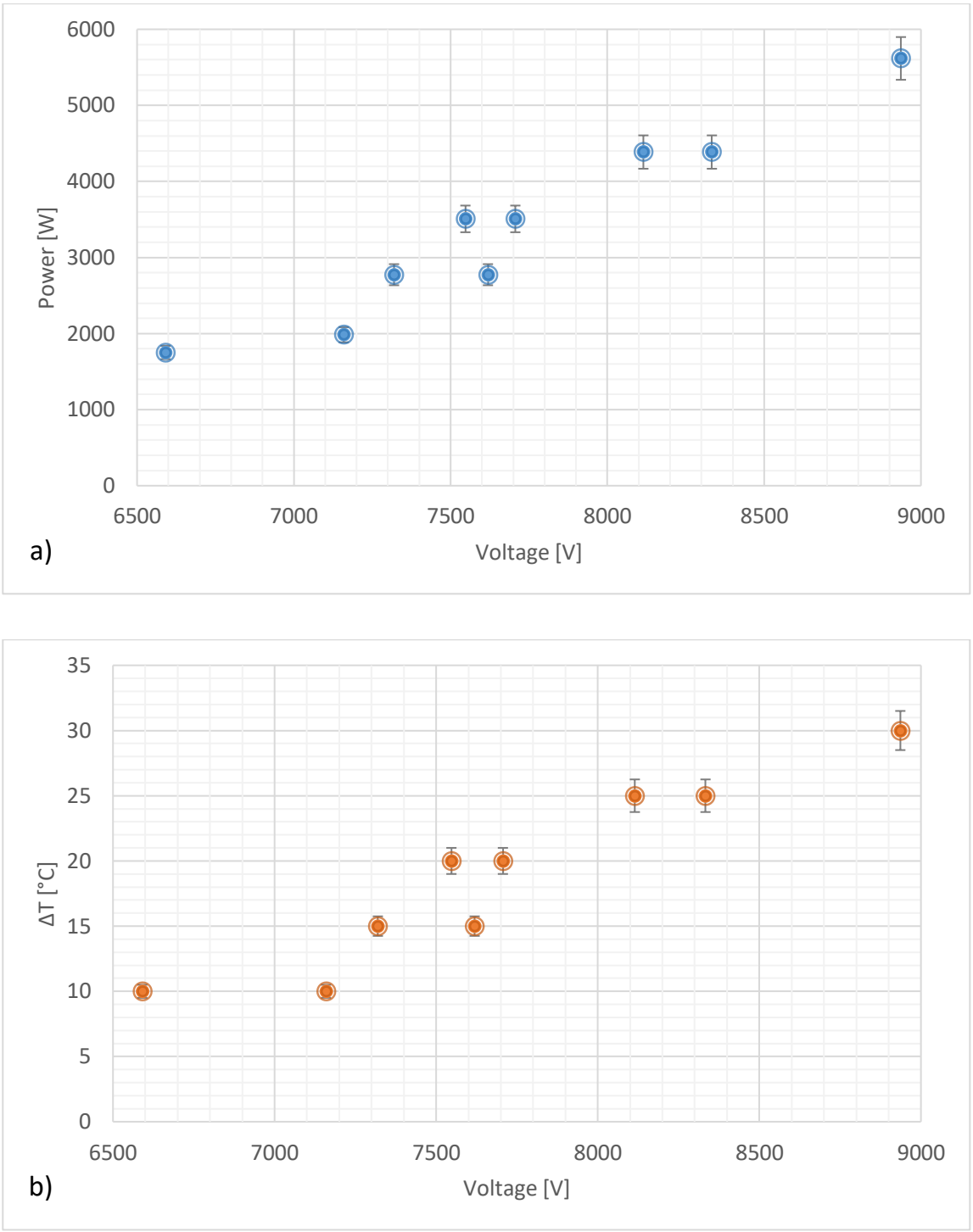

Figure 85 Trend of the a) transferred power and b) the temperature difference as a function of the applicator voltage

As mentioned before, it is clear that the curve has hysteresis since different voltage values correspond to the same power; the same behaviour is found for the thermal difference.

5.2.3.2 TESTS WITH MILK

The values of the relevant physical quantities corresponding to the desired work points were taken from the machine panel, as reported in table 51:

Table 51 RF machine data

Test	Power (W)	Anodic Current (A)
1	2448	1.32
2	3262	1.19

Similarly to what was done with water, also in this case the no-load power was evaluated and therefore the percentage of no-load power and power supplied to the product was calculated as shown in table 52:

Table 52 RF machine data processing

Voltage (V)	ΔT	$\overline{c_p}$ (J/Kg K)	Q (L/h)	P_p (W)	P_v (W)	% P_p	% P_v
5714	10	3916.28	150	2448	4352	36.0%	64.0%
6212	15	3914.32	150	3262	4938	39.8%	60.2%

The experimental results in terms of transferred power and temperature difference were reported on a graph as a function of the voltage applied by the electrode (figure 86).

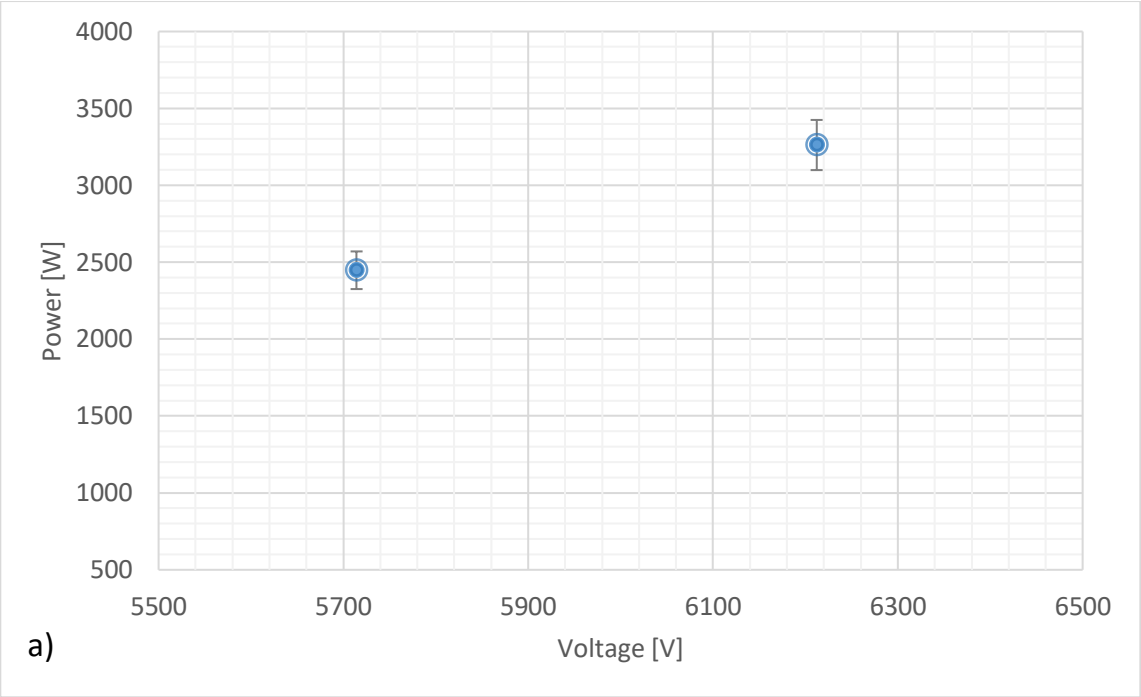

a)

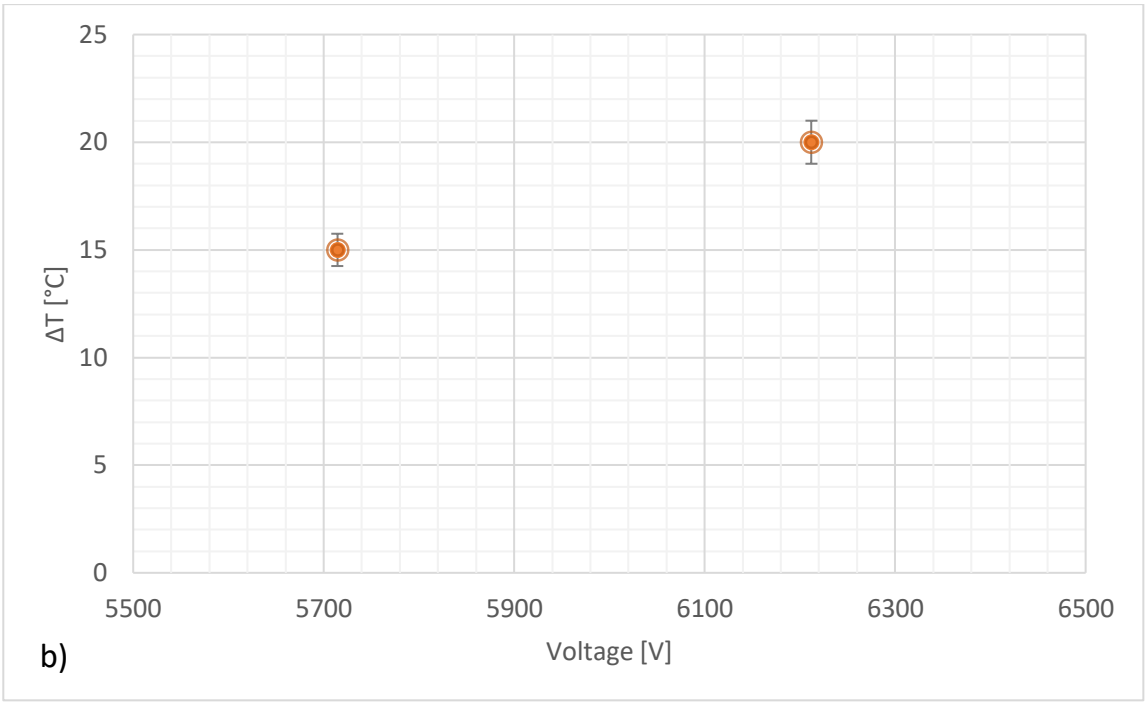

Figure 86 Trend of the a) transferred power and b) the temperature difference as a function of the applicator voltage

5.2.3.3 COMPARISON BETWEEN SIMULATIONS AND EXPERIMENTAL TESTS

As for the simulations and tests carried out with water, the range of simulated voltage values includes the range of voltage values recorded in the experimental tests. The results, presented in figure 87 show a trend of the simulations that well approximates the real behaviour of the machine.

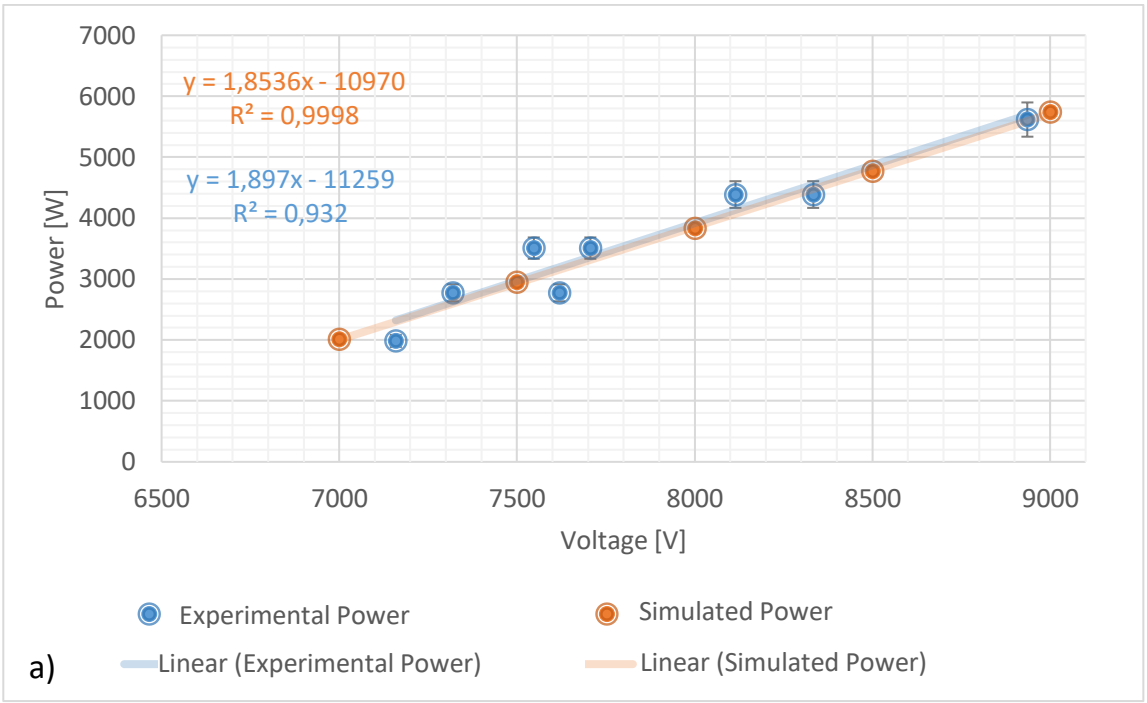

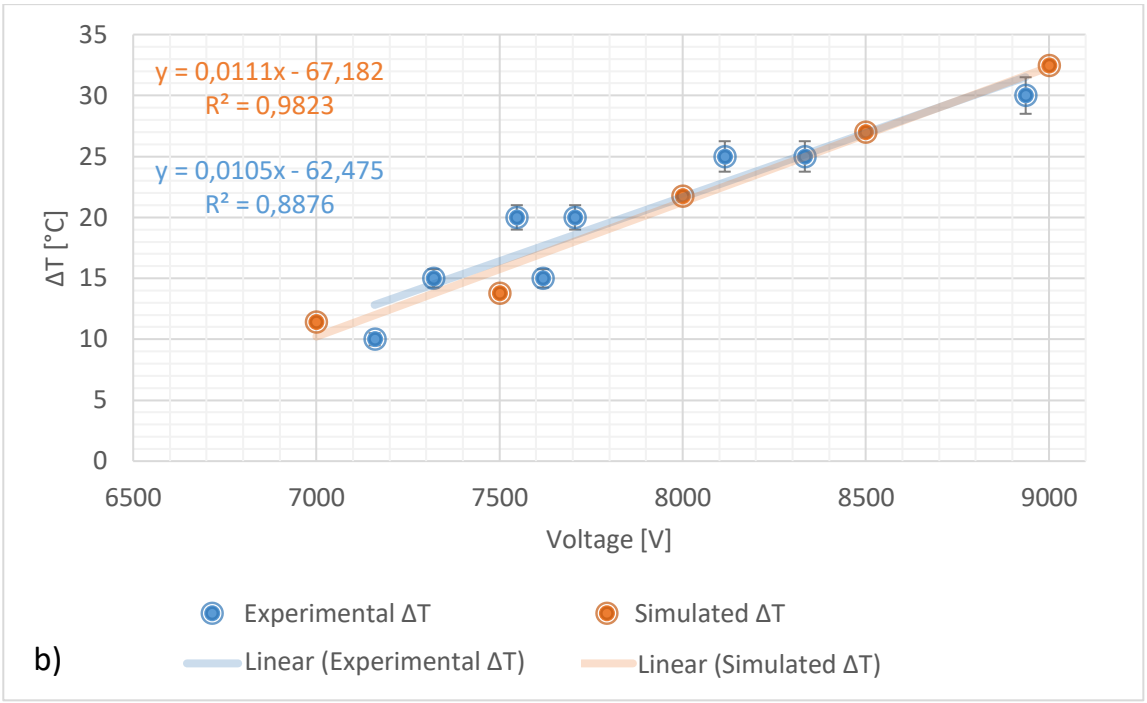

Figure 87 Trends of a) transferred power and b) temperature difference in experimental (blue) and simulation (orange) tests, as functions of the applicator voltage

Also for the tests carried out with milk, it is possible to compare the results of the simulations and experimental tests:

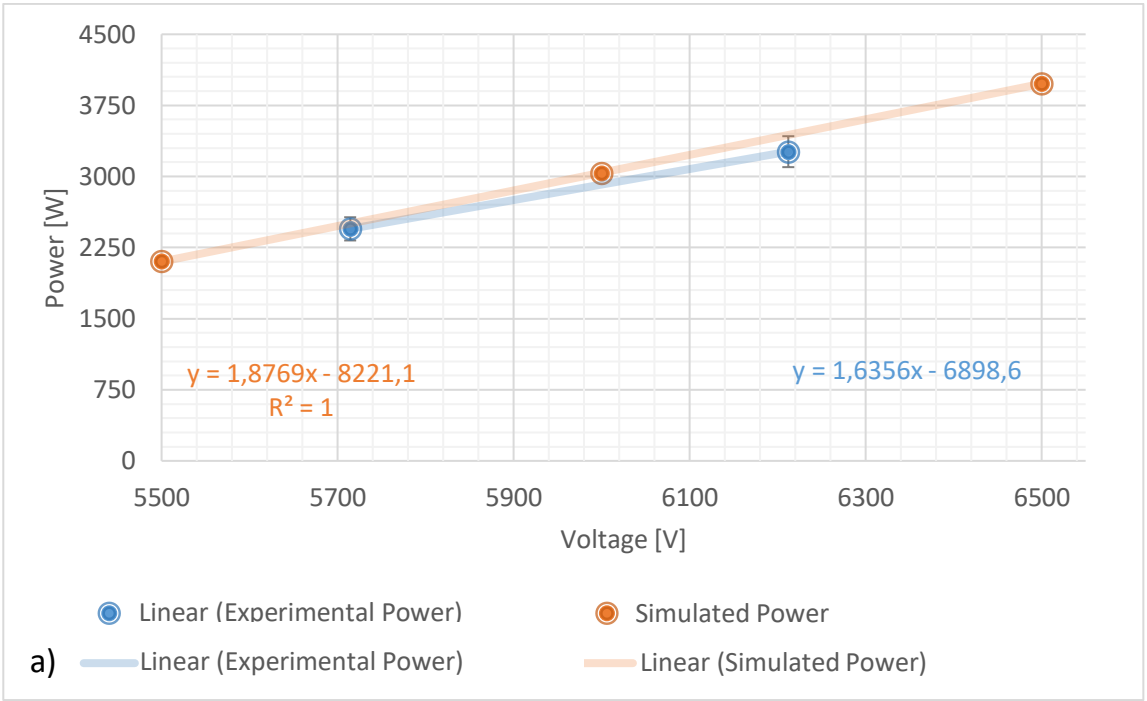

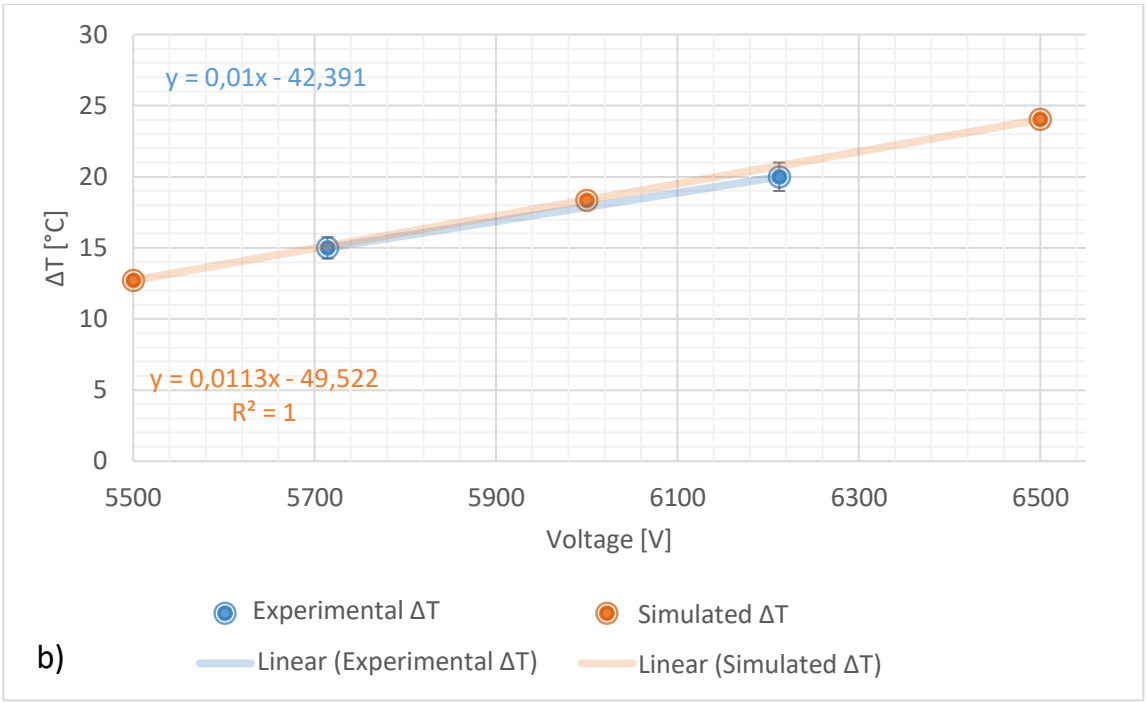

Figure 88 Trends of a) transferred power and b) temperature difference in experimental (blue) and simulation (orange) tests, as functions of the applicator voltage

As is evident from the graphs above, the simulations and the experimental data, both in the case of the tests with water and with milk, show an excellent agreement. So it can be said that the simulations well approximates the real behaviour of the machine.

6. CONCLUSIONS

The evaluation of the dielectric properties of both food and polymeric materials is a phase of fundamental importance for the setting of dielectric heating technologies, whether they are radiofrequency or microwave. To determine these properties, an impedance analyser and the high temperature open-ended coaxial-line probe were used. The coaxial probe allows to investigate the entire frequency range from 1MHz to 3 GHz, thus including the industrial operating frequencies for radio frequency and microwave, that are 27 MHz and 2.45 GHz. The use of this probe is very simple in the case of liquids or fluids as it does not require any type of sample preparation, but the same is not true for solids. This is because the probe needs a perfect contact with the sample surface to be able to correctly measure dielectric properties. This led to create a measurement protocol that would allow to carry out the impedance tests of granular solids.

In the case of liquid materials, a continuous laboratory scale treatment system was also used, which simulated as much as possible a real dielectric treatment system. For the other materials, however, it was necessary to use a static system, with a heating provided by a microwave oven. For granular solids of food origin, the measurement protocol foresees the grinding and compacting of the products flour, in order to obtain a sample of the same composition and density as the original material, but with a larger size that therefore allows the probe to be able to perform the measurements. The accuracy of this protocol was verified with thermal measurements. In future studies, this method can be used for the determination of the dielectric properties of a large number of materials, such as other types of seeds, legumes, cereals, etc.

Furthermore, for all the studied food-borne materials, the dependence of the dielectric properties with the temperature was provided. As already mentioned, knowing this parameter and how it varies during the heating phase is essential to obtain the desired heating in industrial treatment processes.

Two different methods have been developed for polymers: the first involves grinding the pellets up to a size of less than 300 μm, while the second uses a liquid matrix to allow the probe to be coupled. Both methods have shown good results, which must however be investigated and confirmed with further studies and with the use of both other types of materials and liquids.

Finally, simulations using COMSOL Multiphysics® and experimental tests were performed on the radiofrequency heating of both water and milk on the basis of data from laboratory tests. The results of the simulations, relative to the power transferred to the product and the thermal difference between input and output, confirmed the experimental data. The model also allowed to estimate the dependence of conductivity on temperature, at 27.12 MHz, both for water and milk.

APPENDIX I

DIELECTRIC HEATING

Microwave and radiofrequency heating are based on the dielectric heating that is generated when a slightly or moderately conductive material is subjected to non-ionizing electromagnetic irradiation. Radio frequency is an electromagnetic wave that propagates in space with a frequency between 300 kHz and 300 MHz, instead microwave are waves with a frequency between 300 MHz and 300 GHz. Different frequencies correspond to different wavelengths: with an inversely proportional ratio as shown in figure A.1:

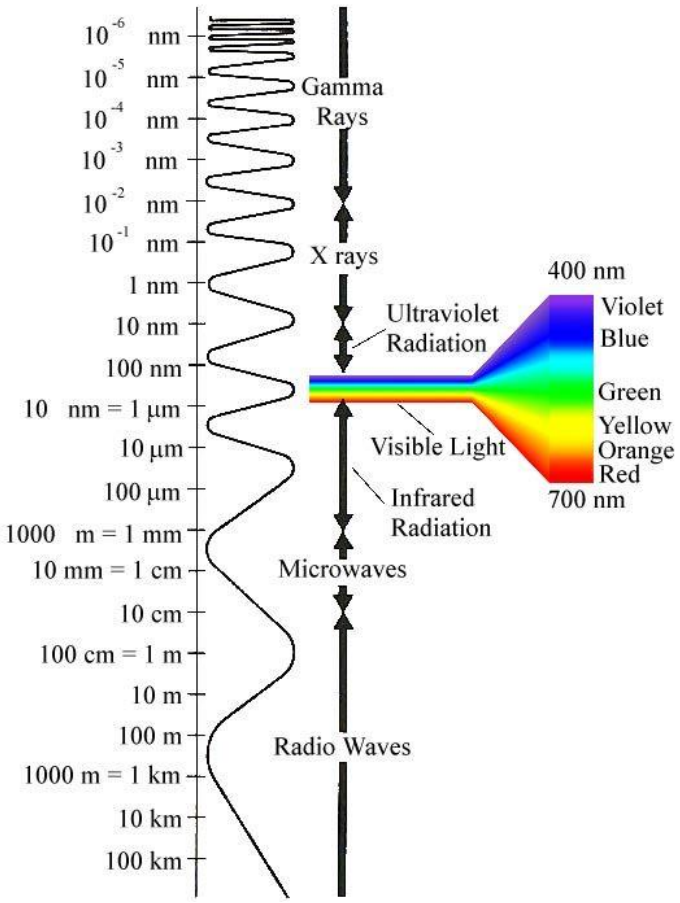

Figure A.1 Electromagnetic spectrum

Each frequency is related to the respective wavelength using the formula:

$$c = \lambda f \qquad \text{(A-1)}$$

Where c = 3.0 × 10^8 m/s is the speed of light, λ is the wavelength (m), and f is the frequency of the EM waves (Hz).

Radio frequency and microwaves fall within the radar range and can, therefore, interfere with communication systems, such as those normally used for cellular communications. For this reason, only certain specific frequencies are allowed for industrial, scientific and medical (ISM) uses. Table A1 shows which ISM frequencies are allowed for Radio Frequency and Microwave, and which wavelengths they correspond to:

Table A1 ISM frequencies for RF and MW and corresponding wavelengths

	RF			MW	
Frequency (MHz)	13.56	27.12	40.68	915	2450
Wavelength (m)	22	11	7.4	0.33	0.12

The applied electric field is proportional to the voltage, which has minimums, zero points and maximums cyclically every λ/4 (where λ is the wavelength of the electromagnetic waves); consequently, the power will have the same behaviour. If the size of the product to be treated is much smaller than the wavelength, this will undergo a uniform temperature increase; otherwise, unwanted hot spots and cold spots will be generated inside the product, corresponding respectively to the maximum and minimum points.

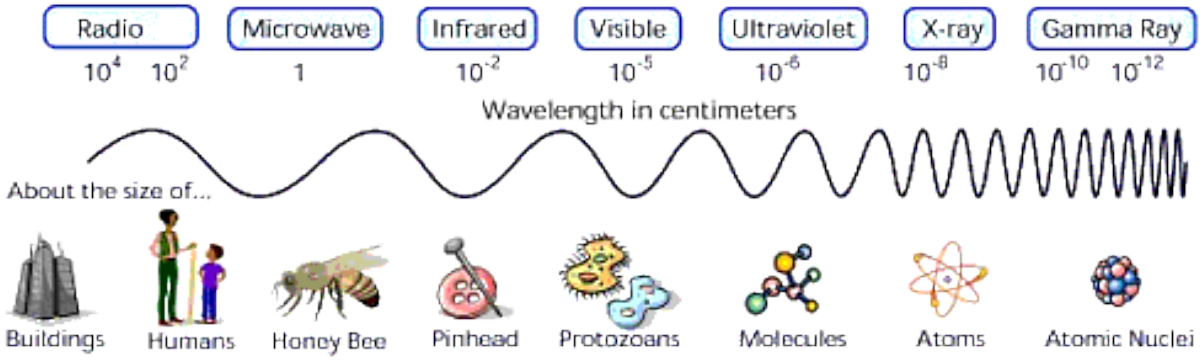

$$\lambda_{RF}|_{27.12\ MHz} = 11{,}06\ m \qquad \lambda_{MW}|_{2.45\ GHz} = 0.12\ m$$

Figure A.2 Wavelengths of different electromagnetic waves

As can be seen from figure A.2, the wavelength λ typical of microwaves is much smaller than that of RF, and is comparable to the size of foods that are processed in a common microwave oven. This leads to a non-uniformity in the transfer of energy. The problem becomes all the more significant the more the size of the object to be treated in microwave increases with respect to the wavelength. It is commonly known that domestic microwave ovens are equipped with a turntable or metal stirrers. These devices are used precisely to try to overcome the field non-uniformities in the microwave oven, trying to homogenize and randomize the electric field in a generic point of the product.

The generation of high frequency alternating electromagnetic fields, which pass through the material and cause it to heat substantially through two physical mechanisms [31]:

- Dipolar rotation - The polar molecules, like water, subjected to the action of an alternating electromagnetic field, tend to orient themselves spatially in a manner dependent on the potential of the electromagnetic field applied to them. Consequently, the molecules will rotate at a speed that is all the greater the greater the propagation frequency of the electromagnetic waves associated with this field. The friction generated by the rotation of two adjacent molecules will cause heat dissipation and, therefore, the heating of the entire volume of material;
- Ionic conduction - The ions are also affected by the action of electromagnetic waves, and will move quickly along the entire volume of the material, with a speed proportional to the frequency of the electric field with which they interact. In this case, the heat will be generated as a result of the friction between ions moving in the opposite direction.

The intermolecular friction transforms the kinetic energy of molecules into heat, resulting in a homogeneous and effective heating action (figure A.3).

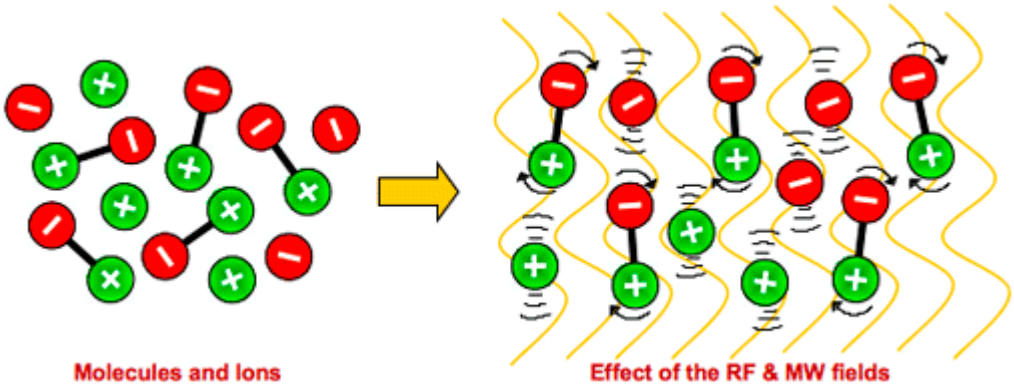

Figure A.3 Orienting effect of the electric field on polar molecules and ions

Dielectric heating can be used when a rapid temperature increasing is needed, because the heating is generated directly inside the material, decreasing the process time, the costs and increasing the product quality.

Food industries, but not only, show a growing interest in the heat treatment of packaged products and radiofrequency can easily adapt to this perspective. In fact, radiofrequency heating may affect both the product and the polymeric material that makes up the packaging. Recently, the use of dielectric heating spreads widely in the treatment of wet food products,

especially for fluid foods, like milk [22], [44] or fruit juice [23] both for the peculiar heating mechanism and for the increasing interest and use in food production. The positive results in terms of treatment times and efficiency [45], pushed to use this technology for low humidity products for which the efficiency of dielectric heating is not so confirmed. For these reasons, it is very important to understand the best way to realize a dielectric heating and do to this and to define the process efficiency, studying dielectric parameters is essential. Dielectric heating for solids or granular materials became very interesting in the industrial scenario and describe the best condition to treat a bulk of these materials is the main challenge for these applications.

DIELECTRIC PROPERTIES

The use of dielectric heating in drying or sanitation processes both for food and non-food products is particularly interesting, but it is very difficult due to the low values of dielectric parameters. Dielectric materials are a class of materials that conduct little or not at all electric current, unlike conductive materials, such as metals, which are instead good electrical conductors. The electrical properties of materials in the context of microwave and radiofrequency heating are known as dielectric properties, which provide a measure of how materials interact with electromagnetic energy. The dielectric properties affect both the distribution of the electromagnetic field and currents in the region occupied by the material itself, and the response of the material to electric fields. Consequently, the dielectric properties will also determine how quickly a material will be heated if subjected to radio frequency or microwaves.

In fact, dielectric properties of most materials vary with several different factors. In hygroscopic materials such as agri-foods, the amount of water in the material is generally a dominant factor. The dielectric properties of materials are described through three important quantities: permittivity ε, permeability μ and conductivity σ. Permittivity and electrical conductivity define the interaction between the material and the electric field, while the magnetic permeability between the material and the magnetic field:

$$D = \varepsilon E \qquad \text{(A-2)}$$

$$B = \mu H \qquad \text{(A-3)}$$

$$J = \sigma E \qquad \text{(A-4)}$$

where *D* is the electric induction field, *E* is the vector of the electric field, *B* the magnetic induction field, *H* the magnetic field, *J* the electric current density. Dielectric properties are most often expressed in relation to those of vacuum:

$$\varepsilon = \varepsilon_0 \varepsilon_r \qquad \text{(A-5)}$$

$$\mu = \mu_0 \mu_r \qquad \text{(A-6)}$$

$$\sigma = \sigma_0 \sigma_r \qquad \text{(A-7)}$$

Where ε_0, μ_0 and σ_0 are the dielectric properties relative to the vacuum, ε_r, μ_r and σ_r are the relative dielectric properties, typical of each material: the electromagnetic characteristics are the key factors in determining the dielectric type heat treatment. For most dielectric materials, permeability plays little or no role in dielectric heating, while permittivity and conductivity play a key role.

Permittivity is a complex quantity used to describe the dielectric properties related to the reflection of electromagnetic waves on the interface and the attenuation of wave energy within the material. The complete mathematical expression is:

$$\varepsilon = \varepsilon_0 \varepsilon_r = \varepsilon_0(\varepsilon_r' - j\varepsilon_r'') = \varepsilon' - j\varepsilon'' \qquad \text{(A-8)}$$

Where:

- ε_r is the relative complex permittivity;
- ε_0 is the permittivity of the vacuum, whose value is constant and equal to $\varepsilon_0 = 8.854 \cdot 10^{-12}$ F/m;
- ε_r' is the relative dielectric constant;
- ε_r'' is the relative loss factor;
- ε' is the dielectric constant;
- ε'' is the loss factor;
- $j = \sqrt{-1}$ is the imaginary unit.

The dielectric constant (ε') is a measure of a material's ability to store electric energy and the loss factor (ε'') is a measure of its ability to dissipate the electrical energy in the form of heat. The dielectric constant decreases as the temperature rises as a result of the increase in Brownian motions of molecules. Dielectric constant and loss factor values are dependent on chemical composition and especially on the permanent dipole moments associated with water and any other molecules making up the material. In general, the moisture relationship

is that higher moisture leads to higher values of both the dielectric constant and the loss factor. Naturally, this relationship is temperature dependent: higher the temperature lowers the moisture content and the dielectric properties. However, water in its pure liquid state appears in food products or other materials very rarely. Most often, it has dissolved constituents, is physically absorbed in material capillaries or cavities, or is chemically bound to other molecules. Depending on the material structure, there may be various forms of bound water, differing in terms of energy of binding and dielectric properties. Moist material, in practice, is usually an inhomogeneous mixture, often containing more than one substance with unknown dielectric properties. Thus, it becomes very difficult to understand and predict the dielectric behaviour of such materials at different frequencies, temperatures, or hydration levels [43].

The ratio of the dielectric loss to the dielectric constant, defined as the loss tangent (tanð), is related to the material's susceptibility to be penetrated by an electrical field and dissipate electrical energy as heat.

$$\tan\delta = \frac{\varepsilon''}{\varepsilon'} = \frac{\varepsilon_r''}{\varepsilon_r'} \qquad \text{(A-9)}$$

Usually, the loss factor is increasing as the temperature increases in the RF range due to the decrease in viscosity (which leads to an increase of the ion mobility), while decreasing for high values of frequency (in the microwave range) because, as the temperature rises, the value of the relaxation time decreases. Matching equations (A-8) and (A-9), we have:

$$\varepsilon = \varepsilon' - j\varepsilon'' = |\varepsilon|\, e^{j\delta} \qquad \text{(A-10)}$$

In the 0.1 MHz to 1000 GHz EM wave frequency range, the mechanisms contributing to the relative loss factor are polarization and ion conduction. The contribution of each mechanism is influenced by the frequency range, temperature, electrical conductivity, moisture content and size of the polar molecules. As mentioned earlier, ion conduction and dipolar rotation are the dominant mechanisms for RF and MW heating:

$$\varepsilon_r'' = \varepsilon_{rd}'' + \varepsilon_{r\sigma}'' = \varepsilon_{rd}'' + \frac{\sigma}{\varepsilon_0 \omega} \qquad \text{(A-11)}$$

In the equation (A-11) the subscripts *d* and *σ* represent the contribution due to dipolar rotation and ion conduction. σ is the conductivity of the material (S/m) and ω = 2πf is the angular frequency of the electromagnetic wave (Hz). Figure A.4 illustrates the contribution of

dipole rotation and ion conduction to the value of the dielectric loss factor.

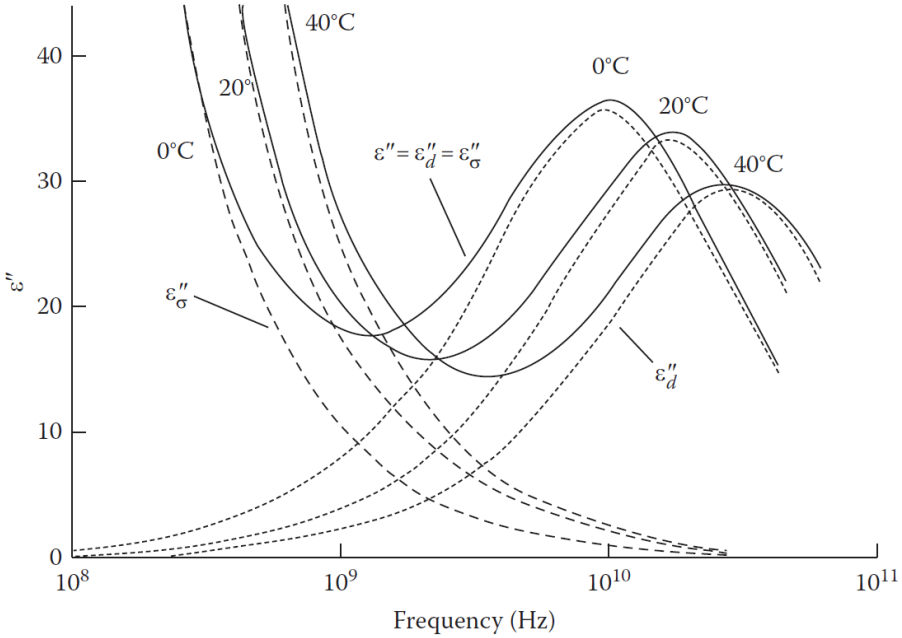

Figure A.4 Contribution of electrical conductivity and relaxation of free water molecules to the global loss factor for a 0.5N sodium chloride solution, depending on frequency and temperature

The global dielectric loss factor is given by the combination of the two contributions presented, to the relative frequency range. As the temperature increases, both the contribution of the ionic conductivity and that of the relaxation peak move to a higher frequency. This phenomenon is caused by the lower viscosity and greater mobility of ions and dipoles at higher temperatures. As can be seen from figure A.4, the contribution of ε_σ'' decreases as the frequency increases, while the contribution of ε_d'' becomes significant for high frequency values, especially in the microwave range (f > 300 MHz).

DIELECTRIC HEATING

Electric heating can be classified into direct, when the electric current is applied directly to the product (ohmic heating), and indirect, when the electric energy is converted into electromagnetic radiation that generates heat inside the product (microwave heating and radio frequencies). A radio frequency system (figure A.5) essentially consists of an RF generator, which produces and makes available an alternating electromagnetic field, and of an applicator, consisting of a pair of electrodes between which the product to be heated is positioned:

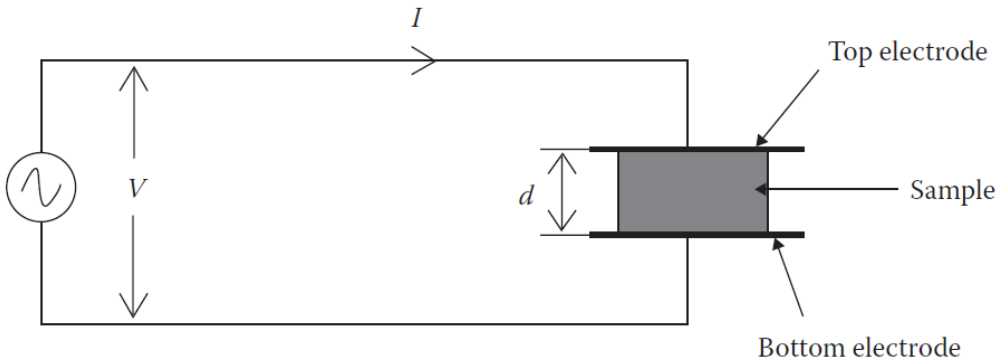

Figure A.5 Simplified RF heating system

The electrodes represent the plates of a capacitor and are positively and negatively charged alternately due to the effect of the electric field. For a flat and parallel plate capacitor, the capacitance can be expressed as:

$$C = \frac{\varepsilon_0 \varepsilon_r' A}{d} \qquad \text{(A-12)}$$

where C is the capacitance (F), ε_0 is the electrical permittivity of the vacuum, ε_r' is the complex relative electrical permittivity of the medium between the plates, A is the surface of the plate (m^2), and d is the space between the electrodes (m).

For an ideal capacitor, there is no current absorption between the two electrodes and the current has a phase angle of $\pi/2$ respect to the voltage. But if there is a dielectric material between the electrodes, it acts as a resistor and the current flowing through the resistor is in phase with the applied voltage. Figure A.6 shows the wiring diagram of a dielectric heating system and the directions of the current; δ is precisely the parameter defined as dielectric loss angle.

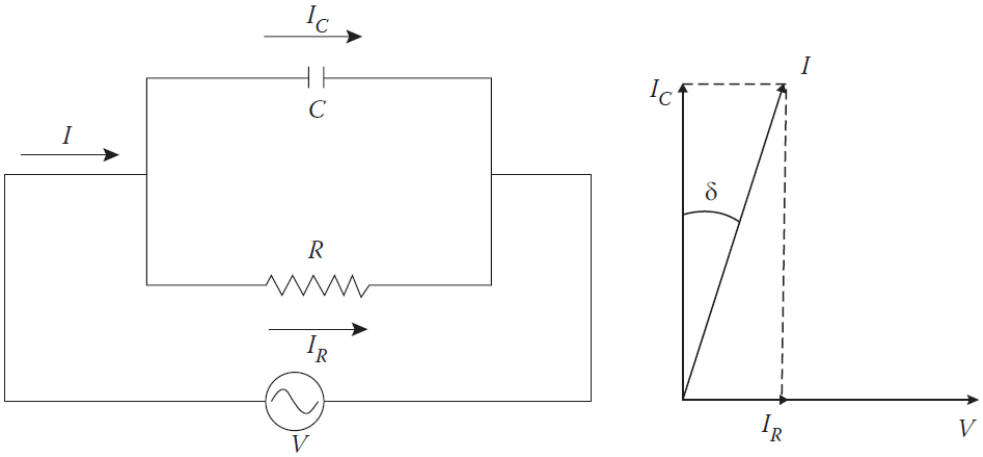

Figure A.6 Wiring diagram of a dielectric heating system

The current through the capacitor (I_c) can be calculated as follows:

$$I_c = \omega VC = 2\pi fVC \qquad \text{(A-13)}$$

Where V is the applied voltage (V) and ω = 2πf the pulsation (Hz). The current through the resistor (IR) is given by:

$$I_R = I \sin\delta = I_C \tan\delta \qquad \text{(A-14)}$$

The power totally dissipated in the load (*Q*) can be expressed as:

$$Q = V\, I_R = VI_C \tan\delta = 2\pi fV^2 C \tan\delta \qquad \text{(A-15)}$$

The relationship between voltage and electric field is:

$$E = V/d \qquad \text{(A-16)}$$

Where E is the electric field (V/m) and d is the distance between the electrodes (m). By replacing (A-16) in (A-15) we get the expression:

$$Q{=}2\pi f \varepsilon_0 \varepsilon_r{}' E^2\, d\, A \tan\delta{=}2\pi f \varepsilon_0 \varepsilon_r{}'' E^2\, d\, A \qquad \text{(A-17)}$$

Where the product d A is the volume of the load and ε_r'' is the relative loss factor. The power dissipated per unit of volume can therefore be expressed as:

$$P{=}2\pi f \varepsilon_0 \varepsilon_r{}'' E^2 = 5.56 \times 10^{-11} f \varepsilon_r{}'' E^2 \qquad \text{(A-18)}$$

where P is the power dissipated per unit volume in the heated material (W/m^3). Equation (A-18) shows that the dissipated power is proportional to the applied frequency, to the relative loss factor of the material and to the square of the applied electric field.

Another important parameter to consider in an RF heating system is the penetration thickness (d_p) of the power. It is defined as the depth of the dielectric at which the power is reduced by a factor of 1/*e* (*e*=2.718) or by 36.9% of its initial value measured on the surface of the material. This quantity, expressed in meters, can be calculated through the dielectric properties using the following formula:

$$dp = \frac{c}{2\pi f \sqrt{2\varepsilon' \sqrt{1+\left(\frac{\varepsilon''}{\varepsilon'}\right)^2 - 1}}} \qquad \text{(A-19)}$$

Where *c* is the speed of light in a vacuum.
In order to ensure uniform heating with the RF treatment, the thickness of the food should be no more than double or triple the penetration thickness.

Dielectric materials, as already mentioned, are characterized by low electrical and thermal conductivity. This implies that when they are heated conventionally, through conduction or convection, the heating rate is low and, often, a temperature gradient is detected between the surface and the innermost parts of the product, where "cold spots" can occur, points that are much colder than the surrounding material. Most foods are dielectric substances, which leads to the high potential for application of RF or MW heating. For these reasons, in the discussion and in the experiments conducted, the heat supplied by convection or conduction was considered negligible. During an electromagnetic heating, the polar molecules tend to rotate to align themselves with the polarity of the electromagnetic field in which they are immersed. Since it changes rapidly depending on the frequency used (for example, 27 million times/s at 27 MHz typical of RF), the friction between adjacent molecules converts electromagnetic energy into heat, thus giving rise to the increase in temperature in the material. As already discussed in the previous paragraphs, this mechanism is known as dipolar rotation. Even ions try to align themselves with the direction of the alternating electromagnetic field through oscillatory motions (polarization or ion conduction). Even if the mechanism is different, the generation of heat always occurs by friction.

As previously said, we can define the power dissipated per unit volume of the material can be expressed as:

$$\mathrm{P} = 2\pi f \varepsilon_0 \varepsilon_r'' \, E^2 \qquad \text{(A-18)}$$

where *P* is the power dissipated per unit volume in the heated material (W/m^3), *f* is the frequency (Hz), and *E* is the electric field intensity within the medium (V/m). The equation shows that the dissipated power is proportional to the applied frequency, to the relative loss factor of the material and to the square of the electric field.

The time rate of temperature rise as a consequence of the power absorption and can be expressed as [46]:

$$\frac{dT}{dt} = \frac{P}{c_p \, \rho} \qquad \text{(A-20)}$$

where c_p is the specific heat of the material at constant pressure (kJ/kg °C) and ρ is its density (kg/m^3).

Matching equations (A-18) and (A-20), it is possible to evaluate the thermal increase in the product following heating [47]:

$$\frac{\Delta T}{dt} = \frac{2\pi f \varepsilon_0 \varepsilon'' E^2}{\rho c_p} \qquad \text{(A-21)}$$

Equation (A-21) allows to evaluate the temperature increase inside a product known the electromagnetic field, its frequency and the physical and dielectric properties of the material. Because E represents the electric field within the medium and it is not possible to evaluate it, considering two successive heating cycles and ΔT sufficiently small, E, ρ and c_p can be assumed to be constant, and then the equation becomes:

$$\frac{dT_i}{dt} = 1.33 \cdot 10^{-11} \frac{f\, E^2\, \varepsilon''_{r,i}}{c_p\, \rho} \qquad \text{(A-22)}$$

$$\frac{dT_j}{dt} = 1.33 \cdot 10^{-11} \frac{f\, E^2\, \varepsilon''_{r,j}}{c_p\, \rho} \qquad \text{(A-23)}$$

Discretising the two equations and dividing them member to member, we obtain:

$$\frac{\Delta \mathrm{T}_i}{\Delta \mathrm{T}_i} = \frac{\varepsilon''_i}{\varepsilon''_j} \qquad \text{(A-24)}$$

Using Equation (A-24), it is possible to correlate the temperature variations due to heating with consequent variations in loss factors. For the mathematical evaluation, only the dielectric property values at MW oven frequency were considered.

The dielectric properties of most materials vary according to several factors. In hygroscopic materials, such as food, the amount of water is generally the dominant factor. In general, as the moisture content increases, the dielectric constant and the loss factor of the dielectric materials also increase, while they rapidly decrease as the water content decreases until a critical level (Mc) of humidity is reached. Below this level, the reduction in the loss factor is not very marked due to the presence of bound water in the dielectric. Finally, during dielectric heating, the wetter areas tend to absorb RF energy more.

The dielectric properties also depend on the frequency of the applied alternating electric field. With the exception of some very low-loss materials, which absorb virtually no energy from RF and MW fields, the dielectric properties of most materials vary considerably with the frequency of the applied electric fields. An important phenomenon that contributes to the dependence of dielectric properties on frequency is that of polarization, which derives from the orientation of molecules that have permanent dipole moments with the electric field. The mathematical formulation developed by Debye to describe this process for pure polar materials is expressed by the relation:

$$\varepsilon = \varepsilon_\infty + \frac{\varepsilon_S - \varepsilon_\infty}{1 + j\omega\tau} \qquad \text{(A-25)}$$

Where:

ε_∞ = relative permittivity at high frequency, or the dielectric constant at such high frequencies that the molecular orientation does not have time to contribute to polarization

ε_s = static relative permittivity, for example the dielectric constant at zero frequency (direct current)

τ = relaxation time or the time required for the polarization to reach a value equal to 1/e times (36.8%) the value corresponding to that of the instant in which the electric field is removed (the dipole returns to a random orientation).

According to the Debye model, the dielectric constant decreases as the frequency increases: to $\omega \rightarrow 0$ corresponds the maximum value equal to ε_s, while for $\omega \rightarrow \infty$ there is the minimum value equal to ε_∞.

By separating equation [28] in its real and imaginary parts, we get:

$$\varepsilon' = \varepsilon_\infty + \frac{\varepsilon_S - \varepsilon_\infty}{1 + \omega^2\tau^2} \qquad \text{(A-26)}$$

$$\varepsilon'' = \frac{\varepsilon_S - \varepsilon_\infty \omega}{1 + \omega^2\tau^2} \qquad \text{(A-27)}$$

These relationships can be illustrated like shown in figure A.7:

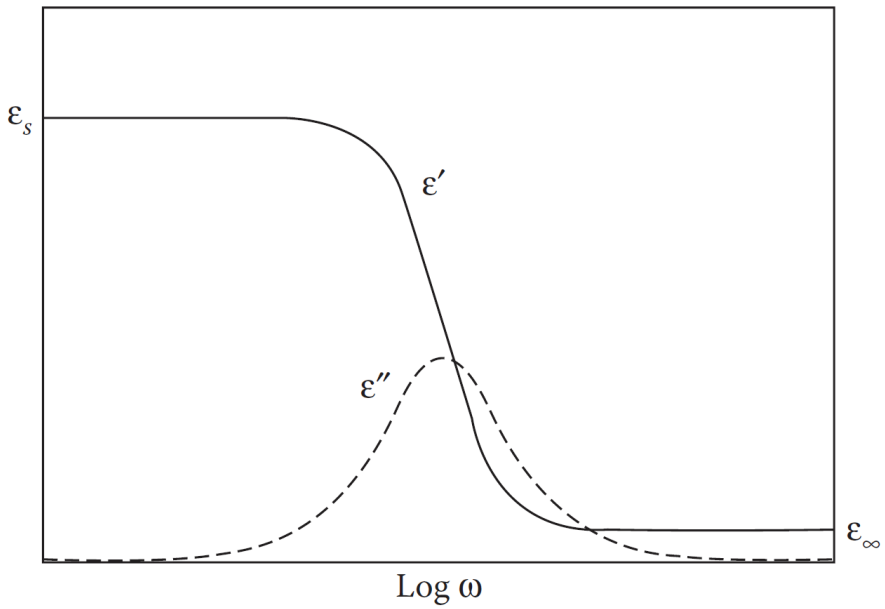

Figure A.7 Dielectric constant and loss factor for Debye model material

At very low and very high frequencies with respect to the molecular relaxation process, the dielectric constant has constant values, respectively ε_s and ε_∞, and the losses are zero. At intermediate frequencies, the dielectric constant undergoes dispersion and dielectric losses occur with the peak loss at the relaxation frequency, $\omega = 1/\tau$. Debye's equation can be represented graphically in the complex plane $\varepsilon'' - \varepsilon'$ as a semicircle with a locus of points ranging from ($\varepsilon' = \varepsilon_s$, $\varepsilon'' = 0$) at low frequencies to ($\varepsilon' = \varepsilon_\infty$, $\varepsilon'' = 0$) at high frequencies. This representation is known as the Cole-Cole diagram (figure A.8):

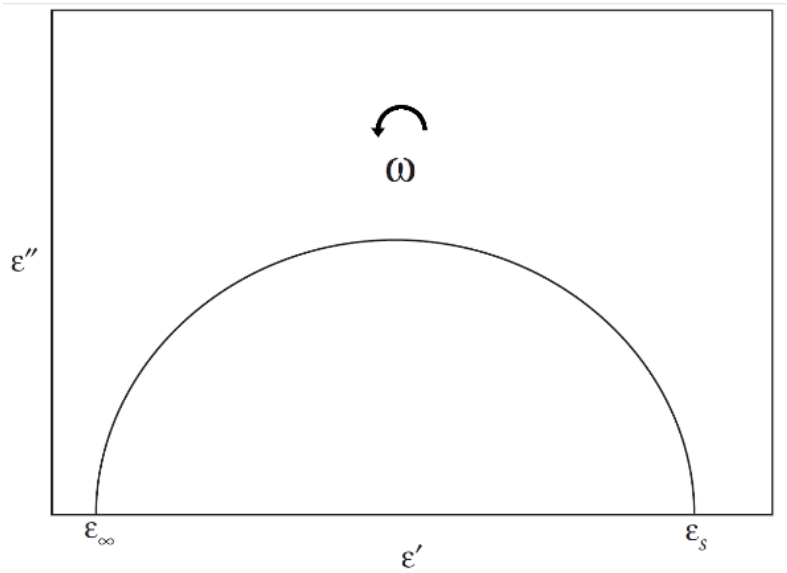

Figure A.8 Cole-Cole diagram for a material following Debye relaxation

However, as few materials of interest consist of pure polar materials with a unique relaxation time, other equations with a higher degree of complication had to be developed to better

describe the frequency dependence of materials with multiple relaxation times or a distribution of relaxation times.

Another fundamental factor for the dielectric properties is the temperature. In general, the loss factor ε'' increases as the temperature in the RF range increases as the term ε_σ'' increases due to the decrease in viscosity (which leads to an increase in ionic mobility), while it decreases for high values frequency (in the microwave range) since, as the temperature increases, the relaxation time value decreases and the value of ε_d'' decreases. The dielectric constant ε' decreases with increasing temperature due to the increase in the Brownian motions of the molecules.

Since the behaviour of a dielectric depends on the amount of mass interacting with the electromagnetic fields, the mass per unit of volume or density will have an effect on the dielectric properties. This is especially important with pulverized or granular materials. To understand the nature of the density dependence of the dielectric properties of such materials, useful relationships between the dielectric properties of solid materials and those of air-particle mixtures, such as granular or pulverized samples of such solids, have been developed.

The first is the Complex Refractive Index (CRI) equation:

$$(\varepsilon)^{1/2} = v_1(\varepsilon_1)^{1/2} + v_2(\varepsilon_2)^{1/2} \qquad \text{(A-28)}$$

the Landau and Lifshitz, Looyenga (LLL) equation:

$$(\varepsilon)^{1/3} = v_1(\varepsilon_1)^{1/3} + v_2(\varepsilon_2)^{1/3} \qquad \text{(A-29)}$$

the Böttcher equation:

$$\frac{\varepsilon-\varepsilon_1}{3\varepsilon} = v_2\frac{\varepsilon_2-\varepsilon_1}{\varepsilon_2+2\varepsilon} \qquad \text{(A-30)}$$

the Bruggeman-Hanai equation:

$$\frac{\varepsilon-\varepsilon_2}{\varepsilon_1-\varepsilon_2}\left(\frac{\varepsilon_1}{\varepsilon}\right)^{1/3} = 1 - v_2 \qquad \text{(A-31)}$$

the Rayleigh equation (also called the Maxwell Garnett equation):

$$\frac{\varepsilon-\varepsilon_1}{\varepsilon+2\varepsilon_1} = v_2\frac{\varepsilon_2-\varepsilon_1}{2\varepsilon_1+\varepsilon_2} \qquad \text{(A-32)}$$

and the Lichtenecker equation:

$$\ln \varepsilon = \upsilon_1 \ln \varepsilon_1 + \upsilon_2 \ln \varepsilon_2 \qquad \text{(A-33)}$$

Where ε is the complex permittivity of the mixture, ε_1 is the permittivity of the medium (for example air) in which the particles of permittivity ε_2 are dispersed, v_1 and v_2 are the volumetric fractions of the respective components and are such that $\nu_1 + \nu_2 = 1$. Furthermore, $v_2 = \rho/\rho_2$, where ρ is the bulk density of the air-particle system of the solid, while ρ_2 is the specific density of the solid. Each of these six mixture equations can be used to calculate the complex permittivity of the bulk of the particles [48]. The Landau & Lifshitz, Looyenga equation is globally the best equation capable of describing the relationship between the permittivity of a solid and its pulverized solid-air mixture.

APPENDIX II

COMSOL MULTIPHYSICS® BALANCE EQUATIONS

The equations of the model that the computer solves for each physics and those necessary for multiphysics coupling will be presented below. In the following equations the tensors have been indicated in bold and capital letters, vectors in bold and lowercase, scalars in lowercase:

- Magnetic and electric fields

The steady state balance equations are:

$$\nabla \cdot \boldsymbol{J} = 0 \tag{A-34}$$

$$\nabla \times \boldsymbol{H} = \boldsymbol{J} \tag{A-35}$$

$$\boldsymbol{B} = \nabla \times \boldsymbol{A} \tag{A-36}$$

$$\boldsymbol{E} = -\nabla V - j\omega \boldsymbol{A} \tag{A-37}$$

$$\boldsymbol{J} = \sigma \boldsymbol{E} + j\omega \boldsymbol{D} + \sigma \boldsymbol{v} \times \boldsymbol{B} + \boldsymbol{J_e} \tag{A-38}$$

where:

∇ = nabla operator;

J = current density [A m^{-2}];

H = intensity of the magnetic field [A m^{-1}];

B = magnetic flux density [T];

A = magnetic potential vector [Wb m^{-1}];

E = intensity of the electric field [V m^{-1}];

V = scalar electric potential [V];

j = imaginary unit;

ω = pulsation [s^{-1}];

σ = electrical conductivity [S m^{-1}];

D = electric flux density [C m^{-2}];

v = instantaneous velocity of the charge [m s^{-1}];

$\boldsymbol{J_e}$ = externally generated current [A m^{-2}].

The default boundary conditions are:

1) Magnetic isolation - All contours $\mathbf{n} \times \mathbf{A} = 0$ (A-39)
   Where:
   n = normal leaving the domain;
2) Electrical insulation - All contours $\mathbf{n} \times \mathbf{J} = 0$ (A-40)

The specific boundary conditions for the problem are:

1) Impedance boundary condition: Ground - Aluminium parallelepiped boundaries
   $V = 0$ (A-41)
2) Concentrated door - ends of the connecting slats

$$Z = \frac{V}{I} \quad \text{(A-42)}$$

   Where:
   Z = characteristic impedance of the port [Ω];
   V = voltage at port [V];
   I = current at port [A].

- Magnetic and electric fields

The equations of matter balance and momentum at stationary are:

$$\rho(\boldsymbol{u} \cdot \nabla)\boldsymbol{u} = \nabla \cdot [-p\boldsymbol{I} + (\mu + \mu_T)(\nabla \boldsymbol{u} + (\nabla \boldsymbol{u})^T)] + \boldsymbol{F} \quad \text{(A-43)}$$

$$\nabla \cdot (\rho \boldsymbol{u}) = 0 \quad \text{(A-44)}$$

to these must be added the equations of the k- ε model:

$$(\boldsymbol{u} \cdot \nabla)k = \nabla \cdot \left[\left(\mu + \frac{\mu_T}{\sigma_k}\right)\nabla k\right] + P_k - \rho\varepsilon \quad \text{(A-45)}$$

$$\rho(\boldsymbol{u} \cdot \nabla)\varepsilon = \nabla \cdot \left[\left(\mu + \frac{\mu_T}{\sigma_e}\right)\nabla \varepsilon\right] + C_{\varepsilon 1}\frac{\varepsilon}{k}P_k - C_{\varepsilon 2}\frac{\varepsilon^2}{k} \quad \text{(A-46)}$$

$$\varepsilon = ep \quad \text{(A-47)}$$

$$\mu_T = \rho C_\mu \frac{k^2}{\varepsilon} \quad \text{(A-48)}$$

$$P_k = \mu_T[\nabla \boldsymbol{u} : (\nabla \boldsymbol{u} + (\nabla \boldsymbol{u})^T)] \quad \text{(A-49)}$$

and the constants of the turbulent model:

$$C_{\varepsilon 1} = 1.44, C_{\varepsilon 2} = 1.92, C_\mu = 0.09, \sigma_k = 1, \sigma_\varepsilon = 1.3, k_v = 0.41$$

where:

ρ = density [kg m^{-3}];

u = velocity vector [m s^{-1}];

p = pressure [kg $m^{-1}s^{-1}$];

I = identity tensor [-];

μ = dynamic viscosity [kg $m^{-1}s^{-1}$];

F = vector of the volume forces [N m^{-3}];

k = turbulent kinetic energy [m^2 s^{-2}];

ε = turbulent dissipation speed [m^2 s^{-2}];

The default boundary conditions are:

1) Wall - all contours

$$\mathbf{u} \cdot \mathbf{n} = 0 \quad \text{(A-50)}$$

$$[(\mu + \mu_T)(\nabla \boldsymbol{u} + (\nabla \boldsymbol{u})^T)]\boldsymbol{n} = -\rho \frac{u_\tau}{\delta_w^+} \boldsymbol{u}_{tang} \quad \text{(A-51)}$$

$$\boldsymbol{u}_{tang} = \boldsymbol{u} - (\boldsymbol{u} \cdot \boldsymbol{n})\boldsymbol{n} \quad \text{(A-52)}$$

$$\nabla k \cdot \boldsymbol{n} = 0, \varepsilon = \rho \frac{C_\mu k^2}{k_v \delta_w^+ \mu} \quad \text{(A-53)}$$

where:

u_τ = friction speed [m s^{-1}];
u_{tang} = tangential speed [m s^{-1}];
δ_w^+= wall lift off in viscous units;

The specific boundary conditions for the problem are:

2) Inlet - fluid inlet surface

$$-\int_{d\Omega} \rho(\boldsymbol{u} \cdot \boldsymbol{n}) d_{bc} dS = m \quad \text{(A-54)}$$

$$k = \frac{3}{2}(U_{ref} I_T)^2, \varepsilon = C_\mu^{3/4} \frac{k^{3/2}}{L_T} \quad \text{(A-55)}$$

where:

d_{bc} = is the thickness of the contour normal to the flow [m];
m = total mass flow [kg s^{-1}];
U_{ref} = reference speed scale [m s^{-1}]
I_T = turbulent intensity [-];
L_T = length of the turbulent scale [m].

3) Outlet - fluid outlet surface

$$[-p\boldsymbol{I} + (\mu + \mu_T)(\nabla \boldsymbol{u} + (\nabla \boldsymbol{u})^T)]\boldsymbol{n} = -\hat{p}_0 \boldsymbol{n} k \qquad \text{(A-56)}$$

$$\hat{p}_0 \leq p_0 \qquad \text{(A-57)}$$

$$\nabla k \cdot \boldsymbol{n} = 0, \nabla \varepsilon \cdot \boldsymbol{n} = 0 \qquad \text{(A-58)}$$

where:

$\hat{p}_0$ = pressure an infinitesimal before the outgoing pressure [Pa];
p_0 = reference pressure, equal to the outlet pressure [Pa];

The *wall lift off in viscous units* is calculated as:

$$\delta_w^+ = \frac{\rho u_\tau \delta_w}{\mu} \qquad \text{(A-59)}$$

Where δ_w is the distance from the wall in which the computational domain is solved through the wall functions; it must never be smaller than half the height h_w of the mesh element near the wall [m].

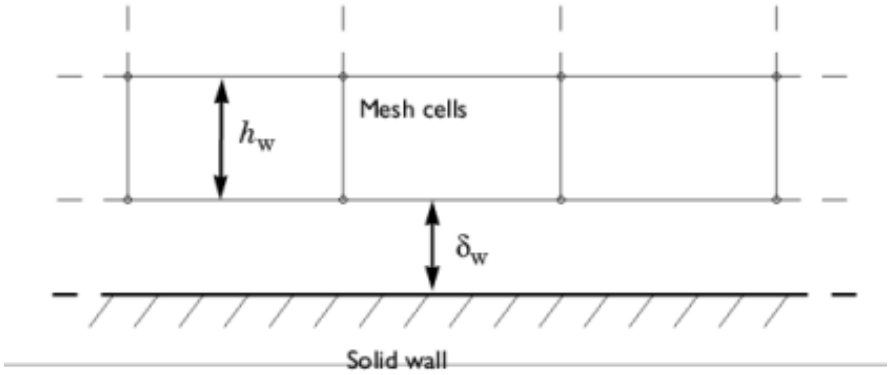

Figure A.9 Representation of the division of the domain between the zone in which the balance equations are solved and the zone in which the wall functions apply

- Heat transfer in fluids

The steady state balance equations are:

$$\rho\, c_p\, \boldsymbol{u} \cdot\, \nabla T + \nabla \cdot\, \boldsymbol{q} = Q + Q_p + Q_{vd} \qquad \text{(A-60)}$$

$$\boldsymbol{q} = -k_t\, \nabla T \qquad \text{(A-61)}$$

Where:

c_p = specific heat at constant pressure [J kg^{-1} K^{-1})];

T = temperature [K];

q = thermal flux [W m^{-2}];

k_t = thermal conductivity [W m^{-1} K^{-1})];

Q = external heat source [W m^{-3}];

Q_p = viscous dissipation [W m^{-3}];

Q_{vd} = point heat source [W m^{-3}].

The default boundary conditions are:

Thermal insulation - all walls

$$-\boldsymbol{n} \cdot \boldsymbol{q} = 0 \qquad \text{(A-62)}$$

This condition is overridden by the two boundary conditions specific to the problem.

1) Temperature $T = T_0$ (A-63)

Where T_0 is the temperature at which the fluid is at the inlet to the applicator tube, set at 353.15 K.

2) Outgoing flow $-\boldsymbol{n} \cdot \boldsymbol{q} = 0$ (A-64)

- Electromagnetic heating

The steady state balance equations are:

$$\rho\, c_p\, \boldsymbol{u} \cdot \nabla T = \nabla \cdot (k_t \nabla T) + Q_e \qquad \text{(A-65)}$$

$$Q_e = \boldsymbol{J} \cdot \boldsymbol{E} \qquad \text{(A-66)}$$

Where is:

Q_e = heat exchanged by an electromagnetic field

- Non-isothermal flow

The steady state balance equations are:

$$-\boldsymbol{n} \cdot \boldsymbol{q} = \rho\, c_p u_\tau \frac{T_w - T}{T^+} \qquad \text{(A-67)}$$

Where:

T_w = temperature at the wall [K];

T^+ = dimensionless temperature.

BIBLIOGRAPHY

[1] A. McElhatton, R. J. Marshall, e K. Kristbergsson, *Food safety: A practical and case study approach*. 2007.

[2] M. S. Rahman, *Handbook of Food Preservation*, vol. 6, n. 3. CRC Press, 2007.

[3] P. Cappelli e V. Vannucchi, *Chimica degli alimenti. Conservazione e trasformazione*, 3° edizion. Bologna: Zanichelli, 2005.

[4] Z. Berk, *Food Process Engineering and Technology*. 2009.

[5] A. K. Haghi e H. Ghanadzadeh, «A study of thermal drying process», *Indian J. Chem. Technol.*, vol. 12, n. 6, pagg. 654–663, 2005.

[6] E. Ferret, L. Bazinet, e A. Voilley, «Heat and Mass Transfers—Basics Enthalpies Calculation and the Different Transfer Modes», in *Gases in Agro-Food Processes*, Elsevier, 2019, pagg. 89–102.

[7] A. Rosenthal, R. Deliza, J. Welti-Chanes, e G. V. Basbosa-Canovas, *Fruit Preservation: Novel and Conventional Technologies - Google Books*. 2018.

[8] Y. H. Hui, C. D. Clary, M. M. Farid, e O. Fasina, *Food Drying Science and Technology: Microbiology, Chemistry, Applications*. DEStech Publications, Inc, 2008.

[9] H. T. Sabarez, J. A. Gallego-Juarez, e E. Riera, «Ultrasonic-Assisted Convective Drying of Apple Slices», *Dry. Technol.*, vol. 30, n. 9, pagg. 989–997, 2012.

[10] D. Friso e M. Niero, *Operazioni unitarie dell'ingegneria alimentare: modelli fisici e matematici, macchine e impianti*. CLEUP, 2010.

[11] D. R. Heldman e D. B. Lund, «Handbook of food engineering, second edition», *Handbook of Food Engineering, Second Edition*. pagg. 1–1025, 2006.

[12] I. Filková e A. S. Mujumdar, «Industrial Spray Drying Systems», in *Handbook of Industrial Drying*, CRC Press, 2020, pagg. 263–307.

[13] Y. L. Xiong, «Influence of pH and ionic environment on thermal aggregation of whey proteins», *J. Agric. Food Chem.*, vol. 40, n. 3, pagg. 380–384, mar. 1992.

[14] J. Hardy, M. Parmentier, e J. Fanni, «Symposium on "Food technology: Can it alter the functionality of nutrients". Functionality of nutrients and thermal treatments of food», *Proc. Nutr. Soc.*, vol. 58, n. 3, pagg. 579–585, 1999.

[15] J. Wang *et al.*, «Effect of high-humidity hot air impingement blanching (HHAIB) on drying and quality of red pepper (Capsicum annuum L.)», *Food Chem.*, vol. 220, pagg. 145–152, apr. 2017.

[16] L. Manzocco, S. Calligaris, D. Mastrocola, M. C. Nicoli, e C. R. Lerici, «Review of non-enzymatic browning and antioxidant capacity in processed foods», *Trends Food Sci. Technol.*, vol. 11, n. 9–10, pagg. 340–346, set. 2000.

[17] M. Mariotti, M. Zardi, M. Lucisano, e M. A. Pagani, «Influence of the heating rate on the pasting properties of various flours», *Starch/Staerke*, vol. 57, n. 11, pagg. 564–572, 2005.

[18] D. Lund e K. J. Lorenz, «Influence of time, temperature, moisture, ingredients, and processing conditions on starch gelatinization», *C R C Crit. Rev. Food Sci. Nutr.*, vol. 20, n. 4, pagg. 249–273, gen. 1984.

[19] M. Zielinska e A. Michalska, «Microwave-assisted drying of blueberry (Vaccinium corymbosum L.) fruits: Drying kinetics, polyphenols, anthocyanins, antioxidant capacity, colour and texture», *Food Chem.*, vol. 212, pagg. 671–680, dic. 2016.

[20] T. Antal, «Comparative study of three drying methods: Freeze, hot airassisted freeze and infrared-assisted freeze modes», *Agron. Res.*, vol. 13, n. 4, pagg. 863–878, 2015.

[21] R. P. F. Guiné, «The Drying of Foods and Its Effect on the Physical-Chemical, Sensorial and Nutritional Properties», *ETP Int. J. Food Eng.*, vol. 4, n. 2, pagg. 93–100, 2018.

[22] X. Zhu, W. Guo, e Y. Jia, «Temperature-Dependent Dielectric Properties of Raw Cow's and Goat's Milk from 10 to 4,500 MHz Relevant to Radio-frequency and Microwave Pasteurization Process», *Food Bioprocess Technol.*, vol. 7, n. 6, pagg. 1830–1839, giu. 2014.

[23] X. Zhu, W. Guo, e X. Wu, «Frequency- and temperature-dependent dielectric properties of fruit juices associated with pasteurization by dielectric heating», *J. Food Eng.*, vol. 109, n. 2, pagg. 258–266, mar. 2012.

[24] P. A. Berbert, D. M. Queiroz, e E. C. Melo, «Dielectric properties of common bean», *Biosyst. Eng.*, vol. 83, n. 4, pagg. 449–462, 2002.

[25] K. Sacilik, C. Tarimci, e A. Colak, «Dielectric properties of flaxseeds as affected by moisture content and bulk density in the radio frequency range», *Biosyst. Eng.*, vol. 93, n. 2, pagg. 153–160, 2006.

[26] S. Trabelsi e S. O. Nelson, «Free-space measurement of dielectric properties of cereal grain and oilseed at microwave frequencies», *Meas. Sci. Technol.*, vol. 14, n. 5, pagg. 589–600, mag. 2003.

[27] I. Shorstkii, X. Q. Koh, e E. Koshevoi, «Influence of Temperature and Solvent Content on Electrical Properties of Sunflower Seed Cake», *J. Food Process. Preserv.*, vol. 39, n. 6, pagg. 3092–3097, 2015.

[28] M. Gao, J. Tang, J. A. Johnson, e S. Wang, «Dielectric properties of ground almond shells in the development of radio frequency and microwave pasteurization», *J. Food Eng.*, vol. 112, n. 4, pagg. 282–287, ott. 2012.

[29] W. Guo, S. Wang, G. Tiwari, J. A. Johnson, e J. Tang, «Temperature and moisture dependent dielectric properties of legume flour associated with dielectric heating», *LWT - Food Sci. Technol.*, vol. 43, n. 2, pagg. 193–201, mar. 2010.

[30] G. B. Awuah, H. S. Ramaswamy, e J. Tang, «Radio-Frequency Heating in Food Processing», in *Electro-Technologies for Food Processing Series*, CRC Press, A c. di 2015, pagg. 501–524.

[31] P. Piyasena, C. Dussault, T. Koutchma, H. S. Ramaswamy, e G. B. Awuah, «Radio Frequency Heating of Foods: Principles, Applications and Related Properties - A Review», *Crit. Rev. Food Sci. Nutr.*, vol. 43, n. 6, pagg. 587–606, 2003.

[32] T. Koral, «Radio Frequency Dielectric Heating re-emerges as an Effective Process in the Food Industry», *42nd Annu. Microw. Symp. Proc. June*, pagg. 1–13, 2008.

[33] J. Tang e T. V. Chow Ting Chan, *Microwave and radio frequency in sterilization and pasteurization applications*, vol. 13. 2007.

[34] L. Wan, P. D. Jakkilinki, M. R. Singer, M. L. Bradlee, e L. L. Moore, «A longitudinal study of fruit juice consumption during preschool years and subsequent diet quality and BMI», pagg. 4–11, 2020.

[35] S. O. Nelson e T. S. You, «Relationships between microwave permittivities of solid and pulverised plastics», *J. Phys. D. Appl. Phys.*, vol. 23, n. 3, pagg. 346–353, mar. 1990.

[36] S. O. Nelson, «Determining dielectric properties of coal and limestone by measurements on pulverized samples», *J. Microw. Power Electromagn. Energy*, vol. 31, n. 4, pagg. 215–220, 1996.

[37] Y.-H. Choi, «Effects of temperature and composition on the thermal conductivity and thermal diffusivity of some food components», *Korean Journal of Food Science and Technology*, vol. 18, n. 5. pagg. 357–363, 1986.

[38] H. G. Kessler e A. Verlag, *Food and Bioprocess Engineering*. Munich, 2002.

[39] L. Riedel, «Thermal conductivity measuments on sugar solutions, fruit juices and milk», *Dairy Sci. Technol.*, vol. 93, pagg. 537–549, 1949.

[40] Y. Nishi, S. Iizuka, M. C. Faudree, e R. Oyama, «Electrical conductivity enhancement of PTFE (Teflon) induced by homogeneous low voltage electron beam irradiation (HLEBI)», *Mater. Trans.*, vol. 53, n. 5, pagg. 940–945, 2012.

[41] Y. A. Çengel, *Termodinamica e trasmissione del calore*. Milano, 2009.

[42] M. E. Sosa-Morales *et al.*, «Dielectric properties of berries in the microwave range at variable temperature», *J. Berry Res.*, vol. 7, n. 4, pagg. 239–247, 2017.

[43] M. S. Venkatesh e G. S. V. Raghavan, «An Overview of Microwave Processing and Dielectric Properties of Agri-food Materials», *Biosyst. Eng.*, vol. 88, n. 1, pagg. 1–18, mag. 2004.

[44] A. A. Laogun, «Dielectric properties of mammalian breast milk at radiofrequencies», *Phys. Med. Biol.*, vol. 31, n. 5, pagg. 555–561, mag. 1986.

[45] A. K. Datta e P. M. Davidson, «Microwave and Radio Frequency Processing», *J. Food Sci.*, vol. 65, n. 8 SPEC. SUPPL., pagg. 32–41, nov. 2000.

[46] S. O. Nelson, «Potential Agricultural Applications for RF and Microwave Energy», *Trans. ASAE*, vol. 30, n. 3, pagg. 0818–0831, 1987.

[47] M. Orfeuil, «Electric process heating». 1987.

[48] S. O. Nelson, «Density-Permittivity Relationships for Powdered and Granular Materials», *IEEE Trans. Instrum. Meas.*, vol. 54, n. 5, pagg. 2033–2040, ott. 2005.